

For Reference

NOT TO BE TAKEN FROM THIS ROOM

Ex LIBRIS
UNIVERSITATIS
ALBERTAEISIS



THE UNIVERSITY OF ALBERTA
RELEASE FORM

NAME OF AUTHOR ALAN DUNCAN GALE
TITLE OF THESIS A HIGH PRESSURE SIMPLE SHEAR APPARATUS
DEGREE FOR WHICH THESIS WAS PRESENTED MASTER OF SCIENCE
YEAR THIS DEGREE GRANTED SPRING, 1981

Permission is hereby granted to THE UNIVERSITY OF
ALBERTA LIBRARY to reproduce single copies of this
thesis and to lend or sell such copies for private,
scholarly or scientific research purposes only.

The author reserves other publication rights, and
neither the thesis nor extensive extracts from it may
be printed or otherwise reproduced without the author's
written permission.

THE UNIVERSITY OF ALBERTA

A HIGH PRESSURE SIMPLE SHEAR APPARATUS

by

(C)

ALAN DUNCAN GALE

A THESIS

SUBMITTED TO THE FACULTY OF GRADUATE STUDIES AND RESEARCH

IN PARTIAL FULFILMENT OF THE REQUIREMENTS FOR THE DEGREE

OF MASTER OF SCIENCE

IN

CIVIL ENGINEERING

DEPARTMENT OF CIVIL ENGINEERING

EDMONTON, ALBERTA

SPRING, 1981

THE UNIVERSITY OF ALBERTA
FACULTY OF GRADUATE STUDIES AND RESEARCH

The undersigned certify that they have read, and
recommend to the Faculty of Graduate Studies and Research,
for acceptance, a thesis entitled A HIGH PRESSURE SIMPLE
SHEAR APPARATUS submitted by ALAN DUNCAN GALE in partial
fulfilment of the requirements for the degree of MASTER OF
SCIENCE in CIVIL ENGINEERING.

Abstract

This research program arose from an interest in the behaviour of earth and rockfill dams during reservoir filling when, relative to the construction phase, increments in major principal stress within the core undergo significant rotation. To better model such processes, study of the shear stress-strain and pore pressure-strain characteristics of core material is of importance. For this purpose, the two main types of simple shear apparatus are reviewed and one of a new design is advocated. It is a modification of that developed primarily at the Norwegian Geotechnical Institute.

This thesis deals mainly with the development of the apparatus. The prototype is described in detail. Appendices contain procedures for preparing samples and conducting tests. The calibration of the apparatus is also described fully.

To assess the performance of the apparatus, a series of tests was carried out. The material tested was derived from that used to construct the core of an earth dam. The samples were saturated by back pressure. They were then consolidated and sheared, to failure, in the undrained state. Throughout, measurements were taken of boundary loads and pore pressures acting, as well as the components of deformation of the sample.

The average shear stress-strain curves are bilinear in form and can be described by the well known hyperbolic

stress-strain formulation. Curves representing the average pore pressure-shear strain relation determined are also presented. The results are discussed but detailed interpretation is limited by uncertainties associated with the state of stress within the sample. However, these preliminary data are considered encouraging.

To conclude, modifications for improving the performance of the apparatus are outlined. The possible nature of future testing programs is also discussed. Finally, the development of a comprehensive constitutive model for the behaviour of compacted soil is advocated.

Acknowledgements

This research was undertaken and completed with the guidance and encouragement of Dr. Z. Eisenstein; to him I am grateful.

Discussions with many other people, on various aspects of my work, helped to clarify or refine ideas. In particular, the comments of Dr. N. R. Morgenstern on simple shear testing, during the early stages of this work, proved very beneficial. Also, many improvements in the design of the apparatus resulted from ideas raised in discussions with Allan Muir and Fathalla El Nahhas. Erman Evgin provided valuable insight into the complex topic of analytical modelling of soil behaviour. As well, John Simmons critically reviewed most of this thesis and suggested numerous improvements.

Dr. D. M. Wood and Dr. T. C. Kenney furnished literature on simple shear testing. Their generosity is gratefully acknowledged.

The technical assistance of Don Fushtey, Hal Soderberg, Gerry Cyre, Steve Gamble and Scotty Rogers was of tremendous benefit. Tom Brown did an excellent job machining the components of the apparatus. The financial assistance received from the National Research Council of Canada and the Department of Civil Engineering, during the course of my research work, is also appreciated.

Finally, I would like to thank all those whose friendship helped make my life as a graduate student such an

enlightening and valuable experience.

Table of Contents

Chapter	Page
CHAPTER 1	
<u>INTRODUCTION</u>	1
1.1 General	1
1.2 Analytical Methods in Earth Dam Design	1
1.3 Description of Two Constitutive Models	3
1.4 Requirements of the Models	4
1.5 Assessment of Two Constitutive Models	8
1.6 Need for Further Research	9
1.7 Aims of Thesis	10
1.8 Contents of Thesis	10
CHAPTER 2	
<u>COMPARISON OF CERTAIN SIMPLE SHEAR APPARATUS</u>	11
2.1 General	11
2.2 NGI Apparatus	11
2.2.1 Description of Apparatus	11
2.2.2 Stress State in NGI Apparatus	15
2.3 Cambridge Simple Shear Apparatus	21
2.3.1 Description of Mark 6 Model	22
2.3.2 Description of Simpler Cambridge Type Apparatus	24
2.3.3 Stress State in Cambridge Type Apparatus	26
2.4 University of Alberta Apparatus	30
2.4.1 Description of Apparatus	30
2.4.2 Stress State in U of A Apparatus	34
2.5 Evaluation of Apparatus	38
CHAPTER 3	

<u>DESCRIPTION OF TESTING APPARATUS</u>	42
3.1 General	42
3.2 Description of Apparatus	42
3.2.1 Testing Frame	42
3.2.2 Vertical Loading System	45
3.2.3 Upper Platen	49
3.2.4 Pedestal	55
3.2.5 Cell Base	57
3.2.6 Cell Wall and Yoke	59
3.2.7 Horizontal Loading System	63
3.2.8 Deformation Gauges	65
3.3 Devices Used During Sample Preparation	66
<u>CHAPTER 4</u> <u>PRESENTATION AND DISCUSSION OF EXPERIMENTAL RESULTS</u> ..	69
4.1 General	69
4.2 Description of Soil Tested	69
4.3 Evaluation of Apparatus and Laboratory Procedures .	71
4.3.1 Membranes	71
4.3.2 Loading Frame	71
4.3.3 Cell Fluid	72
4.3.4 Testing Procedure	72
4.3.5 Lateral Gauge	74
4.3.6 Maintenance of Boundary Conditions	77
4.4 Evaluation of Test Results	80
4.4.1 Factors Influencing Soil's Structure	80
4.4.2 Average Stress Strain Curves	83
4.4.3 Average Pore Pressure Shear Strain Curves ...	86
4.4.4 Reformulation of Results	86

4.4.5 Discussion of Stress State in Sample	89
4.4.6 Work of van Eekelen and Potts	92
4.4.7 Work of Prevost	94
CHAPTER 5	
<u>CONCLUSIONS AND RECOMMENDATIONS FOR FURTHER RESEARCH</u>	97
5.1 General	97
5.2 Review of Thesis	97
5.3 Conclusions	98
5.4 Recommendations for Further Research	100
REFERENCES	102
APPENDIX A	
<u>CALIBRATION OF APPARATUS</u>	108
A.1 Procedure for Friction Determination	109
A.2 Determination of Horizontal Friction Loss	114
A.3 Reduction of Horizontal Load Data	120
APPENDIX B	
<u>SAMPLE PREPARATION</u>	123
B.1 Preparation of Sample	124
B.2 Preparations Involving the Apparatus	127
B.3 Installation of Soil Sample	137
APPENDIX C	
<u>TEST PROCEDURE</u>	155
C.1 General	156
C.2 Test Procedure	156
C.2.1 Initial Readings	156
C.2.2 Back Saturation of Sample	157
C.2.3 K_0 Consolidation	158
C.2.4 Shear Loading	160
C.2.5 End of Test	162

C.2.6 Disassembly of Cell	162
C.3 Detailed Discussion of Back Saturation	166
C.3.1 Seating Load	166
C.3.2 Increments of Cell Pressure	168
C.3.3 Changes in Degree of Saturation	169
C.3.4 Acceptable Degree of Saturation	172

List of Tables

Table	Page
4.1 Test Results	78
4.2 Structure Determining Factors and Processes for Compacted Soil (after Mitchell, 1976, abridged)	81

List of Figures

Figure	Page
1.1 Movements During Construction Period (after Wilson, 1977)	6
1.2 Movements During First Filling of Reservoir (after Wilson, 1977)	7
2.1 NGI Simple Shear Apparatus (after Bjerrum and Landva, 1966)	12
2.2 Boundary Conditions for Three Dimensional Analysis (after Lucks et al., 1972)	17
2.3 Finite Element Mesh for Three Dimensional Analysis (after Lucks et al., 1972)	17
2.4 Results of Three Dimensional Analysis (after Lucks et al., 1972)	19
2.5 Boundary Conditions and Finite Element Idealization for Fourier Analysis (after Lucks et al., 1972)	20
2.6 Results of Fourier Analysis (after Lucks et al., 1972)	20
2.7 Mark 6 Simple Shear Apparatus (after Roscoe et al., 1967)	23
2.8 Boundary Conditions for Roscoe's Analysis (after Roscoe, 1953)	27
2.9 Normalized Stress Distribution Within Cambridge Apparatus (after Roscoe, 1953)	29
2.10 Sectional View of U of A Apparatus	31
2.11 Representation of Platen-Sample-Pedestal System	36
3.1 View of Testing Frame	43
3.2 View of Load Cell and Cell	46
3.3 View of Ram-Load Cap Connection	48
3.4 View of Sample with Lateral Gauge Attached	50

Figure	Page
3.5 View of Upper Platen	51
3.6 View of Drainage Line in Position	53
3.7 Upper Platen Disassembled	54
3.8 View of Pedestal	56
3.9 Schematic View of Cell Base	58
3.10 View of Horizontal Bushing Assembly	61
3.11 Yoke and Load Cap Assembly	62
3.12 Horizontal Loading System	64
3.13 Embedding Fins in Sample	67
4.1 Grain Size Distribution of Altered Mica Dam Core Material	70
4.2 Views of Sample at End of Test #3	79
4.3 Views of Sample #3 Encased in Membrane	82
4.4 Average Shear Stress as Function of Average Shear Strain	84
4.5 Inverse of Secant Modulus as Function of Average Shear Strain	87
4.6 Pore Pressure as Function of Average Shear Strain ..	88
4.7 Stress Ratio as Function of Average Shear Strain ..	90
4.8 Average Shear Stress as Function of Average Vertical Effective Stress	91
4.9 Predicted Behaviour of Drammen Clay (after van Eekelen and Potts, 1978)	93
4.10 Predicted Behaviour of Normally Consolidated Drammen Clay (after Prevost, 1978)	95
4.11 Predicted Behaviour of Overconsolidated Drammen Clay	

Figure	Page
(after Prevost, 1978)	95
A.1 Forces Acting on Load Cap-Vertical Ram Assembly	112
A.2 Net Internal Load as Function of External Load	113
A.3 Idealization of Calibration Curve	116
A.4 Absolute Error as Function of Change in Load Cell Output	118
A.5 Internal Horizontal Load as Function of Applied External Load	119
A.6 Schematic View of Horizontal Ram Showing Forces Acting	121
B.1 View of Compaction Mould	126
B.2 Control System for Apparatus	128
B.3 Valves and Connections on Cell Base	129
B.4 View of Cell Fluid Reservoir	132
B.5 View of Pedestal	135
B.6 Upper Platen with Drainage Line Attached	136
B.7 View of Device for Embedding Fins in Sample	138
B.8 View of Rotation LVDT's and Stand	142
B.9 View of Cell Cap, Load Cap and Cell Wall	146
B.10 View Showing Horizontal LVDT Holder Abutting Bushing Assembly	147
B.11 Procedure for Securing Tie Rods	149
B.12 View of Vertical Load Cell Assembly	151
B.13 View of Horizontal Loading Assembly	153

List of Symbols

Chapter 2

E : Young's modulus

h : one half height of sample in Cambridge apparatus (page 27)

: initial height of sample in U of A apparatus (page 37)

k : angle of shear

K_0 : coefficient of earth pressure at rest

L : length of sample in Cambridge apparatus

r : cylindrical polar co-ordinate direction

s : average applied shear stress

u_x : component of displacement in Cartesian co-ordinate direction

u_y : component of displacement in Cartesian co-ordinate direction

u_z : component of displacement in Cartesian co-ordinate direction

u_r : component of displacement in cylindrical polar co-ordinate direction

u_θ : component of displacement in cylindrical polar co-ordinate direction

u_z : component of displacement in cylindrical polar co-ordinate direction

u : total displacement of upper platen in NGI apparatus (pages 17 and 20)

: horizontal component of displacement in Cambridge apparatus (page 26)

v : vertical component of displacement in Cambridge apparatus

x : Cartesian co-ordinate direction

y : Cartesian co-ordinate direction

z : Cartesian and cylindrical polar co-ordinate direction

γ : shear strain

θ : cylindrical polar co-ordinate

ν : Poisson's ratio

σ_H : horizontal normal stress in U of A sample (page 35)

σ_v : vertical normal stress in U of A sample (page 35)

σ_r : radial normal stress in NGI sample (page 20)

σ_z : vertical normal stress in NGI sample (page 20)

σ_x : horizontal normal stress in Cambridge sample (page 28)

σ_y : vertical normal stress in Cambridge sample (page 28)

τ : shear stress in NGI and U of A samples (pages 18 and 37)

τ_{xy} : shear stress within Cambridge sample (page 28)

τ : shear stress on vertical boundary of Cambridge sample (page 27)

Chapter 4

a : constant in hyperbolic stress-strain formulation

B : pore pressure parameter

b : constant in hyperbolic stress-strain formulation

p : mean normal effective stress

p_o' : in situ vertical effective stress

q : stress difference in triaxial test

u : pore pressure
 γ : average shear strain
 ϵ_v : vertical normal strain
 τ : average shear stress
 τ_{xy} : shear stress in ideal simple shear test (page 95)
 τ_h : measured average shear stress (page 95)
 σ_h : measured average horizontal normal stress (page 95)
 σ_v : measured average vertical normal stress (page 95)
 σ_v' : average vertical normal effective stress (pages 89 and 93)
 σ_{vc}' : vertical normal effective stress upon K_o unloading (page 95)
 σ_y : vertical normal stress (page 95)
 σ_x : horizontal normal stress (page 95)

Appendix A

a : load measured by horizontal load cell
A : weight of load cell, connectors and Bellofram piston;
load on Bellofram
b : frictional force on horizontal ram
B : frictional force due to oil seal and Thompson bushing
c : thrust on horizontal ram due to cell pressure
C : weight of ram-load cap system
D : net upward thrust due to cell pressure
E : reaction of load cell
f : shear load carried by soil sample
q : error in horizontal load

r : true horizontal Bellofram load

t : apparent horizontal Bellofram load

Appendix C

d : diameter of sample

Δd : change in diameter of sample

d_1 : diameter of vertical ram

d_2 : bore of vertical Bellofram

L_1 : load on vertical ram due to cell pressure

L_2 : load on vertical ram due to Bellofram

p_1 : line pressure to cell

p_1' : air pressure reading from regulator gauge

p_2 : line pressure to Bellofram (page 167)

p_2' : air pressure reading from regulator gauge

p_i : initial pressure (absolute) in the pore space

p_2 : final pressure (absolute) in pore space of sample

(page 170)

S_i : initial degree of saturation of sample

S_2 : final degree of saturation of sample

V_i : initial volume of free air within sample

V_2 : final volume of free air within sample

V_w : initial volume of water within sample

CHAPTER 1

INTRODUCTION

1.1 General

A brief review of the considerations that led to the undertaking of the research program begins the chapter. Criteria for the design of an earth dam are introduced. The use of finite element analyses, in such design, to predict stress-deformation behaviour and thus, to help insure proper functioning of the earth dam throughout the course of its working life is then noted. Two constitutive models for the behaviour of compacted clay, that can be incorporated in the above analytical procedures, are also described. Assumptions and approximations implicit in these models are carefully pointed out. The suitability of their use in such analyses is then discussed. Finally, the need for further work in this area is suggested.

The chapter concludes with a statement of the aims of this research work and an outline of the remaining portions of the thesis.

1.2 Analytical Methods in Earth Dam Design

In designing an earth dam, the principal objective is to arrive at a functional design that minimizes the long term total cost of the project. Recently, the fundamentals of such a basic design were outlined (USBR, 1977). Among other things,

- a. "The slopes of the embankment must be stable during construction and under all conditions of reservoir operation, . . ." and,
- b. "Seepage flow through the embankment, foundation, and abutments must be controlled so that no internal erosion takes place and so there is no sloughing in the area where the seepage emerges."

(USBR, 1977, p. 210).

Thus, it is clear that the ability to accurately predict the stress-deformation and pore pressure response of an earth dam during all stages of its working life would be invaluable in such an undertaking. However, this is an extremely complex task. Where justified, numerical analyses, such as those employing the finite element method, can be used as a guide to engineering judgment. In particular, interest has recently been focussed on the performance of earth dams upon first filling of the reservoir. Kulhawy and Gurtowski (1976) discuss the results of a parametric study to determine the relative effect of certain factors on the potential for hydraulic fracturing. Seed et al. (1976) have conducted a finite element analysis to determine the stress state within the Teton Dam in an attempt to elucidate the causes leading to its failure. For this reason, the following discussion concerning the predicting of earth dam behaviour will be restricted to the periods of construction and first filling of the reservoir.

The major steps in any such analysis are:

- a. the selection of an appropriate model, or models, to represent the stress-strain behaviour of the material within the dam,
- b. the determination of input parameters including constitutive moduli, and
- c. the interpretation of the results.

1.3 Description of Two Constitutive Models

Of special interest here is the manner in which the stress-strain characteristics of the material comprising the dam are portrayed. Therefore, in the following paragraphs, two constitutive models will be described. One of these, that developed by Duncan and Chang (1970), appears widely in the literature, especially in North America (Duncan et al., 1978; Seed et al., 1975). The other, drawn from recent work (Chang, 1976), is more complex, involving the concepts of elastoplasticity. It is felt that this summary constitutes an adequate representation of the current level of sophistication among such models and will provide the basis for a discussion, later in the chapter, of their predictive capabilities.

In the first method referred to above, the dam is constructed in steps. During the placement of each new layer, every element's behaviour is governed by a two dimensional, linear constitutive relationship in which only normal stresses produce normal strains and, similarly, only shear stresses produce shear strains. The constitutive moduli are expressable in terms of stress level dependent

pseudo-elastic parameters derived from the results of triaxial tests appropriate to the problem under consideration (Duncan et al., 1978). It is assumed that the problem is one of plane strain. A similar formulation can be employed during the simulation of behaviour upon reservoir filling.

In seeking a versatile constitutive relationship for compacted soil Chang (op. cit.) adapted the work of researchers at Cambridge University on remoulded soils.

The soil is modelled as an elastoplastic work hardening material. On loading, both elastic and plastic strains may occur. A composite yield surface governs the plastic behaviour once it has been assumed that an associated flow rule is followed. When unloading takes place all deformation changes are elastic. Finally, at failure, the effective stress state is assumed such as to satisfy a linear relationship involving mean and deviatoric effective stress invariants.

1.4 Requirements of the Models

In evaluating a particular constitutive model, one is concerned chiefly with its predictive capability and that required. The latter is determined by, among other things, uncertainties introduced through construction practice and control and, for present purposes, the complexity of the expected stress deformation paths followed at points within the dam during construction and first filling of the

reservoir. The nature of these loading paths is reviewed briefly in the succeeding paragraphs. Although important, considerations of construction practice and control will not be dealt with explicitly.

An idealized example, due to Wilson (1977), shown in Figures 1.1 and 1.2, illustrates the form of the deformations occurring within an earth dam during construction and first filling of the reservoir. It would then seem reasonable, considering as well any variation in material stiffness throughout the dam, that one should expect an accompanying pattern of stress changes of some complexity. Evidence in support of this position can be found in the work of, among others, Penman and Charles (1979), Kulhawy and Gurtowski (1976) and Squier (1970). The possibility of stress transfer between core and shells due to varying material stiffnesses is well known. In discussing the processes ongoing during reservoir filling, Nobari and Duncan (1972,a) note the imposition of water loads on the upstream foundation and the upstream core-shell interface. This would be accompanied by a reduction in effective stress in the upstream shell due to buoyancy effects (Nobari and Duncan, *op. cit.*). Within the core, one might expect a marked reorientation of principal stress increments. Data drawn from the publications of Nobari and Duncan (1972,b) and Stewart (1979) support this hypothesis.

Thus, the basic framework of the two constitutive models has now been discussed and the nature of the

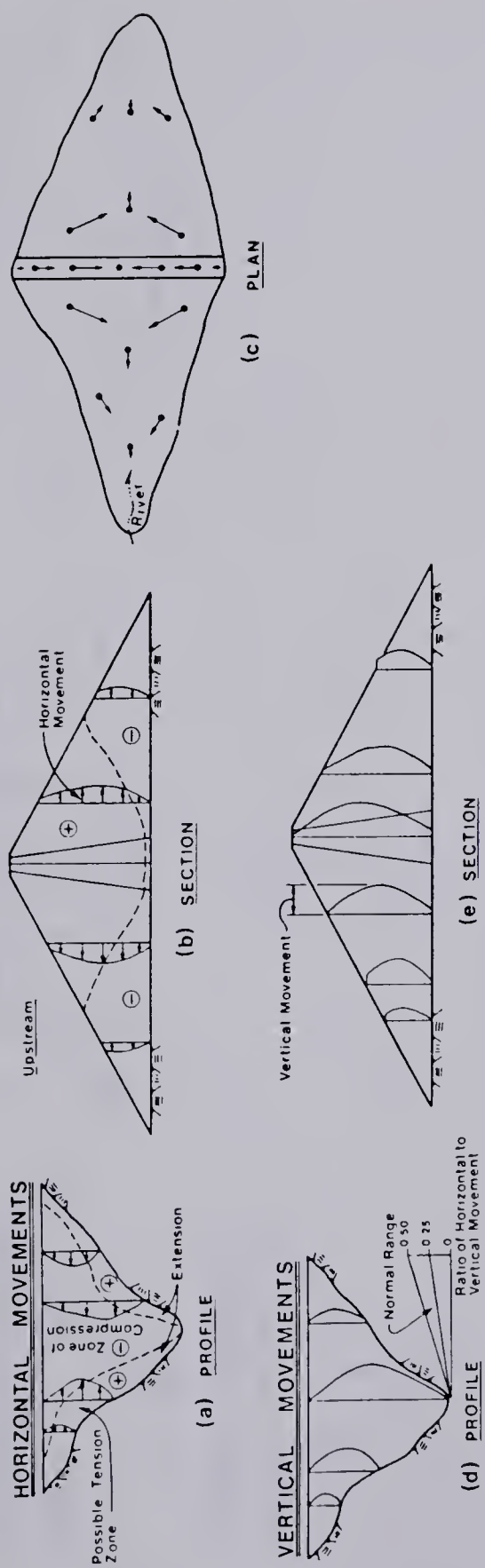


Figure 1.1 Movements During Construction Period
(after Wilson, 1977)

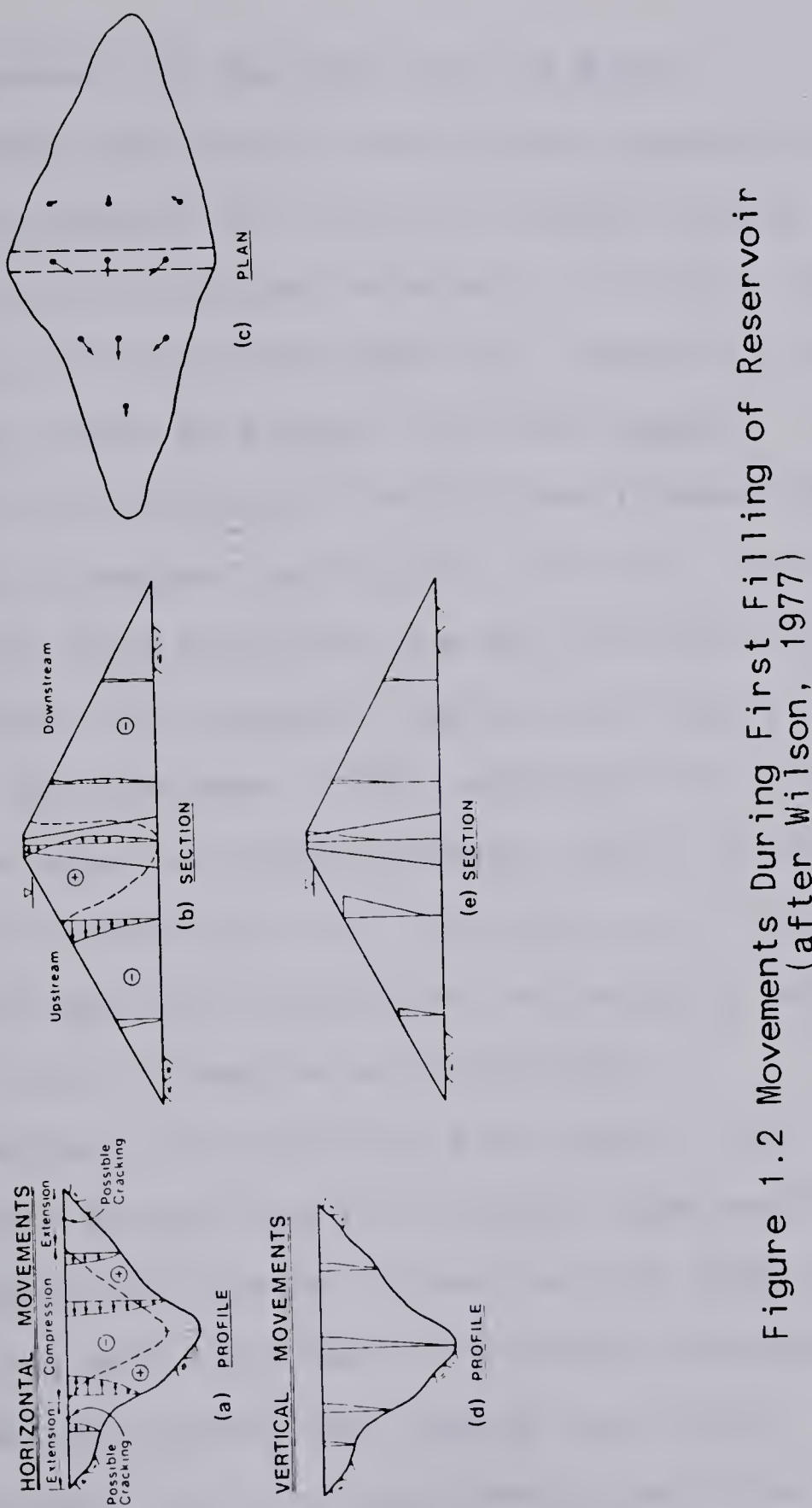


Figure 1.2 Movements During First Filling of Reservoir
(after Wilson, 1977)

processes to be modelled reviewed. With this information in mind, an evaluation of their suitability follows.

1.5 Assessment of Two Constitutive Models

Duncan and Chang's formulation represents a practical, reasoned approach to the task of modelling soil behaviour during construction and reservoir filling. This, as well as the ease with which the empirical parameters can be obtained, serve to explain its wide appeal. However, the simplifications implicit in its development must be borne in mind when interpreting results. Further, to the author's knowledge, pore pressures are not predicted as part of such an analysis; for example, the work of Seed et al. (1976), Kulhawy and Gurtowski (1976) and Nobari and Duncan (1972,b).

The model utilized by Chang (1976) is more rigorous and complete in form than the previous one, although the necessary empirical parameters are equally easy to obtain. As well, pore pressures are predicted.

However, in evaluating its capabilities, attention was restricted to the case of triaxial, compressive, loading. It would be of interest to see how the model would fare in predicting soil behaviour, including pore pressures, under different but controlled loading conditions. Also, for the dam analysed, no field measurements were then available for comparison, although good agreement was found with the limited results of a nonlinear hyperbolic analysis, for the case of steady seepage, presented. Thus, more evidence of

the usefulness of the model under the just mentioned conditions would be desirable.

1.6 Need for Further Research

On the basis of the preceding paragraphs, it is felt that research in the area of simple shear testing of compacted soil would be of value. The reasons are :

- a. the experimental data would be of interest in an attempt to better understand the nature of soil behaviour, within the core of an earthdam, during reservoir filling; specifically the interrelationship of applied shear stress, shear strain and pore pressure
- b. such data would also allow a more complete verification of a general elastoplastic model for compacted soil.

To date, little has been published dealing with the effect of the continuous rotation of principal stress increments on the material behaviour of compacted clay. As far as is known, there is only one paper on the subject (Thurner, 1973); few results are given, emphasis being placed on a description of the testing apparatus and experimental procedure.

1.7 Aims of Thesis

The aims of the present research work are then twofold:

- a. to design and build a simple shear apparatus suitable for testing samples of compacted soil at elevated pressures, and
- b. to demonstrate, by comparing experimental and expected results, that the data derived from such tests are meaningful.

1.8 Contents of Thesis

The contents of the remaining chapters are as follows:

Chapter 2 - the factors determining the selection of the particular simple shear apparatus used for the present study

Chapter 3 - a description of the simple shear apparatus

Chapter 4 - the presentation and discussion of experimental results

Chapter 5 - conclusions and recommendations for further research.

Appendices A, B and C deal with calibration of the apparatus and procedures for sample preparation and testing.

CHAPTER 2

COMPARISON OF CERTAIN SIMPLE SHEAR APPARATUS

2.1 General

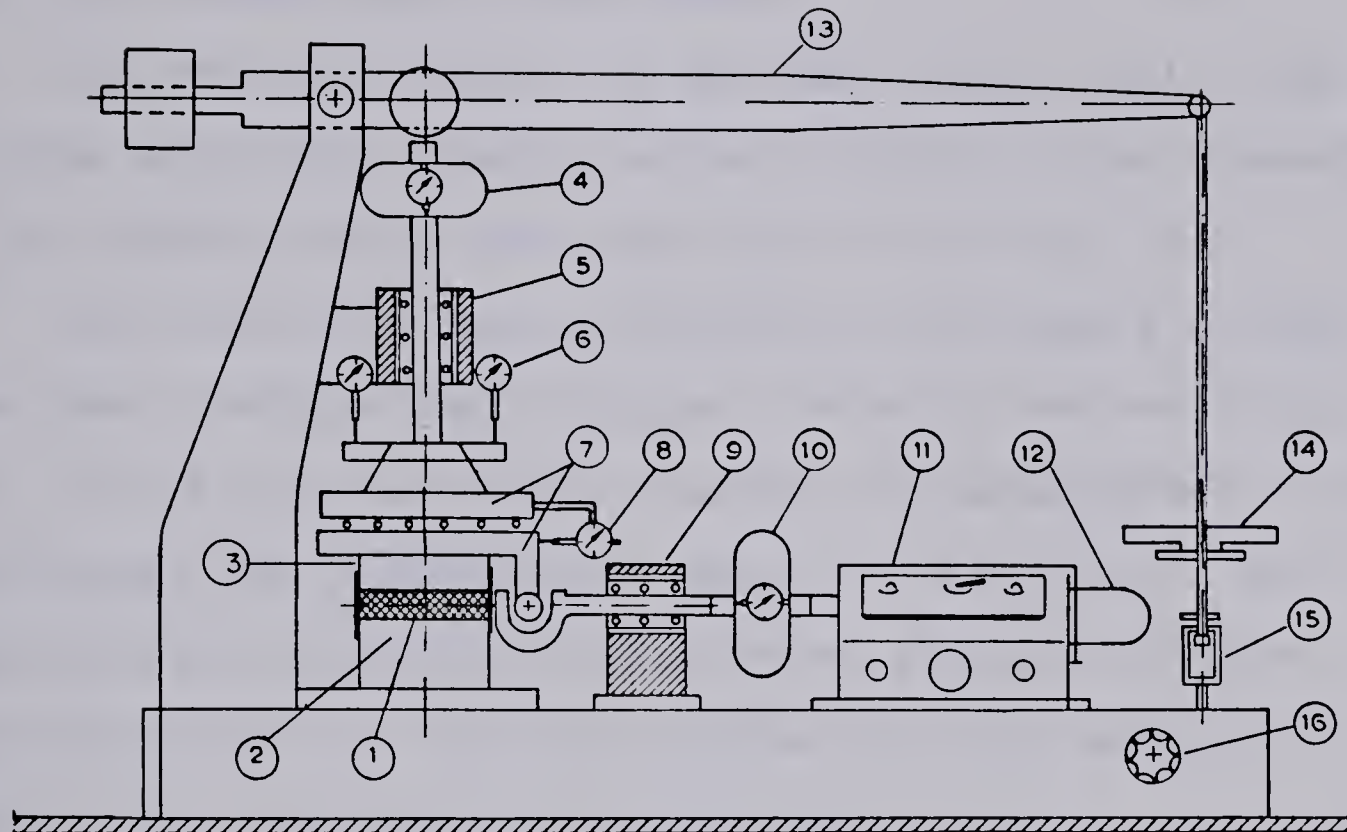
The two main types of simple shear apparatus are discussed briefly. Emphasis is placed on the nature of accompanying sample preparation, apparatus assembly and test procedure, as well as the physical quantities that can be measured during each type of test. The relative merits of each apparatus are discussed. To conclude, the choice of an appropriate apparatus is made and an outline is presented of the accompanying analytical scheme for treatment of the experimental data.

2.2 NGI Apparatus

The NGI simple shear apparatus employed by Bjerrum and Landva (1966) is a further development of that presented by Kjellman in 1951.

2.2.1 Description of Apparatus

Figure 2.1 presents a sectional view of the device. The sample tested is 8 cm in diameter and may range from 1 to 2 cm in height. It is encased in a rubber membrane reinforced with a spiral winding of wire. Ideally, the role of the reinforced membrane is to maintain a condition of no lateral strain in a horizontal plane; more will be said of this later. During a test, the upper platen (3, Fig. 2.1) is



Legend

- 1 Sample and membrane 2 Pedestal 3 Upper Platen 4 Load gauge for vertical load
 5 Ball bushing 6 Dial gauges for measurement of vertical deformation 7 Load cap,
 Upper and Lower 8 Dial gauge for measurement of horizontal deformation 9 Ball
 bushing 10 Load gauge for horizontal force 11 Gear box 12 Exchangeable servogear
 motor 13 Lever arm 14 Weights 15-16 Clamping and adjusting mechanism used for
 constant volume tests

Figure 2.1 NGI Simple Shear Apparatus
 (after Bjerrum and Landva, 1966)

connected to the lower load cap (7, Fig. 2.1). The lower load cap can slide independently of the upper one, being separated by roller bearings. However, vertical load may still be transmitted to the sample.

The vertical load on the specimen can be controlled by a screw controlled loading mechanism which can be connected to the loading rod of the lever arm (15, 16, Fig. 2.1).

The horizontal load is applied to the sample through the lower load cap and the upper platen by the horizontal ram. For strain controlled loading, the displacement of the horizontal ram is guided by a motor (12, Fig. 2.1). The apparatus can also be used to conduct stress controlled tests but this will not be discussed here nor are the appropriate components shown in Figure 2.1.

The vertical and horizontal loads acting on the sample are measured using load gauges (4, 10, Fig. 2.1). Dial gauges (6, 8, Fig. 2.1) indicate the vertical and horizontal deformation which the upper platen and, presumably, the upper surface of the sample have undergone.

The apparatus may be used to perform drained and constant volume tests on specimens strained, approximately, in simple shear and plane strain. The model of the NGI apparatus used by Ladd et al. (1972) was able to apply a maximum vertical load of 7845 N and maximum horizontal load of 3925 N to the sample. The area of the sample was 50 square centimetres. Further, it was able to test soft clays, stiff clays, silt and sand. The membranes used by

Ladd et al. were of two kinds; one reinforced by constantan wire, the other by stainless steel suture thread. The former could withstand a maximum horizontal stress of 1.8 kg/sq cm, the latter could be subjected to a maximum horizontal stress of 5 kg/sq cm.

In preparing for a test, the sample is mounted on the pedestal (2, Fig. 2.1) and encased in a reinforced membrane with the upper platen positioned as required. To begin a test, the sample can be consolidated simply by adding weights to the lever arm (14, Fig. 2.1). The change in height of the sample is noted by observing the change in the appropriate dial gauge readings (6, Fig. 2.1).

After consolidation, a drained shear test can be run by leaving the vertical load, acting on the sample, untouched and imposing a horizontal displacement on the upper platen, at a desired rate.

The rate would be such as to allow complete dissipation of pore pressures during the shearing process. Measurements are taken of the horizontal load, horizontal deformation and vertical deformation. Berre (1969) notes the use of constantan wire reinforced membranes as "strain gauges" to get an indication of the value of the radial stresses acting in the sample during a test. This technique has been utilized in more recent work by, for example, Wood and Budhu (1980) among others.

Bjerrum and Landva (1966) state that due to difficulties in the prevention of drainage, undrained simple

shear tests were conducted as constant volume tests. During such tests, drainage from the sample was permitted, the rate of application of shear strain being such as to allow dissipation of pore pressures and the vertical load acting on the sample was altered so that the height of the sample remained constant. Given that the reinforced rubber membrane maintained the perimeter of the sample constant, its total volume remained constant as in an undrained test. The change in vertical stress required to maintain the volume constant was then interpreted as equal in magnitude but opposite in sense to the change in average pore pressure that would occur in a truly undrained test under constant total vertical normal load. Bjerrum and Landva (1966) indicate that this hypothesis was verified by conducting a truly undrained simple shear test in which the pore pressure was measured at the base of the specimen.

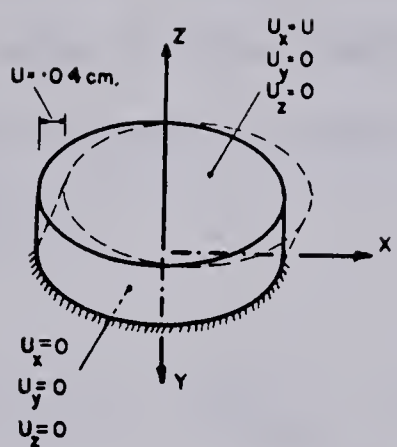
2.2.2 Stress State in NGI Apparatus

In determining the stress state within the NGI apparatus it is best to begin by establishing the boundary conditions. The upper and lower horizontal surfaces of the sample are assumed to remain planar and parallel to one another during shear. Each point on the upper surface is assumed to undergo the same displacement relative to the lower surface of the sample which is taken as remaining fixed. The boundary condition on the side of the sample is really one of constant perimeter (Wood and Budhu, 1980).

However, for the purposes of finite element analysis other, more approximate, conditions are chosen.

Lucks et al. (1972) conducted analyses of a sample of dimensions identical to those used in NGI simple shear devices at that time. The samples were assumed to be representable by an isotropic, linearly elastic solid and to undergo infinitesimal strains. Two analytical methods, each employing the finite element method, were used. The first employed three dimensional solid parallelepiped elements with nodes at each of the eight corners. The second, less rigorous, utilized a formulation for axisymmetric bodies unsymmetrically loaded. Plane elements expanded in a Fourier series about the axis of the sample were used. More information on these finite element formulations can be found in the paper by Lucks et al. and those to which they refer.

The sample analyzed was 8 cm in diameter and 2 cm high. The isotropic, elastic properties were Young's modulus 200 kg/sq cm and Poisson's ratio .49. The boundary conditions were largely as outlined before; the horizontal surfaces of the sample remained parallel and at a constant distance from each other. However, the side of the sample was allowed to deform freely. Figures 2.2 and 2.3 indicate the boundary conditions and the idealized finite element mesh for the sample of the rigorous analysis. In the Fourier series analysis, an initial vertical consolidation stress of 1 kg/sq cm and horizontal consolidation stress of .5 kg/sq cm



Note: displacements specified are boundary conditions.

Figure 2.2 Boundary Conditions for Three Dimensional Analysis
(after Lucks et al., 1972)

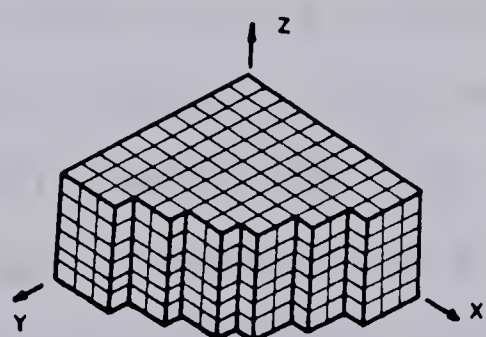


Figure 2.3 Finite Element Mesh for Three Dimensional Analysis
(after Lucks et al., 1972)

were assumed.

The results of the rigorous three dimensional analysis are presented in Figure 2.4. Were complementary stresses assumed to act on the side of the sample, such imposed horizontal boundary displacements would result in a uniform shear stress of magnitude

$$\tau = \frac{\gamma E}{2(1+\nu)} = \left[\frac{.04}{2} \right] \frac{200}{(1+.49)2} \text{ kg/cm}^2 \quad 2.1$$

$$= 1.34 \text{ kg/cm}^2 (131 \text{ kPa})$$

One can see by study of the figure how uniform the induced shear stress state is.

Lucks et al. (1972) note that the results of the two analyses agree quite closely. Figure 2.6 presents the variation of the vertical normal stress through different sections of the sample, yielded by the Fourier analysis. The axis with respect to which θ is measured is shown in Figure 2.5(b). It lies along a diameter of the specimen and parallels the line of action of the shear load. Thus, for the layer of elements portrayed, the nonhomogeneities in vertical stress reach a maximum for $\theta = 0^\circ$ (parallel to the shear load) and vanish for $\theta = 90^\circ$. Note, similarly, the variation in radial stress with both elevation and angular position within the sample.

As noted by Roscoe (1953), if no complementary shear stresses are provided on the side of the circular sample

X									
1.35	1.35	1.35	1.36	1.36	1.37	1.38	1.38	1.29	0.84
1.35	1.35	1.35	1.36	1.37	1.37	1.38	1.37	1.31	0.79
1.35	1.35	1.35	1.36	1.37	1.38	1.39	1.37	1.27	0.88
1.35	1.35	1.36	1.36	1.37	1.38	1.38	1.36	0.97	
1.35	1.36	1.36	1.36	1.38	1.38	1.37	1.27	0.84	
1.35	1.36	1.36	1.36	1.38	1.36	1.35	0.97		
1.36	1.36	1.37	1.35	1.39	1.35	1.26	0.86		
1.36	1.36	1.38	1.35	1.31	1.45	0.97			
1.38	1.37	1.30	1.46	0.99					
1.42	1.39	1.02							

(a) SHEAR STRESS ALONG HORIZONTAL PLANE AT MID - HEIGHT

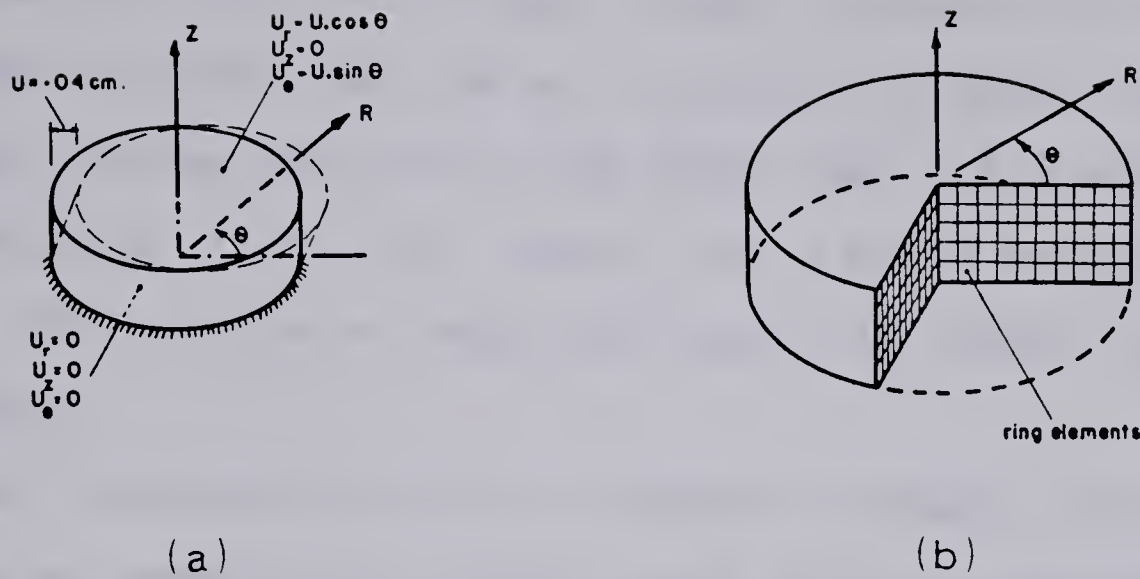
Z									
1.34	1.34	1.33	1.33	1.32	1.31	1.30	1.23	1.29	1.31
1.34	1.34	1.34	1.35	1.35	1.35	1.35	1.34	1.31	1.00
1.35	1.35	1.35	1.36	1.36	1.37	1.38	1.38	1.29	0.84
SYMMETRIC									

(b) SHEAR STRESS FOR POINTS IN A - A SECTION

Z							
1.33	1.33	1.33	1.32	1.31	1.29	1.28	1.25
1.35	1.35	1.35	1.35	1.35	1.33	1.34	1.08
1.35	1.36	1.36	1.36	1.38	1.36	1.35	0.97
SYMMETRIC							

(c) SHEAR STRESS FOR POINTS IN B - B SECTION

Figure 2.4 Results of Three Dimensional Analysis
(after Lucks et al., 1972)



Note: displacements specified are boundary conditions.

Figure 2.5 Boundary Conditions and Finite Element Idealization for Fourier Analysis
(after Lucks et al., 1972)

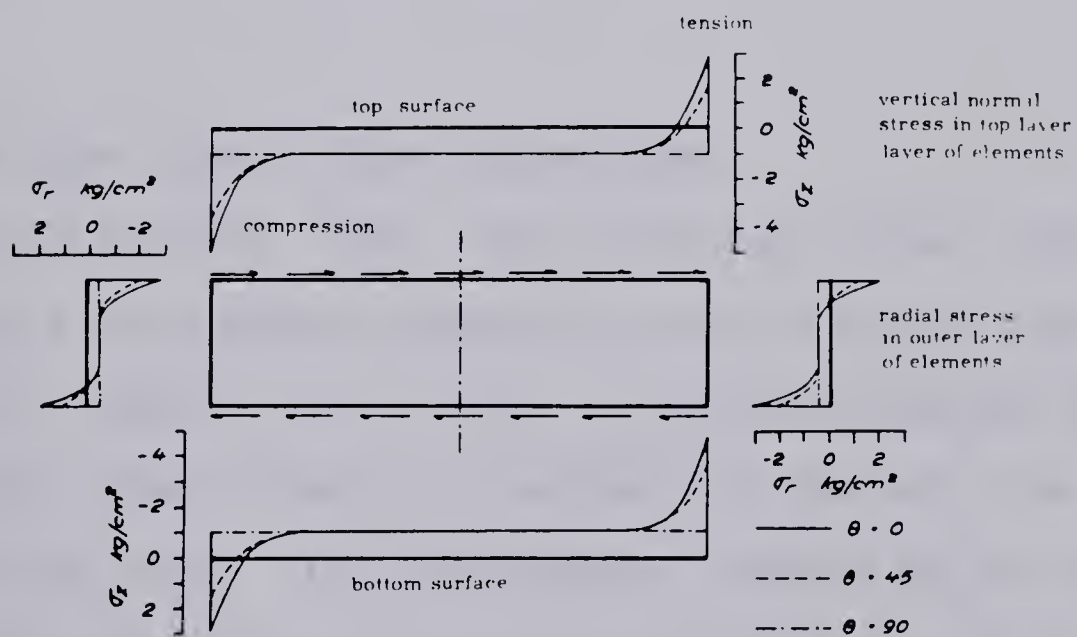


Figure 2.6 Results of Fourier Analysis
(after Lucks et al., 1972)

then the distribution of shear stress increments upon an increase in shear load can not involve only those components of shear stress parallel to the shear load. For example, on the perimeter of the soil sample, for a given horizontal plane, the traction at each point must lie tangent to the perimeter.

Any tendency for relative movement between the soil sample and pedestal or platen, where such is inhibited, is likely to cause some degree of stress transfer, rendering the stress state within the sample more complex. In this regard, the interaction of the soil sample and wire wound membrane is of interest. Such an enhanced nonhomogeneity of stress state would also be expected upon actual, but nonuniform, slippage between the soil sample and pedestal or upper platen (Prevost and Hoeg, 1976).

2.3 Cambridge Simple Shear Apparatus

To the present time, there have been seven different models of simple shear apparatus constructed at Cambridge University (Wood et al., 1979). The basic design of the three most recent models is markedly different from that of the previous ones. The deformation imposed on the sample is more uniform and allows measurement of sufficient boundary loads that the magnitudes and directions of the principal stresses can be determined independently of the principal strains at all stages of a test (Roscoe et al., 1967).

The mark 7 apparatus contains certain improvements over previous models (Roscoe, 1970). However, it is sufficient, for present purposes, to discuss the mark 6 model (Roscoe et al., 1967).

2.3.1 Description of Mark 6 Model

Figure 2.7 presents a sectional view of this apparatus. The sample (15, Fig. 2.7) is square in plan with a side length of 10 cm. The height of the sample is about 2 cm. It is surrounded by load cells designated by the letters a-h in the figure. Two other load cells may be positioned parallel to the plane of the figure to measure the load acting, on either side of the sample, in the normal direction, or they can be replaced by rigid sides transparent to X or γ -rays. The load cells a-h can measure the shear load and normal load acting on them as well as the eccentricity of the normal load.

The lower bearing plate is hinged to one end flap (7,5, Fig. 2.7). The other end flap (6, Fig. 2.7) is constrained to remain in contact with the right hand edge of load cell f, at all times, by a bearing. The lower bearing plate is bolted to the base plate which can move horizontally along rollers (8,10, Fig. 2.7). The rollers are supported by the loading frame base (11, Fig. 2.7).

The load cells a-c are mounted on the block (12, Fig. 2.7) fitting into the independent upper bearing frame. One end flap (6, Fig. 2.7) is hinged to this frame, which also

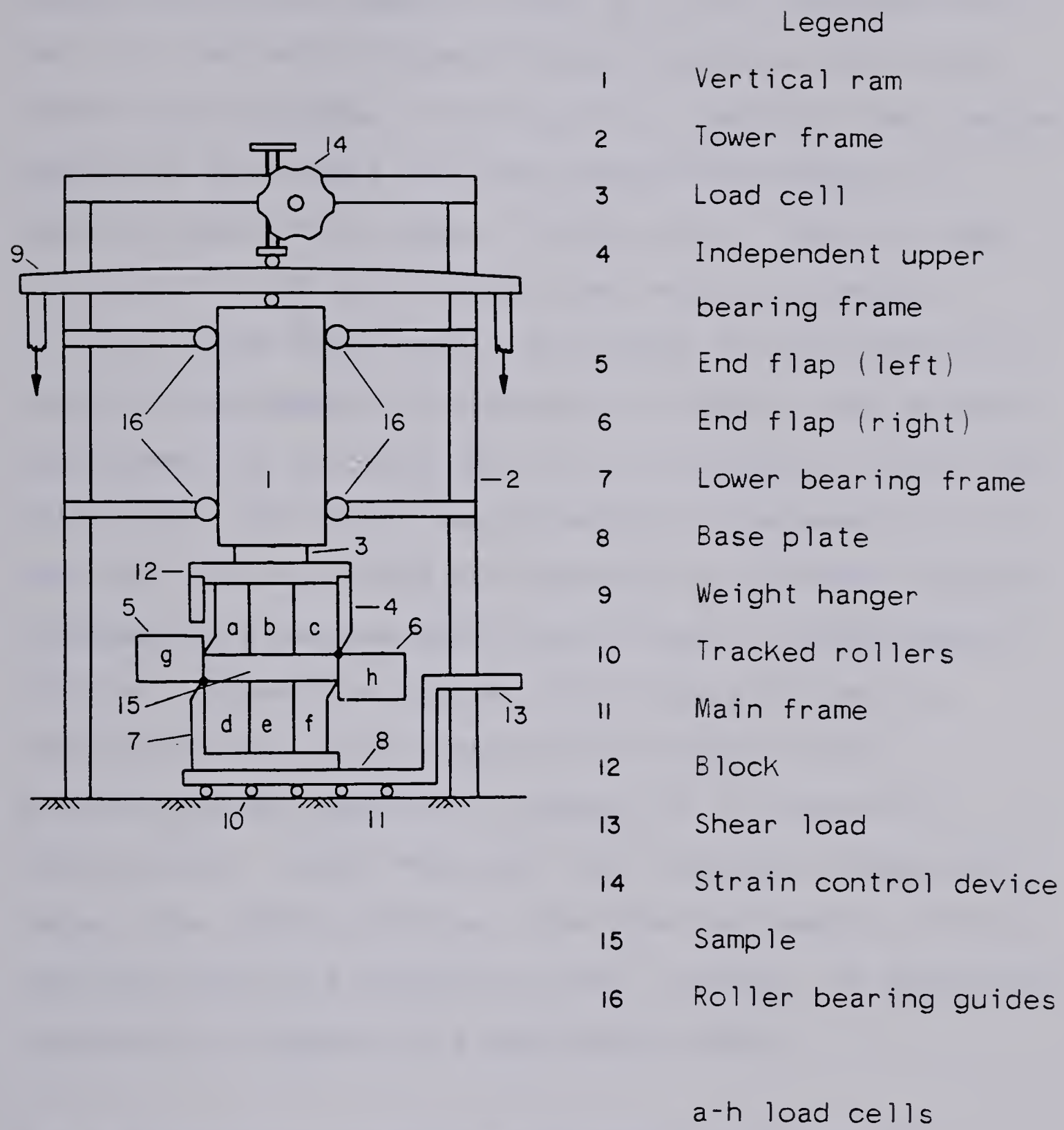


Figure 2.7 Mark 6 Simple Shear Apparatus
(after Roscoe et al., 1967)

guides the movements of the other (5, Fig. 2.7).

A load cell measures the total normal and shear load transmitted to the sample (3, Fig. 2.7). It is connected in turn to a ram which is constrained to move vertically by roller bearing guides (1, 16, Fig. 2.7). Vertical loads can be applied to the sample in stress controlled fashion by applying loads to the hanger (9, Fig. 2.7). There is also the capability of strain controlled vertical loading.

The strain state within the sample is calculated from external measurements of deformation; that is, the maximum displacement of the shear box in the horizontal and vertical directions. The instantaneous height of the sample is also measured. The apparatus was designed to withstand stresses accompanying a maximum mean normal stress of approximately 700 kPa. The maximum angular distortion which may be imparted to the vertical ends of the sample is 45°. Referring to the load cells labeled a-f in Figure 2.7, Roscoe et al. (1967) note that the clearance between them ranged from .004 to .005 cm. When testing samples of clay, the gaps could be filled with latex. However, no indication is given of an appropriate testing procedure.

2.3.2 Description of Simpler Cambridge Type Apparatus

A less complex form of the Cambridge type of simple shear apparatus was used by Dunlop et al. (1968) to test clays in the undrained state. The sample to be tested was 6 cm square and 2 cm high. The vertical sides of the sample

are surrounded by a rubber membrane attached to the upper and lower platens. In turn, they are in contact with the upper and lower horizontal surfaces of the sample respectively. The membrane is surrounded by metal walls. With the application of shear load to the sample, the upper platen can move both vertically and horizontally. At all times, it remains parallel to the lower platen. As the upper platen moves horizontally, the end walls rotate to impose, in a gross sense, a state of simple shear deformation. Vertical loads can be applied to the sample. For the particular suite of tests described by Dunlop et al. (1968), the horizontal loads were applied in a strain controlled manner. Lateral normal loads, those acting on the vertical walls of the apparatus, were not measured. Prior to a test, the samples were consolidated one-dimensionally, being subjected to a pressure greater than their previous overburden pressure. Since the top cap in the simple shear device had a rather restricted range of travel, consolidation was carried out in a large consolidometer. After this, the samples were trimmed to the appropriate dimensions and installed in the simple shear device.

Further consolidation of the sample was then initiated to insure that it was properly seated and normally consolidated under the desired pressure. A back pressure was applied to make sure that the specimens were fully saturated.

Upon completion of the final phase of consolidation, with further drainage from the sample prevented, a shear load was applied to the sample at an average rate sufficient to cause failure within 1.25 to 3.75 hours. It is noted that, with failure occurring during this length of time, the estimated degree of equalization of non uniform pore pressures ranged from 92% to 98%.

2.3.3 Stress State in Cambridge Type Apparatus

In trying to determine the approximate nature of the stress state within an early model of the simple shear apparatus, Roscoe (1953) assumed the soil to be isotropic and linearly elastic. The boundary conditions were as outlined in Figure 2.8, where u denotes the horizontal deformation, v the vertical deformation, κ the angle of shear and τ the shear stress, all referred to the coordinate axes shown. The problem is two dimensional in nature with the sample being six units long and two units high. From the diagram, it can be seen that no vertical load has been applied to the sample; the case analysed is one of undrained shear. Poisson's ratio is assigned a value of one half.

The solution can be expressed in the form of an infinite series with the constants being determined by fitting them to the above mentioned boundary conditions. In discussing the results of the stress analysis, Roscoe (1953) noted the following:

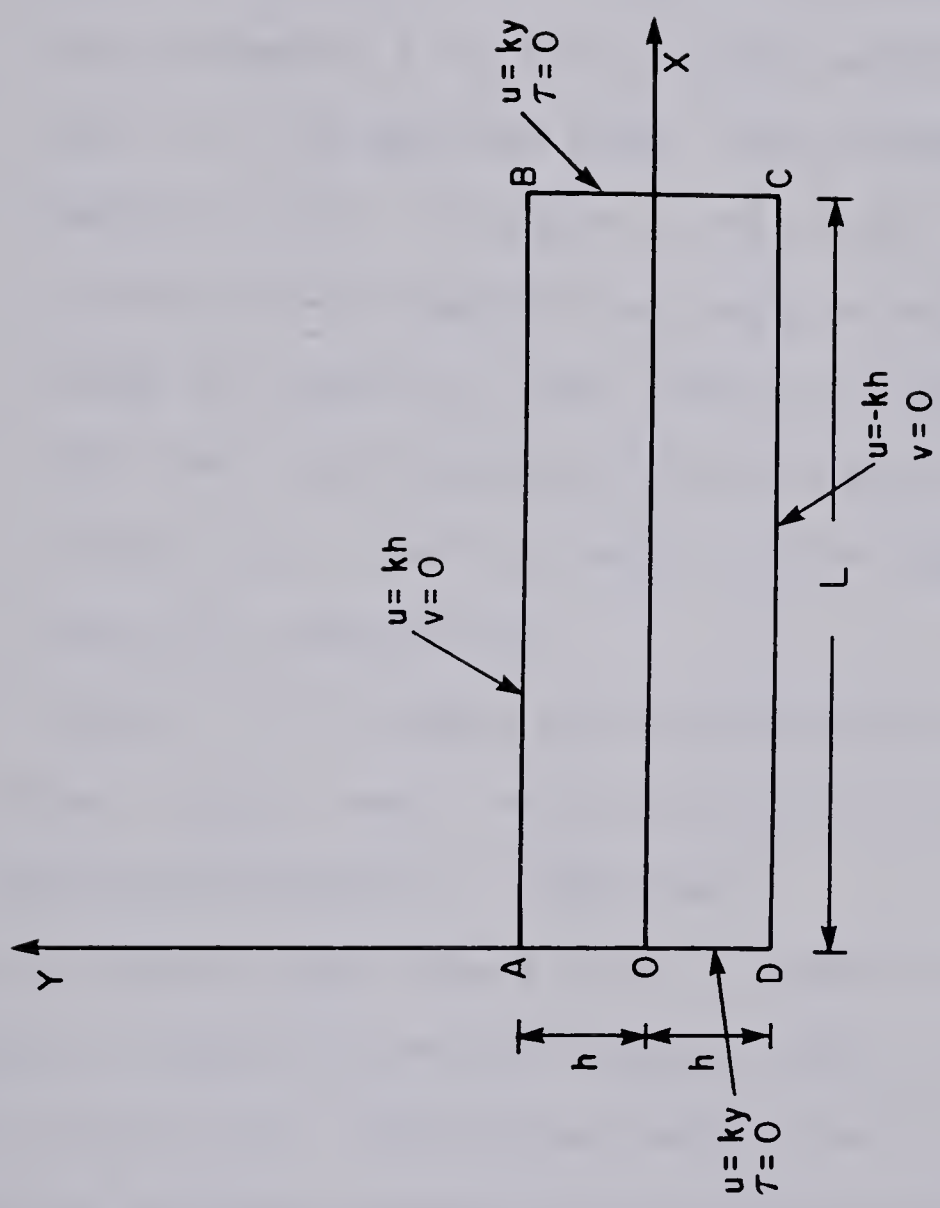


Figure 2.8 Boundary Conditions for Roscoe's Analysis
(after Roscoe, 1953)

- a. the vertical normal stress, σ_y , is zero for all values of x along the horizontal centerline of the sample ($y=0$)
- b. over the upper and lower surfaces of the sample the distribution of the vertical normal stress is nonuniform. The computed variation of σ_y over the upper surface of the sample is given in Figure 2.9. The parameter s is the average applied shear stress, that is, the applied shear load divided by the sample's area. The variation of σ_y along the lower surface of the sample is simply a reflection of that along the upper surface, about the abscissa.
- c. that the distribution of the horizontal normal stress, σ_x , over the ends of the sample is similarly nonuniform.

In Figure 2.9 is shown the distribution of normalized shear stress, τ_{xy}/s , over the top surface of the sample; that over the bottom surface is identical.

In a recent paper, Wood et al. (1980) discuss a procedure for determining the stress state in the central region of the latest Cambridge simple shear apparatus. It is based on the measurements of the load cells that bound the sample. Further, a method is advanced for ascertaining the complete stress state in simpler forms of the apparatus where only the total shear and normal loads applied to the sample are measured. However, as yet, the latter approach is restricted to sands.

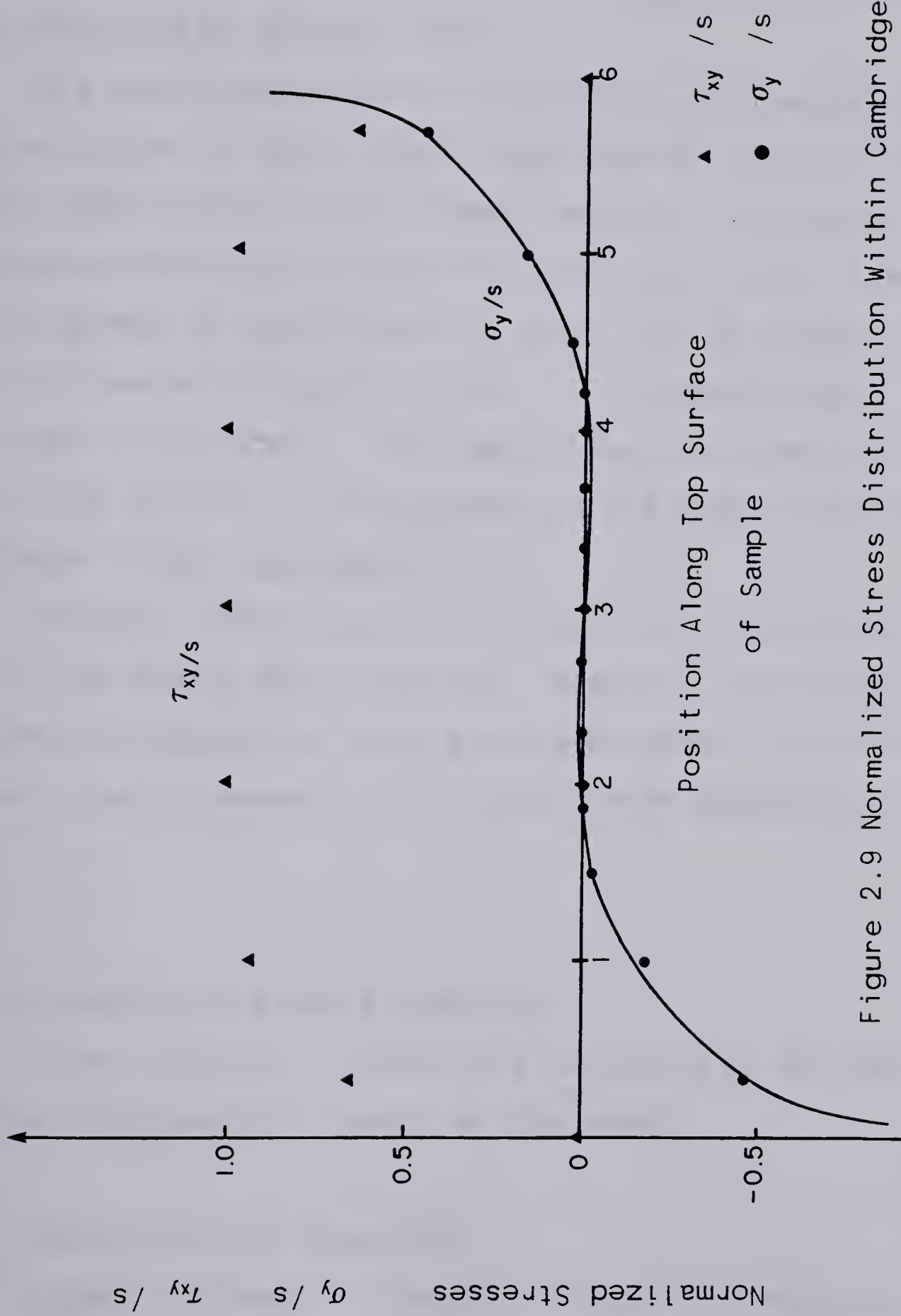


Figure 2.9 Normalized Stress Distribution Within Cambridge Apparatus
(after Roscoe, 1953)

An example of the stress state on the boundary of a medium loose sample of sand tested in the mark 6 apparatus is given by Roscoe et al. (1967). It is similar in form to that predicted by Roscoe (1953).

In studying the nature of the stress state existing in samples tested in their simple shear device, Dunlop et al. (1968) employed the finite element method. The material response was modelled as nonlinear and anisotropic. Details of the method of determining the moduli can be found in the paper by Duncan and Dunlop (1969) or, in greater detail, in the report cited above. The imposed boundary conditions were quite similar to those used in the analysis conducted by Roscoe (1953); see page 27.

No graphs indicating the uniformity of the stress state within the sample were presented. However, the related problem of progressive failure was considered. Its effect on test results depends upon the post peak behaviour of the soil.

2.4 University of Alberta Apparatus

In this section, a possible alternative to the two devices discussed previously is introduced.

2.4.1 Description of Apparatus

Figure 2.10 shows a schematic view of the apparatus. The sample to be tested is circular in plan and encased in a conventional latex membrane. The upper platen (5, fig. 2.10)

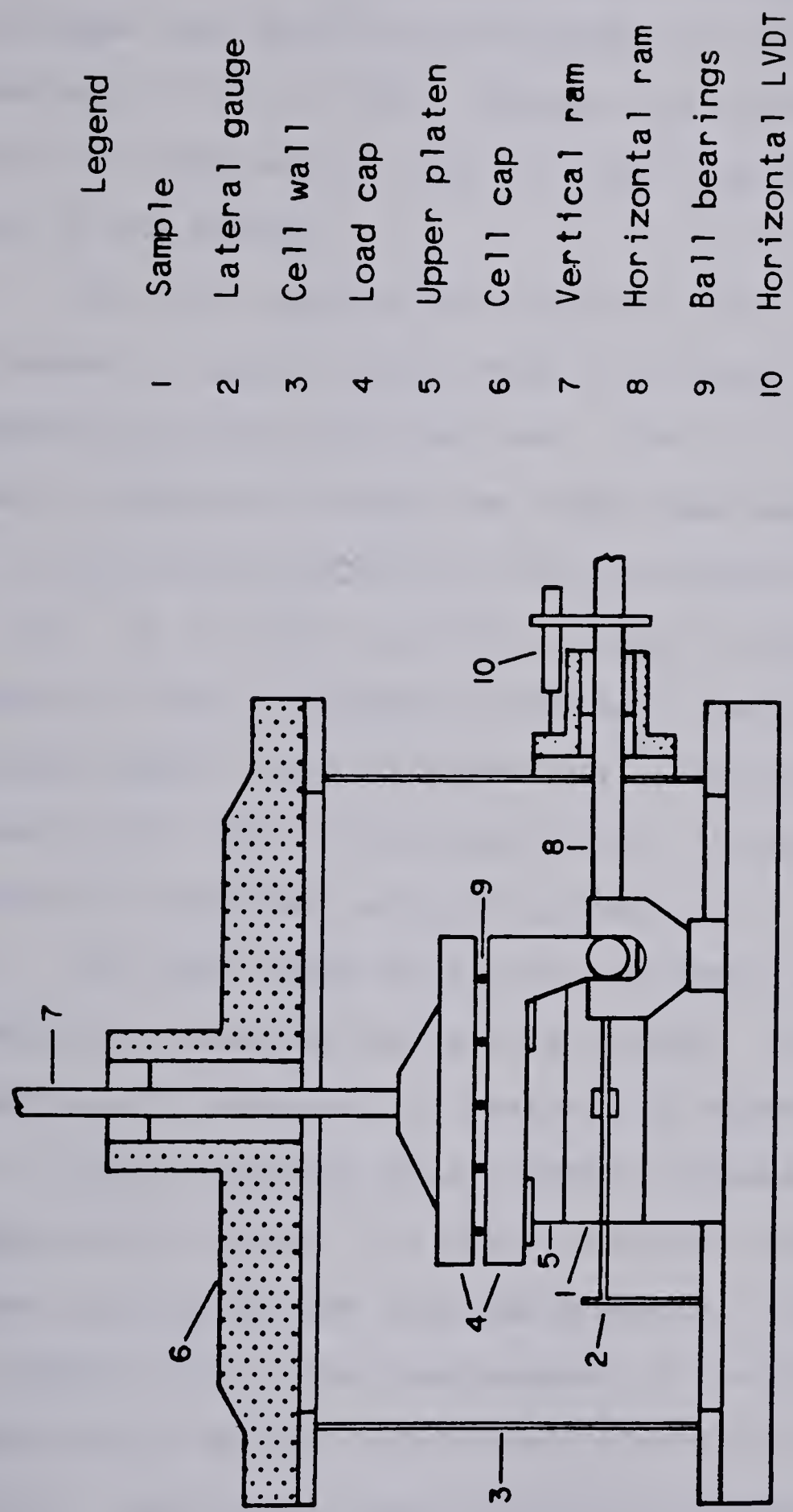


Figure 2.10 Sectional View of U of A Apparatus

is connected to the loading cap assembly by means of a pair of collars. The lower load cap can slide independently of the upper one due to the presence of a layer of ball bearings (9, Fig. 2.10). However, as can be seen, any vertical compressive load will still be transmitted from the ram to the sample.

Vertical load can be applied to the sample by means of a pneumatic jack or Bellofram, not shown in the figure, connected to the vertical ram. Similarly, horizontal load can be applied, through the lower load cap and upper platen, by a Bellofram connected to the horizontal ram (8, Fig. 2.10). It is also possible to apply a cell pressure to the sample. Fins, embedded in the soil sample on its top and bottom faces, allow transmission of the shear load to the sample and, then, to the cell base. Stress controlled tests would be conducted using this apparatus.

The rams' loads acting on the upper surface of the sample are measured using load gauges. The lateral load, due to cell pressure, is measured by means of a transducer.

Linear variable displacement transducers (LVDT's) are used within the cell to detect vertical movement of the lower section of the load cap assembly. These are not shown in Figure 2.10. The displacement of the horizontal ram is measured by an LVDT positioned outside the cell (11, Fig. 2.10). The vertical and horizontal movements, just described, are assumed to be those of the upper surface of the sample as well. A lateral strain gauge (2, Fig. 2.10) is

used to detect any change in the length of a reference diameter. It is assumed that this measurement reflects the behaviour of all sample diameters. The pore fluid pressure is measured at the base of the sample, by means of a transducer.

The technology employed in this apparatus being conventional, it does not appear difficult to design one capable of withstanding relatively high pressures; on the order of 2800 kPa maximum working cell pressure. Both drained and undrained tests can be performed. The samples would be strained, approximately, in simple shear and plane strain.

The specimen is compacted in a split ring mould, then placed on the pedestal, the mould removed and the membrane positioned. The lateral gauge (2, Fig. 2.10) is then set up. With the horizontal ram (6, Fig. 2.10) in place, the cell wall can then be positioned and the partially assembled apparatus installed in the testing area proper. Next, the load cap assembly (4, Fig. 2.10) is attached to the upper platen (5, Fig. 2.10) and the cell cap (6, Fig. 2.10) fastened. Finally, the rams (7, 8, Fig. 2.10) are connected to load cells which are attached, in turn, to pneumatic rams or Belloframs. Various electrical lines taking the output from the measuring devices to an automatic recording unit can be connected at this time as well. The cell would then be filled with a nonconducting fluid not causing the degradation of latex membranes.

In running an undrained test, the sample is consolidated under conditions of no lateral strain; the diameter of the sample being maintained constant by an appropriate manipulation of one or both of the boundary loads. Back pressure can also be applied, through a line leading to the upper surface of the sample, if required.

After completion of the consolidation phase, increments of shear load are applied; the length of each being sufficient to allow equalization of excess pore pressures. Again, the boundary loads are altered, as required, to maintain the measured sample diameter constant.

At all times, pertinent data are recorded automatically.

2.4.2 Stress State in U of A Apparatus

The boundary conditions to be used for a stress analysis of the sample subject to shear loading are similar to those of Lucks et al. (1972) mentioned previously. Upon shear loading each point on the upper surface of the sample is assumed to experience an identical horizontal displacement, the horizontal surfaces of the sample remaining parallel to one another. The, initially, vertical sides of the sample are not acted upon by a cell pressure.

To analyse the stress state in the sample simulating all phases of the loading sequence, one must model the interaction of the soil, upper platen and pedestal. The pedestal is taken to be identical in form to the upper

platen. It is then the exterior horizontal surfaces of the upper platen and "pedestal" to which the appropriate displacement boundary conditions are assigned. Along the vertical surfaces of the sample, platen and pedestal, force boundary conditions are imposed. These conditions are depicted graphically in Figure 2.11. The complete sample was not analysed; the section considered was the one passing through the axis of the sample and parallel to the line of action of the applied shear load. It corresponds to the $\theta = 0^\circ$ section of Lucks et al. (1972). A two dimensional, plane strain, linear elastic analysis was run. That the $\theta = 0^\circ$ section deforms under conditions of plane strain follows from the symmetry of the loading condition and sample itself about that plane.

For an assumed vertical stress of σ_v within the soil sample, the required horizontal stress, to be applied on the vertical faces of the sample is:

$$\sigma_H = \left[\frac{\nu}{1-\nu} \right] \sigma_v = K_o \sigma_v \quad 2.2$$

where ν is Poisson's ratio. The vertical displacements to be imposed on the exterior horizontal surface

horizontal force
calculated from
cell pressure

horizontal deformation determined from shear load
vertical deformation determined from vertical load

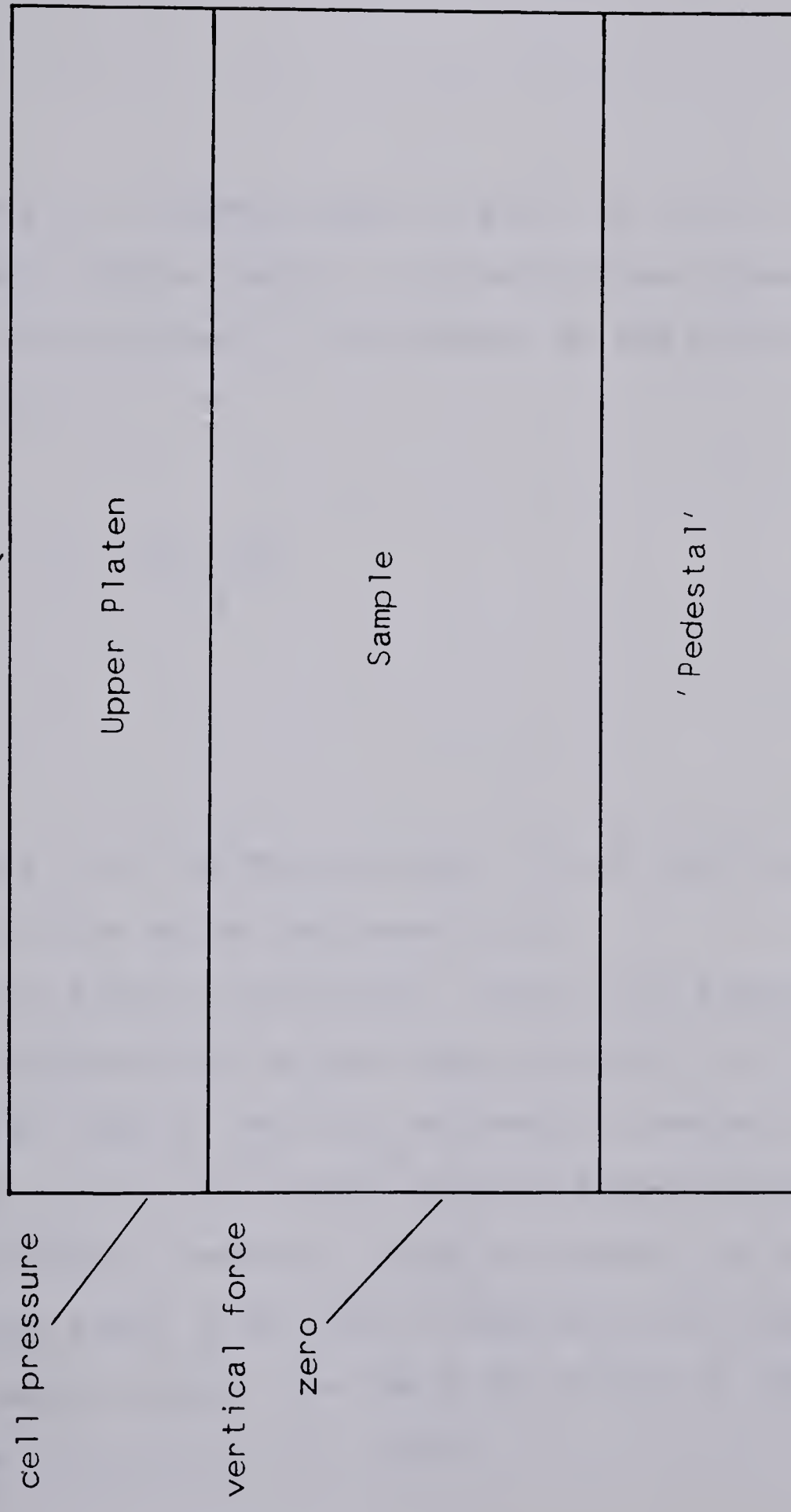


Figure 2.11 Representation of Platen-Sample-Pedestal System

of the upper platen are:

$$v = \left[\frac{\sigma_v}{E} \right] [1 - 2\nu K_o] h \quad 2.3$$

where E is Young's modulus and h is the initial height of the soil sample; both in appropriate and compatible units. The horizontal displacement of the platen's upper surface is:

$$u = \frac{2\tau [1 + \nu] h}{E} \quad 2.4$$

where τ is the desired shear stress and the other parameters are as defined previously.

Given a set of analytical results and assuming that the normal loads applied to the sample (whether in the form of horizontal load or vertical deformation boundary conditions) are such as to avoid stress transfer between the sample and upper platen or "pedestal", one can assess the uniformity of the stress state in vertical planes passing through the axis of the sample, other than the $\theta = 0^\circ$ plane, by referring to the work of Lucks et al. (1972).

A parametric study was then conducted to determine a reasonable sample size. The comments that were made previously concerning the effects on stress state homogeneity of the cylindrical nature of the sample (page 21) and possible slippage between the sample and platen or pedestal (page 21) may be made once again.

2.5 Evaluation of Apparatus

In choosing an apparatus for this testing program, of particular interest are:

- a. the ease of construction of the apparatus
- b. the nature of sample preparation and apparatus assembly
- c. the complexity of the test procedure
- d. the physical quantities that can be determined and,
- e. the uniformity of the stress state.

As will have become clear by the discussion of the various potential apparatus, each has its shortcomings. However, for present purposes, the University of Alberta apparatus would appear suitable. In a mechanical sense, its design is relatively simple. Samples can be prepared using conventional techniques and slightly modified equipment. The membranes encasing the sample are easy to fabricate and position. Further, the apparatus can be used to run tests over a wide range of pressures. The test procedure might seem tedious, involving as it does the adjustment of boundary loads to maintain the reference diameter constant.

However, in a recent paper Franke et al. (1979) describe a servomechanism that accomplishes this. Perhaps some variation of this development might ultimately be incorporated.

The chief difficulty that surrounds simple shear devices is the nature of the stress state within the sample. The boundary conditions are not specified purely in terms of stresses, but displacements and stresses so, to an extent, one must presume a constitutive law to hold or make other assumptions before proceeding with an analysis of the test data.

In the recent versions of the Cambridge device one attempts to circumvent the major uncertainties associated with a boundary value analysis through measurement of boundary tractions using load cells, assuming that stresses in the central region of the sample are uniform (Wood and Budhu, 1979). However, in the case of undrained tests, one cannot proceed similarly because with nonhomogeneous states of stress near the boundaries of the sample come equally variable pore pressures regimes; their equilibration cannot be prevented and the state of stress in the central regions of the sample can therefore not be isolated.

In the case of the apparatus utilized by Dunlop et al. (1969), one must specify primarily displacements on the boundary of the sample and then, with the aid of a technique like the finite element method, determine the stress distribution within the sample. Proceeding in this way, one

must be sure that the boundary conditions in fact are as presumed (Prevost and Hoeg, 1976; Finn et al., 1971) lest the analytical results lose their meaning. The nature of the stress-strain law assumed also affects the validity of the results obtained.

With the circular simple shear devices, unless one is content to deal only with average, boundary values of stress, analytical techniques must also be used to determine the nature of the stress state within the sample. The idea of interpreting such test results in terms of boundary stresses should be approached with caution due to:

- a. stress nonhomogeneities evident, even assuming an ideal soil model,
- b. the tendency for some nonuniform horizontal deformation during shear (Duncan et al., 1968)
- c. the possibility of the horizontal normal stress changes, required to maintain a K_0 condition, varying around the sample's perimeter in light of the actual ability of the reinforced membrane or cell pressure to provide such restraint, and
- d. the equilibration of pore pressures within the sample.

However, the derivation of a suitable soil model to be used in the prediction of stress-strain behaviour and pore pressure response upon rotation of principal stress increments would be given impetus by the experimental and analytical work recently completed in this area. Then, with

such a capability, the results of an ideal simple shear test, one in which there are no stress nonhomogeneities, could be recovered. More will be said of this in a later chapter.

The level of technology reflected in the design, and the simplicity of laboratory procedures, in conjunction with an appropriate model of soil behaviour, would seem to permit the University of Alberta device to elucidate the behaviour of compacted soil upon rotation of principal stress increments. Further, it is suggested as a reasonable choice for use in the following study.

CHAPTER 3

DESCRIPTION OF TESTING APPARATUS

3.1 General

In this chapter a description of the various parts of the apparatus is given. When felt appropriate, considerations of machining and design are noted.

3.2 Description of Apparatus

For convenience, this section has been subdivided. The testing frame will be described first.

3.2.1 Testing Frame

This component is situated on a robust table constructed solely of hollow rectangular mild steel tubing. The prime consideration in choosing the material for the table was its availability. A view of the testing frame is given in Figure 3.1. The base is formed by a mild steel plate 155 cm long, 76 cm wide and 1.3 cm thick, braced on the underside by hollow rectangular tubing welded in place. In specifying the length of weld one must keep in mind the thickness of the table and its consequent deformation during welding. The vertical uprights, 218 cm long, were machined from precisely milled, high strength alloy steel shafting. Material of this high quality was used due to the great length of the uprights and the complexity of the apparatus, necessitating fine tolerances. Collars, located on the

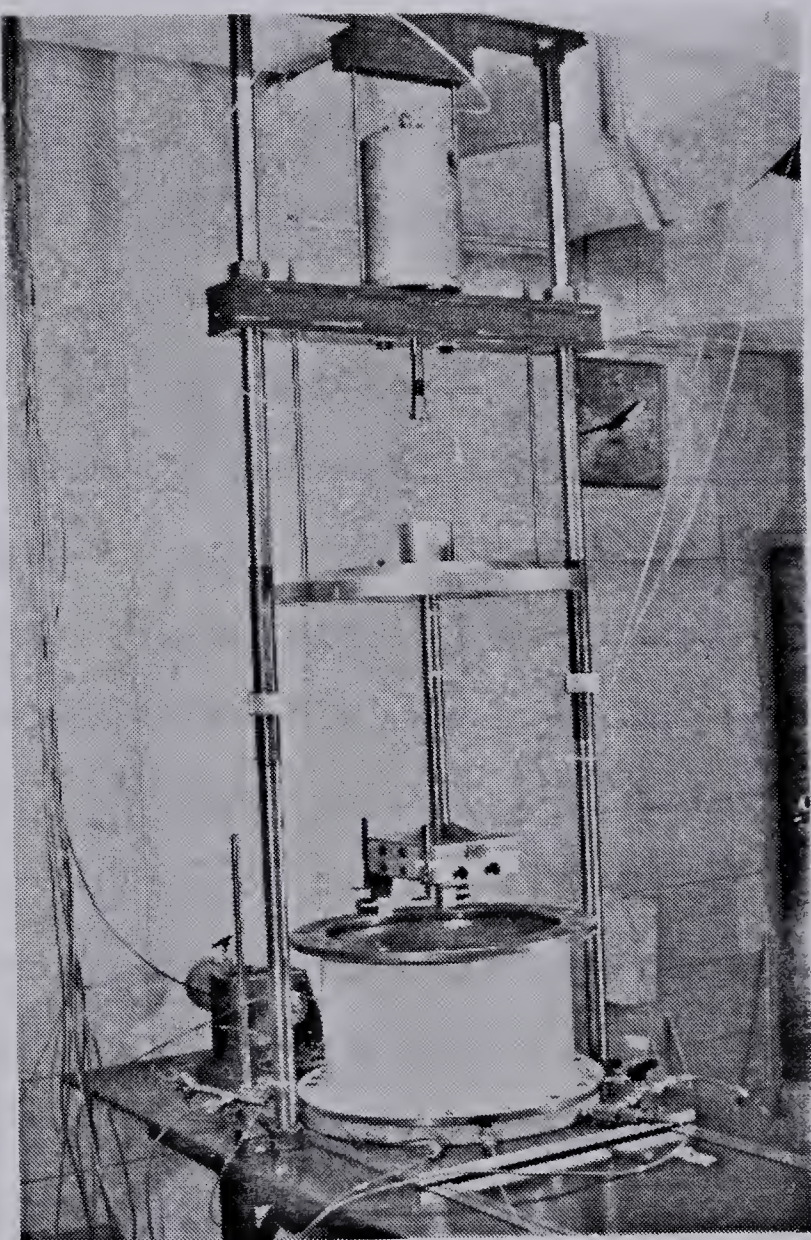


Figure 3.1 View of Testing Frame

underside of the base, are threaded to accept the vertical supports. At the very top of Figure 3.1 may be seen part of the uppermost crosspiece. The crosspiece is supported on its underside by large mild steel nuts. To secure the crosspiece firmly in position, two other such nuts may be advanced downwards along the vertical supports until they come into contact with its upper surface. The purpose of this member is to provide support for a pneumatic ram.

The ram has a bore of 5 cm and maximum working pressure of 1400 kPa. During assembly and disassembly of the cell it may be used to raise or lower various components. This point is discussed more fully in the appendices on testing.

The middle crosspiece is connected to the ram. This component serves to enable transmission of force from the pneumatic ram, through two .95 cm diameter steel rods, to the lowest or main crosspiece.

The main crosspiece can thus be raised and lowered along the vertical supports. The diameter of the central threaded portion of the vertical supports is greater than that of the unthreaded portion above so that the nuts used to secure the main crosspiece may slide freely as its elevation is changed. When not being moved, the main crosspiece is supported by two other mild steel nuts, which are located just below the cell cap in Figure 3.1. Finally, two steel rods connect it to the cell cap. This allows the raising and lowering of the cap.

3.2.2 Vertical Loading System

The Bellofram, used to apply the vertical deviatoric load, is situated on the main crosspiece. Bolts prevent its moving during the application of load. The Bellofram has a maximum working pressure of 860 kPa and bore of 14 cm.

Figure 3.2 shows the cell as it would look shortly before a test was run, several tie rods having yet to be inserted. In the middle of the picture one can see the vertical load cell. It is made of aluminum. A hollow plexiglas cylinder encases the load cell, preventing accidental damage to the strain gauges mounted on its side.

Two adapters link the Bellofram ram and vertical load cell. The first, conical in profile, allows transmission of force over a wider area. It screws into the Bellofram ram and is threaded to accept a male thread from the rotational adapter below it. The second or rotational adapter incorporates a thrust bearing oriented in a horizontal plane. Due to this design feature, compressive loads can be borne and yet, under no load, one half of the adapter may be rotated independently of the other. Since it is inadvisable to rotate the belofram ram at any time, such a fitting proves quite valuable during assembly and disassembly of the apparatus. The rotational adapter screws into the load cell. A small connector links the vertical load cell and ram.

The ram is precisely machined, hardened and ground along its length for smooth travel through the bushing in

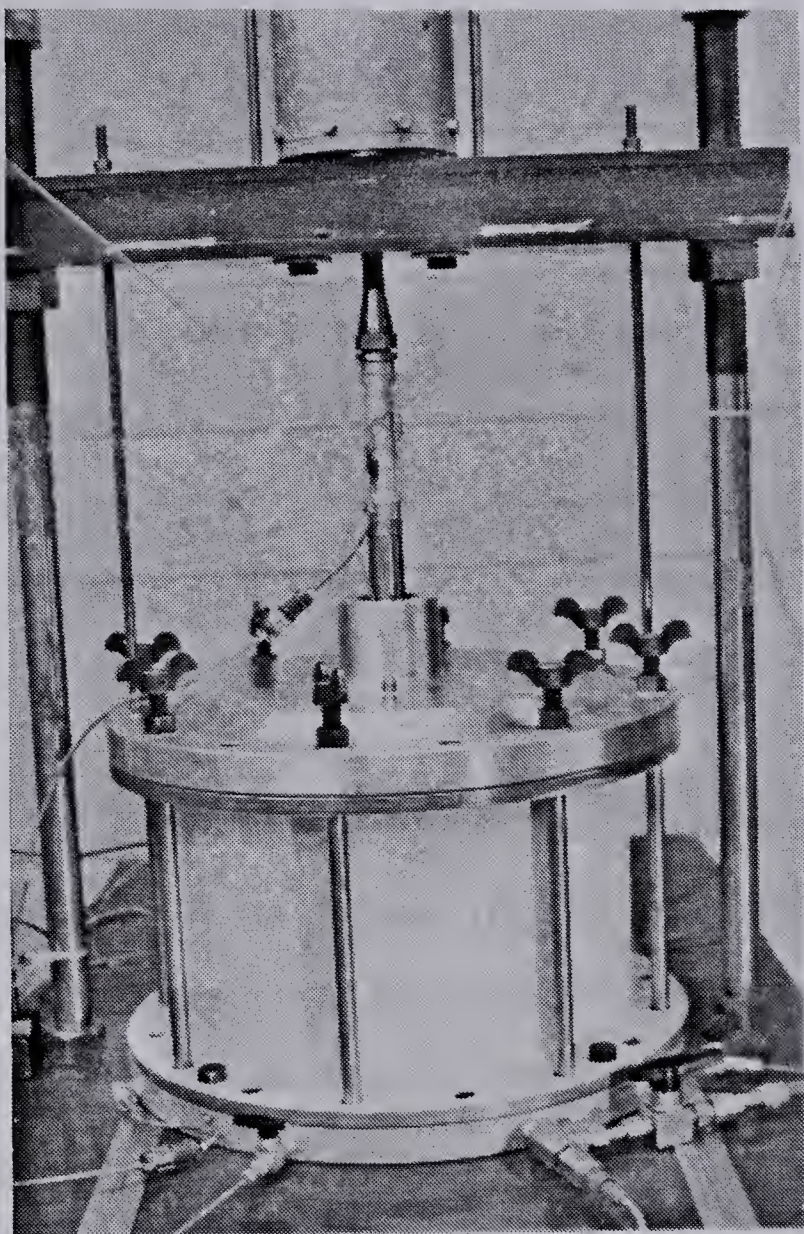


Figure 3.2 View of Load Cell and Cell

the cell cap. Further, as shown in Figure 3.3, the vertical ram screws into the top of the upper load cap. It is very difficult to machine a material of this hardness, so, to effect such a connection, it was necessary to drill and thread a hole in the end of the ram, into which was screwed an adapter of an exposed threaded diameter equal to that of the ram. The need for the load cap to remain normal to the axis of the vertical ram and, hence, for a rigid connection between the two components was discussed in the chapter in which the stress state within the sample was described.

The load cap is composed of three distinct parts:

- a. the upper load cap, mentioned previously,
- b. a Teflon sheet, immediately below it, and,
- c. the lower load cap.

Twenty three holes were drilled, in staggered rows, in the Teflon sheet. A ball bearing is positioned in each one. The diameter of the holes is slightly greater than that of the bearings; the thickness of the Teflon sheet is slightly less. Connector plates, positioned on each of the long sides of the load cap, limit relative movement between the upper and lower load caps. Due to the presence of small end flaps, one of which can be seen bolted to the upper load cap in Figure 3.3, and the just mentioned limits to the relative movement of the lower load cap, the displacement of the Teflon sheet relative to the upper load cap can be no greater than that of the lower load cap. Figure 3.3 represents a condition of no relative displacement of the

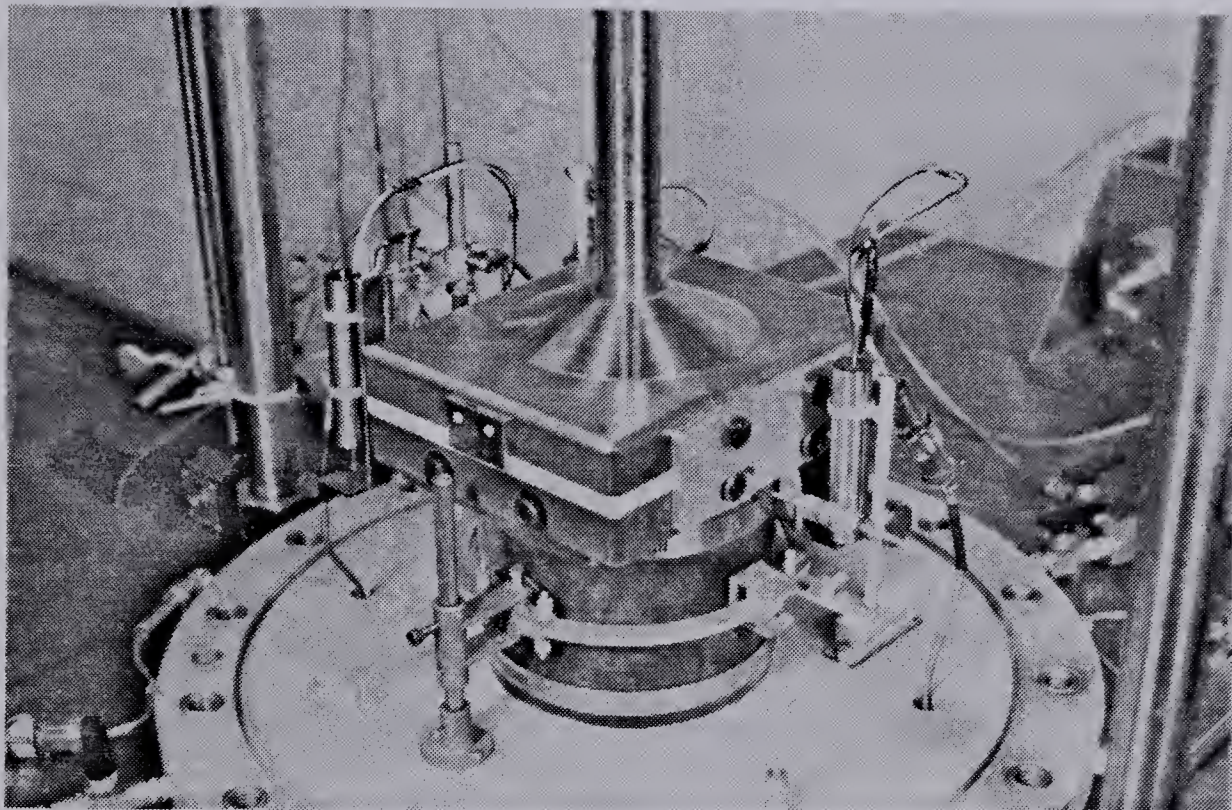


Figure 3.3 View of Ram-Load Cap Connection

components of the load cap.

This design insures maintenance of the integrity of the load cap, allows transmission of vertical load to the sample yet, even under such load, permits horizontal movement of the lower load cap. The magnitude of the resistance to any such movement, due to friction between various components of the apparatus, will be discussed later. The maximum travel of the lower load cap is about 1.3 cm.

3.2.3 Upper Platen

The load cap rests on the upper platen of the sample. Two collars incorporated in the lower load cap, may be lodged against the upper platen by tightening several Allen head cap screws. These collars enable proper positioning of the load cap during sample assembly and, hence, ensure that the displacement of the lower load cap will be equal to that of the upper platen during the test. From the vantage point for Figure 3.4, the horizontal component of displacement is from left to right.

A close up view of the upper platen is seen in Figure 3.5. The brass disc and attached stainless steel line, occupying the recessed area in the platen, are components of a drainage line through which pore fluid may drain from the sample, if the appropriate valves are open. One can also see an O-ring, inset in the disc, and the ends of two screws, tightening which the O-ring seal may be formed. To prevent drainage around the heads of the screws, Teflon

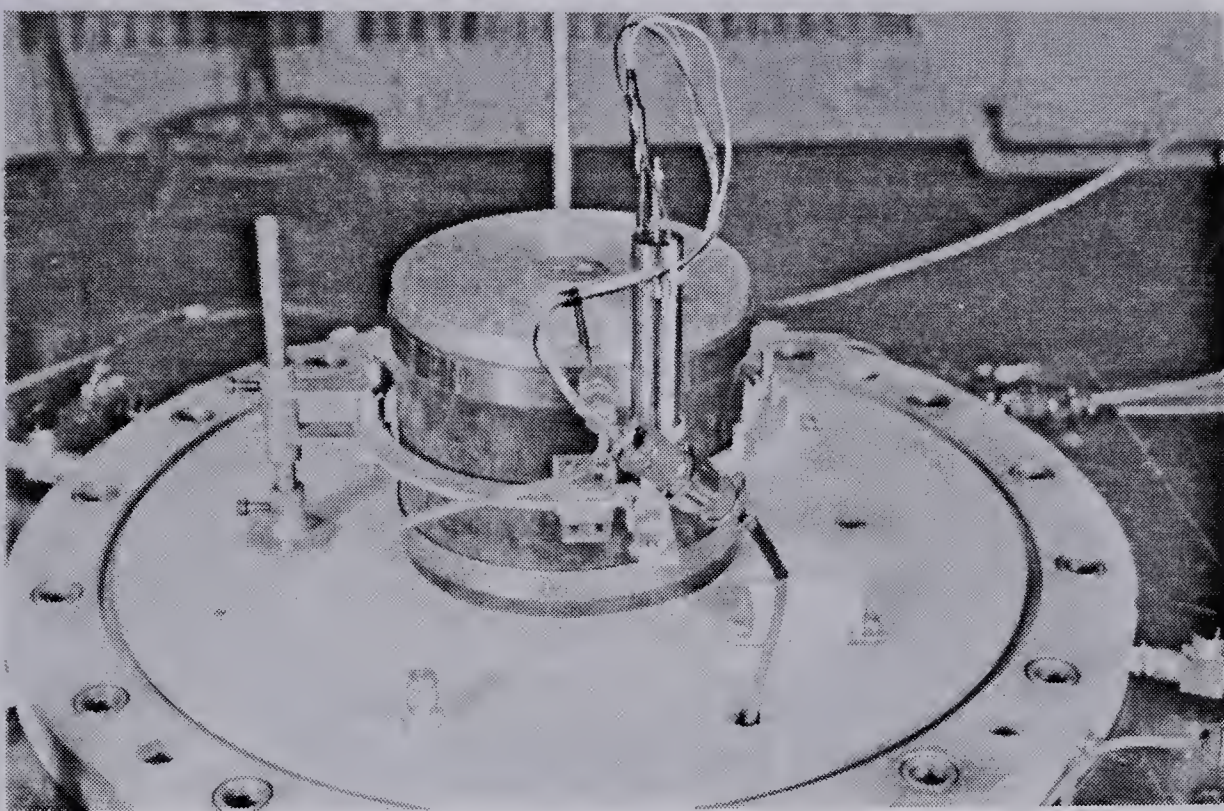


Figure 3.4 View of Sample with Lateral Gauge Attached

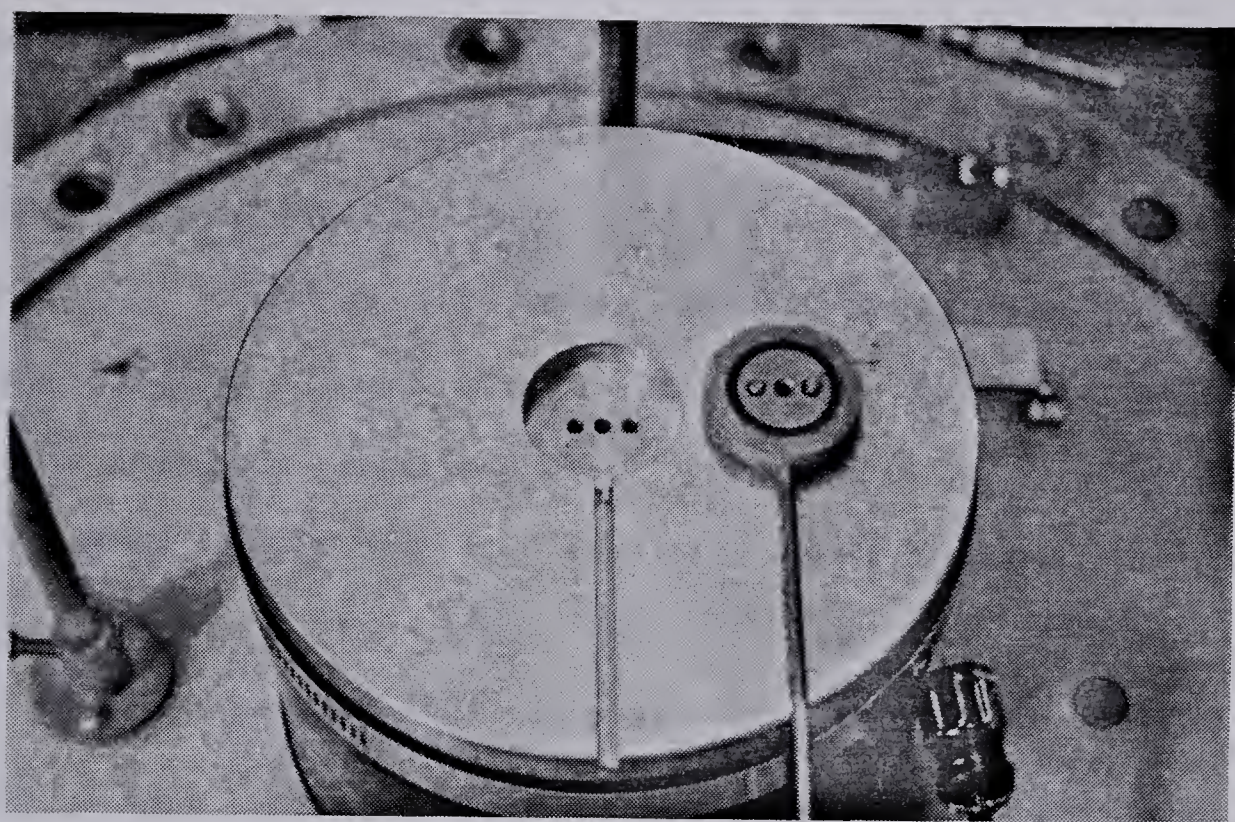


Figure 3.5 View of Upper Platen

gaskets may be used. Figurew 3.6 shows the drainage line in position.

The platen itself, upside down and disassembled, may be seen in Figure 3.7 . Uppermost is the finned plate with the recessed porous stone below. The finned plate is attached to the upper platen, proper, by means of aluminum screws. In tightening the screws, one must be careful not to tighten them too much, thereby stripping the threads. Note, that the holes for the screws are countersunk. Drainage of the pore fluid from the sample takes place through the numerous small diameter holes drilled in the finned plate. The fins, triangular in profile, insure that the horizontal deformation of the upper platen and upper surface of the soil sample are identical. Their spacing was arbitrary, being thought great enough to allow easy embedment in the soil, yet small enough to allow transmission of the desired shear force. The ratio of fin to sample height was selected after reference to the work of Hvorslev and Kaufmann (1952) and Bishop et al. (1971). The porous stone is cut from coarse, sintered stainless steel. It is connected to the upper platen drainage line, shown in Figure 3.5, by a line drilled vertically through the upper platen, proper.

The upper platen, proper, is not of uniform diameter, as can be seen in Figure 3.7 . The diameter of the finned plate is equal to the larger diameter. During sample preparation, two O-rings may be slipped over the region of smaller diameter and lodged against that of the larger

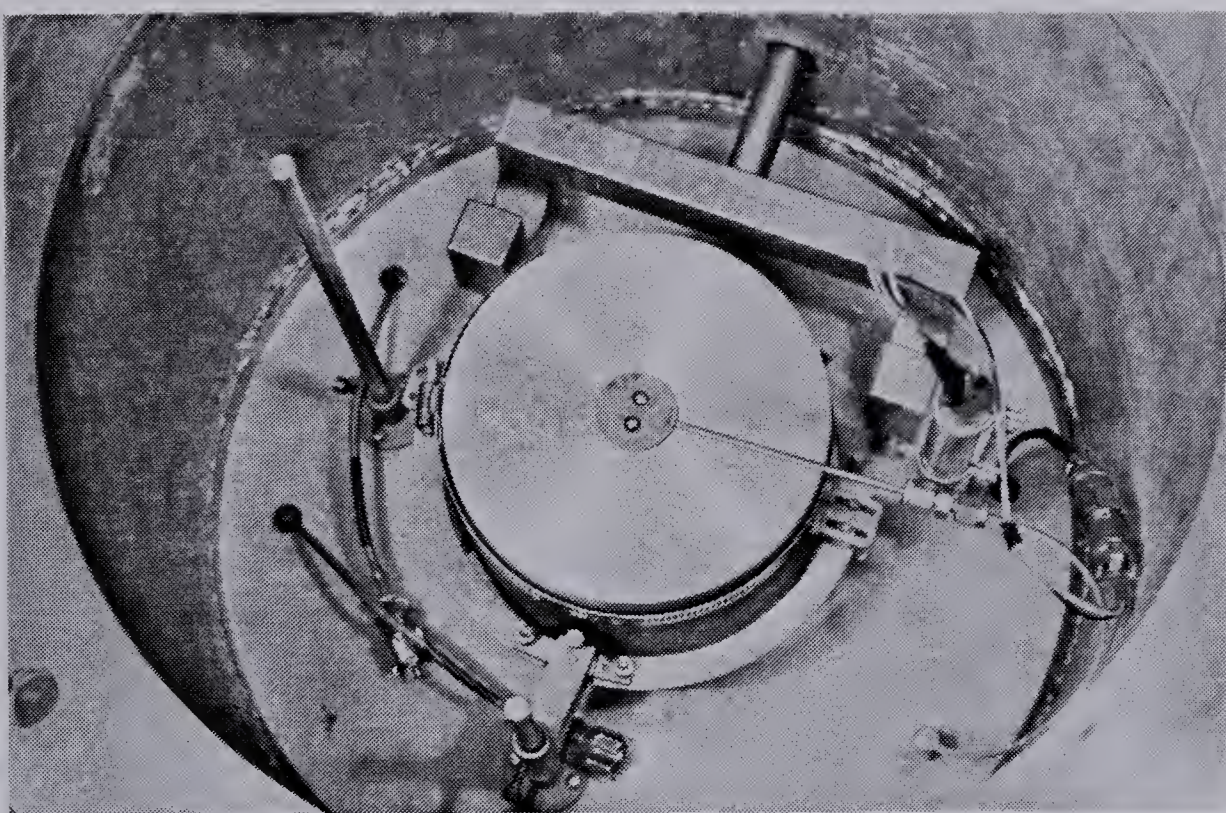


Figure 3.6 View of Drainage Line in Position

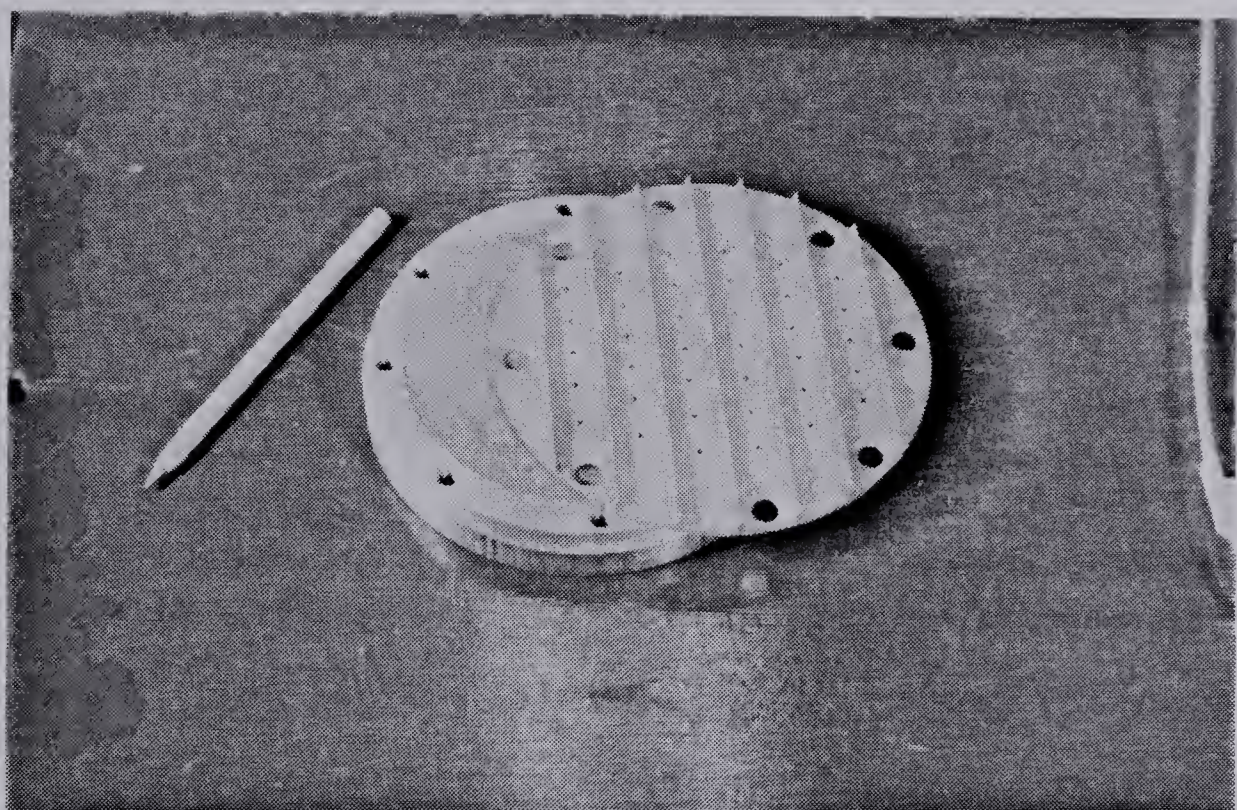


Figure 3.7 Upper Platen Disassembled

diameter. The finned plate, when screwed into place, then prevents the O-rings from slipping out of position.

During a test, two other O-rings will encircle the lower platen or pedestal, on which the sample rests. Metal strapping is used to press the rubber membrane, enclosing the sample, against the sets of O-rings, thus isolating the sample from the cell fluid. The lower set of O-rings can be seen in Figure 3.8 .

3.2.4 Pedestal

Like the upper platen, the pedestal, proper, has a recessed area for a porous stone and screw holes allowing attachment of a finned plate. Lines allowing drainage of fluid and measurement of pore fluid pressure run down through the pedestal and into the cell base. The finned plate prevents the lower surface of the sample from translating horizontally under the action of the deformation imposed on the upper surface. As with the upper platen, the fins are aligned normal to the axis of the horizontal ram. The pedestal fits into a recessed area in the cell base, being secured by Allen head cap screws that pass through the cell base and lodge in holes drilled and threaded in the underside of the pedestal. An O-ring which runs around the underside of the pedestal, near its perimeter, prevents the inflow of cell fluid. Further, smaller O-rings surround the base drainage and pore pressure lines.

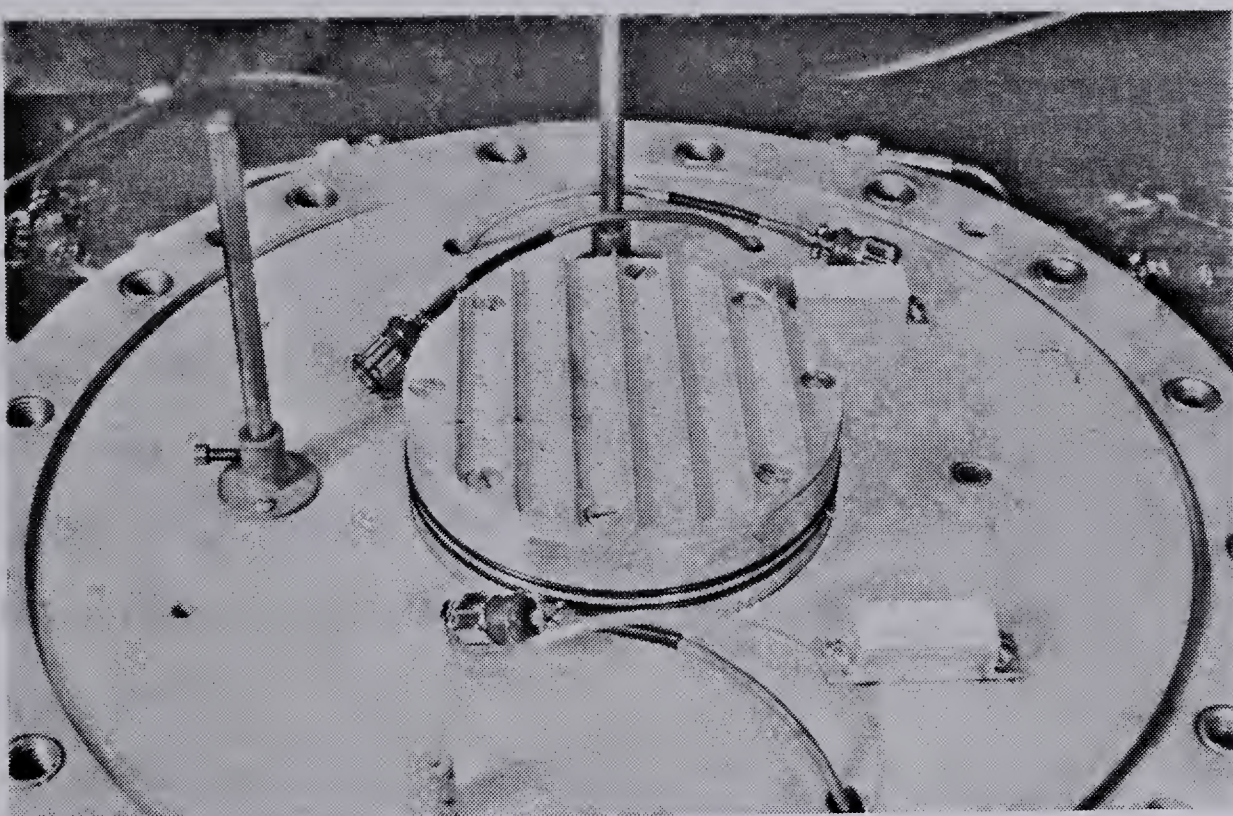


Figure 3.8 View of Pedestal

3.2.5 Cell Base

The cell base is constructed of aluminum. Various views of the base are presented in Figures 3.3, 3.4 and 3.8. A schematic view is shown in Figure 3.9. The lines for pore fluid pressure measurement and base drainage pass predominantly through the cell base, appearing on its exterior vertical surface. The pore fluid pressure transducer is located there. One of the valves on the base drainage line is also located there. Care had to be taken in drilling these lines as they are rather long and it was necessary that their final form be such as to allow the complete flushing of entrapped air bubbles during sample preparation.

Within the cell, during a test, are several electrical measuring devices. The leads for these devices are passed through lines, of a diameter larger than those just discussed, drilled in the cell base. They are reconnected, ultimately, to a data acquisition system. That device can monitor and/or record their output. There are three such lines. A seal must be formed around the electrical leads, where they leave the cell base, to prevent gross leakage of fluid from the cell. However, small amounts of leakage can be tolerated since the cell pressure is generated by a constant pressure source and sample volume change is monitored using electrical devices.

The remaining lines drilled through the cell base form parts of systems allowing draining of the cell and enabling

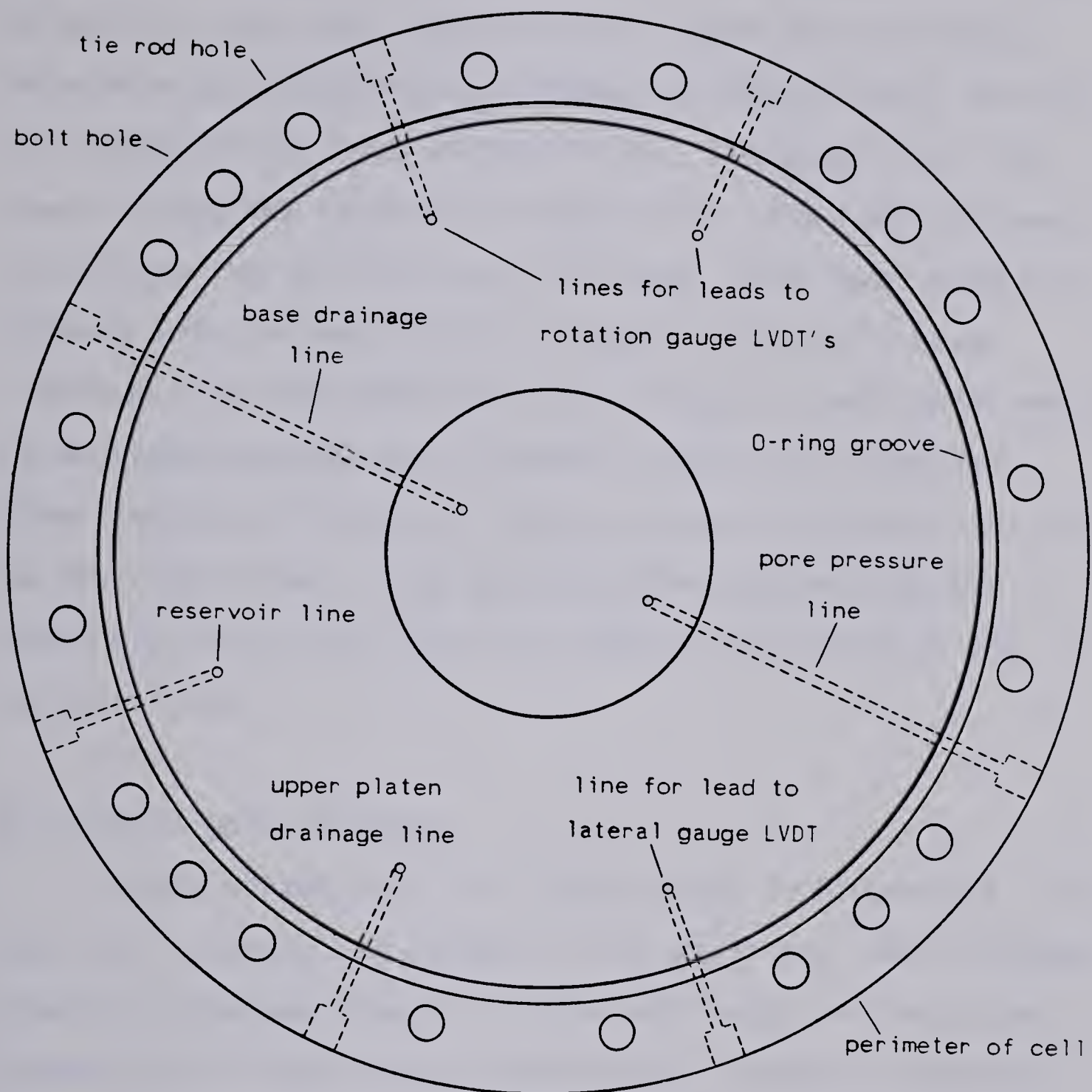


Figure 3.9 Schematic View of Cell Base

drainage of the sample from its upper surface, respectively. A transducer, located on the former line, on the perimeter of the cell base, is used to measure cell pressure. It can be seen in the right foreground of Figure 3.2. O-rings provide a seal between the flanges of the cell wall and the cell base and cell cap respectively. The groove for the lower O-ring may be seen in Figure 3.8. Tie rods are used to connect the cell cap and cell base. The lower ends are screwed into hardened inserts lodged in the cell base. Aluminum is a soft metal and the threads of such holes would be degraded quickly were hardened inserts not provided. Other features of the cell base, as seen in Figure 3.8, will be described later. The consideration determining the thickness of the cell base was ease of machining of the various lines.

3.2.6 Cell Wall and Yoke

A view of the cell wall may be seen in Figure 3.2. The cell wall, proper, is welded to the upper and lower flanges. Given the average diameter of the cell wall, 40 cm, some distortion of the flanges and cell wall might be expected upon such welding. To circumvent the problem, flanges 1.3 cm in thickness were used, the welding was done, and only then were the surfaces of the flanges, in contact with the cell cap and base, machined. The holes for the tie rods were then marked and drilled.

The horizontal load to which the load cap is subjected

during a test is applied by a yoke passing through the cell wall. Beyond the wall, the yoke passes through a bushing housed in a fitting which is in turn bolted to a base on the cell wall. This is shown in Figure 3.10 . O-rings must be provided to prevent leakage of cell fluid along the interface between the above mentioned base and fitting.

In Figure 3.11 are pictured two vertical arms that extend from the underside of the lower load cap. At the lower extremities of the arms are horizontally oriented roller bearings held in place by pins passing through the respective arms. The roller bearings form line contacts with the arms of the yoke. It is beneficial to use them to transmit the horizontal load from the yoke to the load cap as vertical deformation is not impeded even if the load cap is under horizontal load. In the initial testing position, the maximum possible vertical movement of the load cap permitted by the design of the yoke is approximately 1.3 cm. It should be noted that, notwithstanding deformation due to the applied load, the arms of the yoke, in contact with the roller bearings, are at all times vertically oriented. This insures that the load, as transmitted to the load cap, has a negligible vertical component. In Figure 3.8, two small rectangular supports for the yoke may be seen. Teflon covered, the supports offer little resistance to the horizontal movement of the yoke yet prevent its rotation.

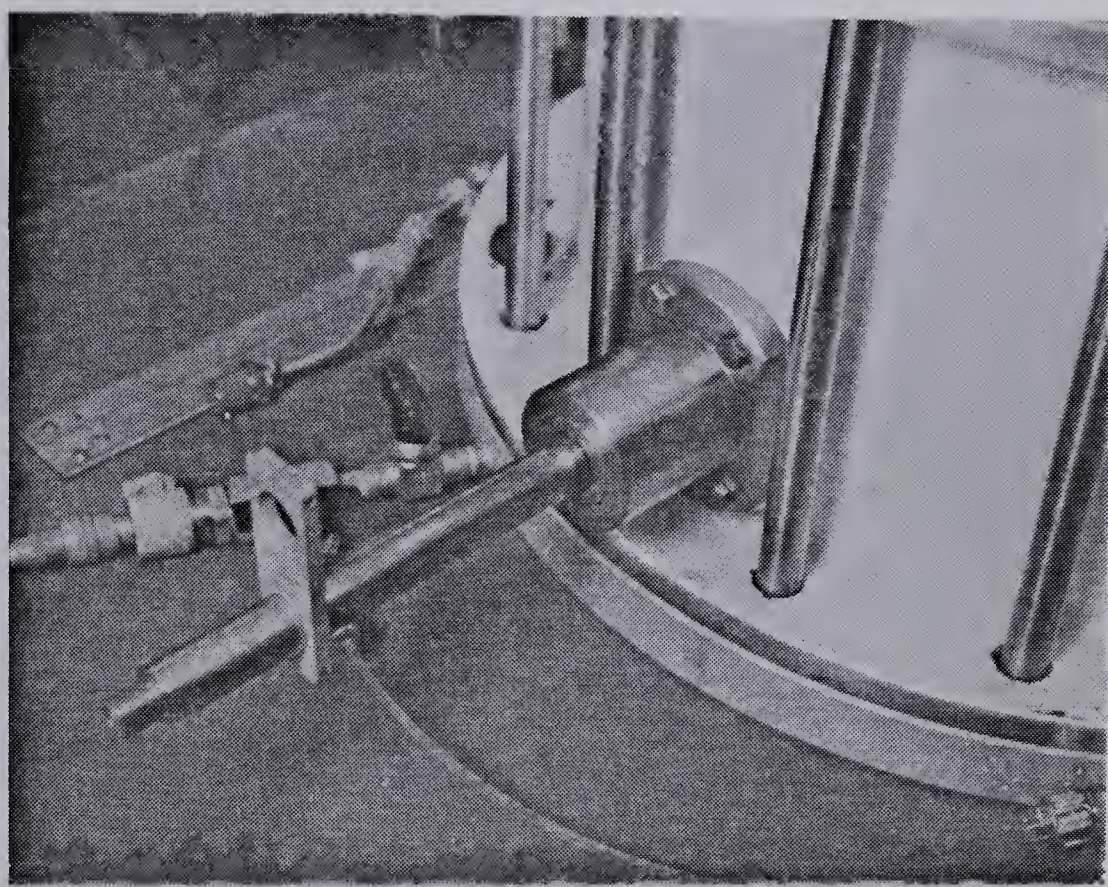


Figure 3.10 View of Horizontal Bushing Assembly

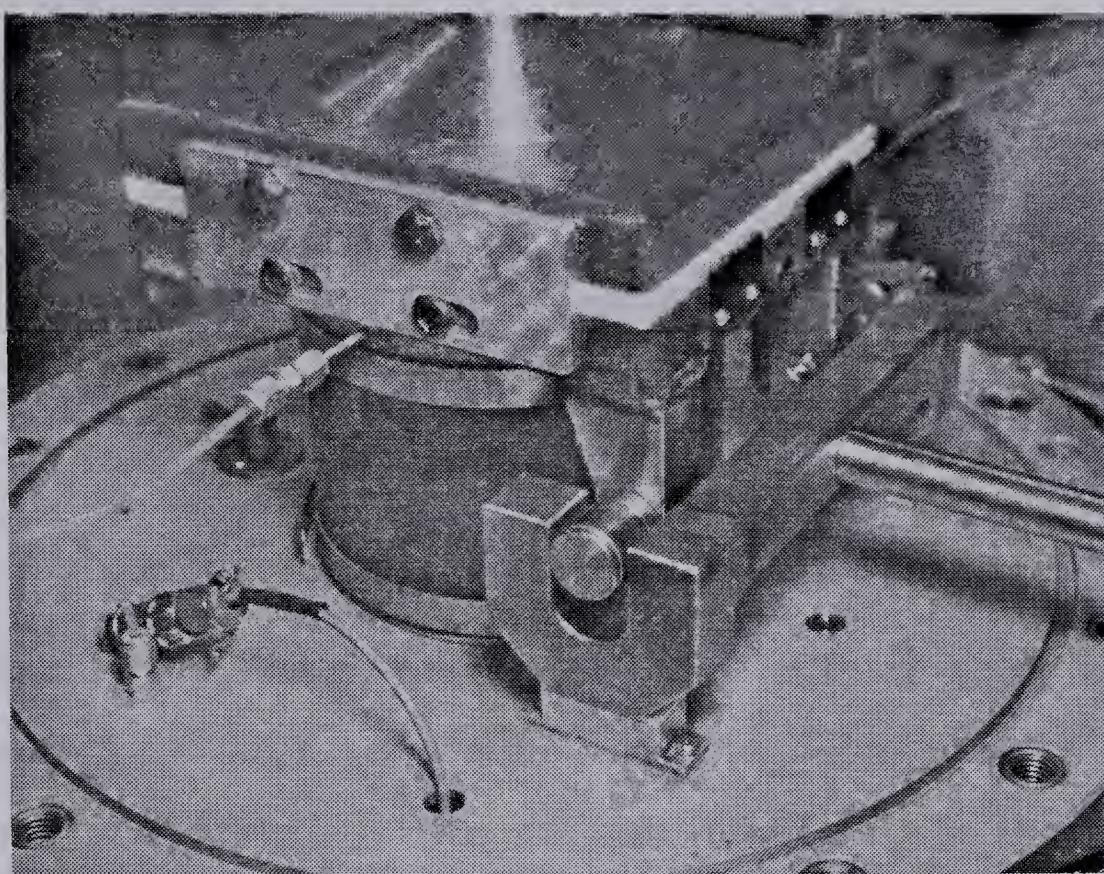


Figure 3.11 Yoke and Load Cap Assembly

3.2.7 Horizontal Loading System

The complete horizontal loading system may be seen in Figure 3.12 . It consists of, in turn:

- a. the yoke
- b. a load cell
- c. a rotational adapter
- d. a spacer and,
- e. the horizontal belofram.

During construction of the apparatus, care was taken in aligning the various components so that frictional forces due to the interaction of the yoke and bushing would be minimized. The load cell, similar in design to the one discussed previously, measures the load applied by the horizontal belofram. This is not necessarily the load to which the sample is subjected, since other forces may also act on the yoke; for example, the above mentioned frictional forces. The determination of the actual magnitude of this load will be discussed in an appendix.

The adapter plays the same role as the one linking the vertical load cell and Bellofram but must bear a tensile load during a test. On occasion, the spacer is used to restrict the movement of the horizontal loading system. Its function is described in more detail in Appendix C. The horizontal Bellofram is bolted to its stand which, in turn, is bolted to the base of the loading frame. To insure horizontal force equilibrium, the cell itself must be able to resist horizontal load. Two of the four bolts used to

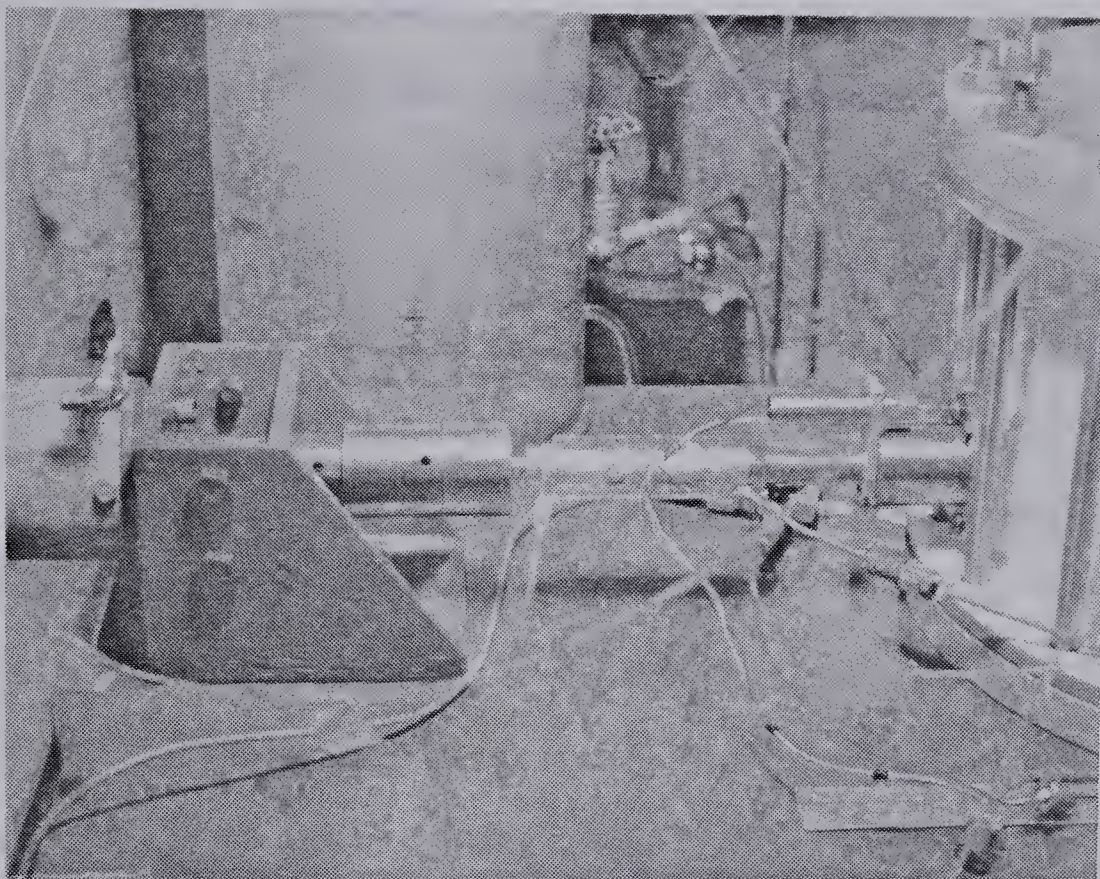


Figure 3.12 Horizontal Loading System

secure the cell may be seen in Figure 3.2 .

3.2.8 Deformation Gauges

Lastly, the components for the measurement of deformation within the cell must be discussed. A gauge was designed to monitor the average lateral deformation of the sample. Several views of the gauge may be seen in Figures 3.4 and 3.6. In principle, its design and operation are the same as those of the one described by Fredlund (1973). Perhaps the main difference is that in the present case the pads resting on the sample's membrane are not of a radius of curvature equal to that of the sample, but planar, oriented parallel to the line of action of the imposed shear load. This must be so to allow horizontal deformation of the sample to take place while, at the same time, recording diameter change.

The other gauge, part of which can be seen on the far side of the load cap in Figure 3.3, consists essentially of two LVDT's that measure the vertical components of movement of the lower load cap at two discrete points. The probes of the two LVDT's rest on separate horizontal pads connected to the lower load cap. These can be seen in Figure 3.1 . The rotation of the lower load cap and, hence, of the upper platen, may be important in determining the stress state within the sample. Considerations in the design of the gauge were the limited space available and the ease of its installation during assembly of the cell.

An LVDT, mounted on the yoke, outside the cell, measures the horizontal displacement of the lateral loading system and, it is assumed, the sample. It may be seen in Figure 3.12. The presence of the spring to maintain the position of the probe should be noted.

3.3 Devices Used During Sample Preparation

The split ring compaction mould is of standard design but unusual dimensions. It is used to form samples 5 cm in height and 15 cm in diameter. When embedding the finned plates in the soil sample, the compaction mould is placed on the pedestal, as shown in Figure 3.13. Due to the design of the mould's base, there is a gap between the bottom of the soil sample and the bottom of the compaction mould. This allows the compaction mould to be centered on the pedestal by the finned plate. It is important that the fins be oriented in the direction normal to the line of action of the shear load. In the case of the lower finned plate this can be assured by the pattern of screws holes in the pedestal. This is not so for the upper platen; a somewhat complex alignment and loading system was designed. Two rods are threaded into holes in the cell base (the bottom has been drilled out of the base for the bar supporting the lateral strain gauge). A crosspiece links these two uprights. This is shown in Figure 3.13. Below it, a slotted 15 cm diameter disc sits on the upper platen, which is resting directly on the soil sample. Previously, two

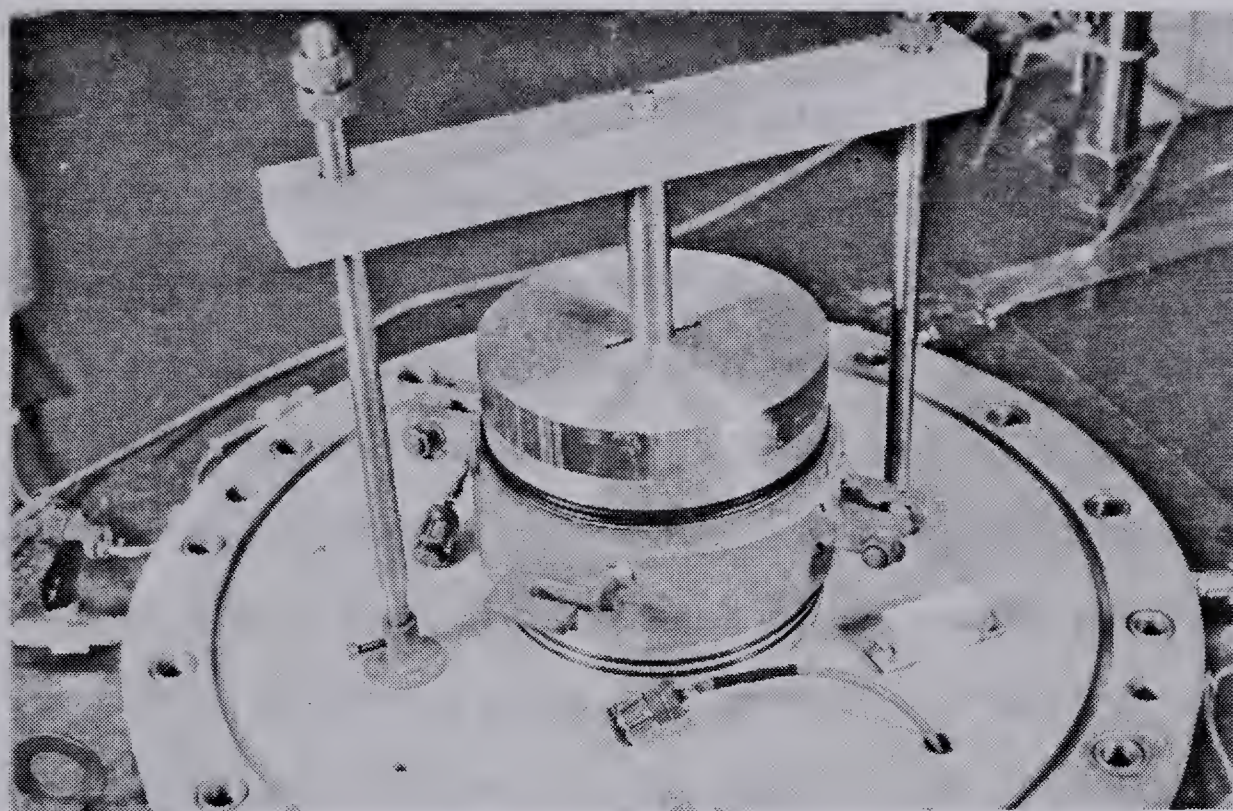


Figure 3.13 Embedding Fins in Sample

small holes had been drilled, with their long axes parallel to one another, through the small rod connecting the crosspiece and the disc. The holes were oriented at right angles to the axis of the rod. Into these holes were then hammered roll pins. Finally, slots to accept the roll pins were milled in the crosspiece and disc. Thus, postioning the rod as shown in Figure 3.13, one fixes the orientation of the disc relative to the crosspiece. The upper platen can then be positioned, by matching marks made in its own surface and that of the disc, so that the fins are normal to the direction of shear. Further, applying a uniform load to the crosspiece allows the fins to be embedded in the soil. The sample is prepared with the cell base resting on a movable plate positioned at one end of the loading frame base. When the load cap is about to be attached, the pin securing the plate is removed and the plate is moved to the position shown in Figure 3.1 . The track along which it runs may also be seen. The plate is made of aluminum, the wheels are light roller bearings.

CHAPTER 4

PRESENTATION AND DISCUSSION OF EXPERIMENTAL RESULTS

4.1 General

In this chapter, an assessment of the performance of the apparatus is made. As well, aspects of the laboratory procedures employed are evaluated. The experimental data are then presented and reviewed in the light of expected results. To conclude, the uncertain nature of the stress state within the sample is noted and methods of analysis, to resolve the attendant difficulties, are discussed briefly.

4.2 Description of Soil Tested

The material from which a sample was derived formed part of a boxed sample of Mica Dam core material taken in the area of one of the abutments. The method of sample preparation is described in Appendix B. Routine index tests were run on the material to be tested; the liquid limit was 18.3%, the plastic limit 15.4%. The specific gravity of soil solids was found to be 2.79. Figure 4.1, on the following page, shows the grain size distribution based on the results of sieve and hydrometer analyses.

The bulk density of the compacted material was 2.23 gm/cc, the water content being approximately 15%. An average degree of saturation would then be about 95%, given the mean void ratio of .44 . The grain size distribution and moulding water content were chosen to enable the fins to be

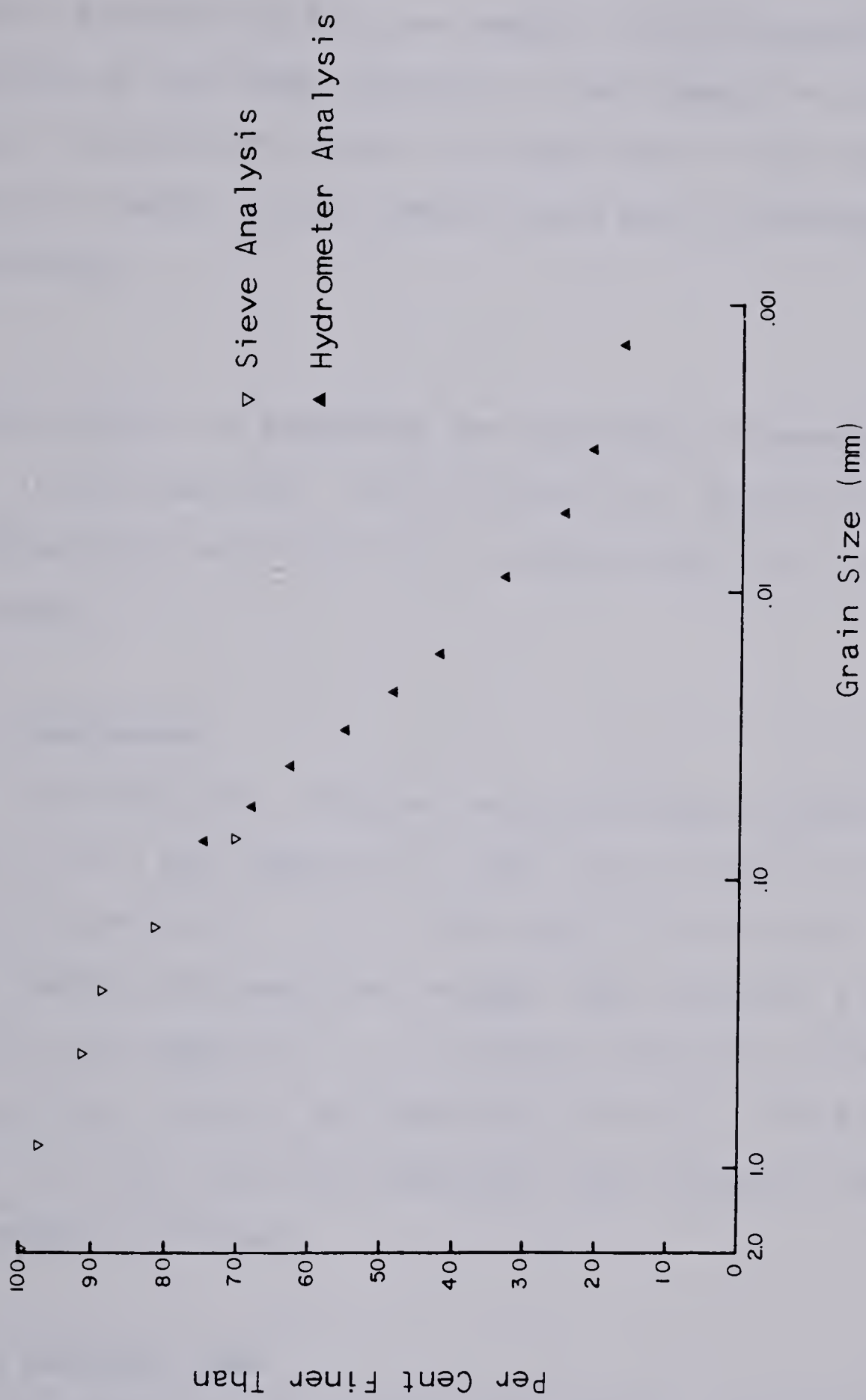


Figure 4.1 Grain Size Distribution of Altered Mica Dam Core Material

embedded in the soil sample easily and to ensure a tight contact between the fins and sample. This necessitated the covering of the inner surfaces of the compaction mould with plastic wrap before beginning compaction of the sample. However, stable, intact samples were easily produced thereafter.

4.3 Evaluation of Apparatus and Laboratory Procedures

In this section, various aspects of the performance of the apparatus and laboratory procedures used will be reviewed.

4.3.1 Membranes

The membranes, produced using techniques based on the work of Vaid and Campanella (1973), were simple to fabricate and performed well. At no time were difficulties experienced with membrane leakage, but the metal straps, binding the membrane to the pedestal and upper platen, respectively, had to be tightened carefully. Care was also taken to insure that the membrane, positioned on the sample, was nowhere wrinkled.

4.3.2 Loading Frame

The design of the loading frame base, incorporating an area where the cell base could be positioned during sample assembly, proved acceptable as did the performance of the pneumatic ram. With a small amount of practice one was able

to control its movements quite closely. Further, there was little friction apparent with relative movement between the vertical uprights and main crosspiece.

4.3.3 Cell Fluid

In choosing a fluid to be used in the cell one must consider, under these circumstances,

- a. whether its conductivity is such as to affect the signal of measuring devices within the cell,
- b. the tendency of the fluid to degrade the latex membranes, over the period of a test, and,
- c. its immiscibility in water.

Glycerin, manufactured by Fisher Scientific Co., was found to be essentially nonconductive. Further, in special preliminary tests run at cell pressures of 1400 kPa over a period of several days, it did not affect the structure of the membranes. The fact that glycerin is soluble in water makes it relatively easy to clean up after a test. However, care must be taken to ensure that the fluid used in tests has not been contaminated with water. This can be determined periodically by checking its conductivity.

4.3.4 Testing Procedure

The process of filling the cell was time consuming, taking approximately two hours. Every twenty minutes or so the fluid level within the reservoir was checked; if necessary, more fluid was added.

It was found preferable for two people to work together on sample and apparatus assembly from positioning of the sample on the pedestal to filling of the cell. However, it was essential that there be two people only from the positioning of the sample to the attaching of the cell cap; on the order of several hours.

In the initial stages of a test, prior to each increment in cell pressure, a seating load was applied to the vertical ram to prevent its being forced out of position by the cell pressure. The calculated increase in air line pressure to the vertical Bellofram, 5% of the subsequent cell pressure increase, proved sufficient.

The above undrained increments in cell pressure preceded K_o consolidation of the sample and the application of horizontal shear load. Their original purpose was to raise the pore pressure to an appropriate level prior to the application of back pressure that would eventually cause saturation of the sample. The cell pressure would then again be increased, in undrained increments, and K_o consolidation begun. Also, it was planned that these load increments would involve no lateral strain. However, the pore pressure response to the increases in cell pressure was such that increments in deviatoric load, to maintain a K_o condition, were not applied for fear the effective lateral stress within the sample would tend to zero. Further, it was realized that, for practical purposes, the sample could be saturated by undrained loading. The cell

pressure was thus raised, in steps, past the level at which back pressure was to have produced full saturation, to its final level and K_0 consolidation then took place against the just mentioned back pressure (or in stages, with the final back pressure equalling the above mentioned value).

Values of the parameter B for undrained load increments at pore pressure levels equal to or greater than the final applied back pressure were always at least .99. Also, the component of vertical stress, due to the various increments of seating load during this period of undrained loading, proved negligible. As desired, the assumption of full saturation of the sample was then felt warranted.

4.3.5 Lateral Gauge

The boundary loading during the episodes of consolidation and shear loading was determined to a large degree by the performance of the lateral strain gauge. With a change in the reference diameter indicated by the strain gauge, the vertical deviatoric load would be altered by a certain amount to restore the reference diameter to its original length. Although the present gauge is similar in design to that utilized by others (Fredlund, 1973; Law, 1975) its performance was not entirely satisfactory. Certain other difficulties, associated with its use, presented themselves in the course of the testing program. Details of both of these concerns are noted in the following paragraphs.

In the first test, although the gauge was responsive to changes in sample diameter during consolidation (against 568 kPa back pressure), too large a vertical load was applied in trying to return the reference diameter to its original length. After reducing the vertical load, without a comparable change in lateral gauge readings, it was decided simply to allow the sample to tend, through consolidation, towards its initial diameter. The gauge's readings reflected the decrease in diameter. During the application of shear load, the readings of the gauge did not change.

In the second test (consolidation against 606 kPa back pressure), the method of maintaining the reference diameter constant was improved and worked successfully. However, it appears that on this occasion the wires of the gauge's LVDT interfered with the free movement of its probe; after two successful attempts to return the reference diameter to its initial value, the gauge indicated a constant diameter despite further consolidation of the sample. With the application of shear load, the output remained unchanged until late in the test when there was some movement indicated.

During the third test, the sample was loaded to a cell pressure of approximately 1400 kPa with little response shown by the lateral gauge. In an attempt to better demonstrate the efficacy of the gauge, the sample was consolidated in stages with the back pressure being reduced successively to approximately 1120, 840 and 630 kPa,

respectively. For present purposes, it was assumed that a linear effective lateral stress versus effective vertical stress graph would constitute sufficient evidence of proper performance; however, an actual calibration test would have been preferable.

While the backpressure was set at approximately 1120 kPa the gauge seemed responsive to the deformation of the sample during consolidation. On two occasions, successful attempts were made to return the reference diameter to its original length by increasing the vertical load. However, thereafter, the lateral gauge did not indicate any movement although some would have been expected, and the vertical load experienced a slight decrease in magnitude due to leakage of air from the Bellofram.

During the second stage of consolidation, it seemed to be much less responsive despite a slight altering of the vertical load. This behaviour was exhibited in the final consolidation stage as well. No further change in lateral gauge readings was noted except at the very end of the test with the removal of boundary loads.

It is felt that attention should be devoted to upgrading the performance of the lateral gauge. Each change in sample diameter must be reflected by a change in LVDT output. Both the method of supporting the lateral gauge arms and that of displacing the LVDT probe should be examined.

With the end of consolidation, in each test, drainage

from the sample was prevented and the shear load applied. Table 4.1, on page 78, indicates the loading conditions just prior to shear. The cell pressure and average total vertical stress were maintained constant thereafter.

4.3.6 Maintenance of Boundary Conditions

During the course of shear loading, to insure as homogeneous a stress state as possible and representative measured quantities, it is desirable that there be:

- a. no rotation of the upper platen,
- b. no bulging of the sample; a constant lateral dimension maintained,
- c. homogeneous deformation of the sample even in the region of the platens, and,
- d. no wrinkling of the membrane.

In the first test, the only test in which two LVDT's were used in the cell to measure vertical deformation, a very small amount of platen rotation was noted during the final two stable load increments. It is thought that this may have been connected with the early stages of failure plane formation. Visual inspection of the other two samples, at the end of the respective tests, revealed the upper and lower surfaces of the samples to be horizontal and parallel. Figure 4.2 shows the sample at the end of test #3. The nature of the deformation is generally characteristic of that in the other tests except that in test #2 a discrete failure plane did not form. In profile,

Test Number	Total Vertical Stress (avg.)	Cell Pressure (kPa)	Pore Pressure Prior to Shear (kPa)	Increase in Pore Pressure During Shear* (kPa)	Stress Ratio* (τ/σ_v')
1	1060	1002	568	200	.7
2	1231	1094	607	280	.7
3	1492	1405	607	460	.65 ⁺

prior to and during shear

* at 7% average shear strain (equilibrium)

+ curve shows discontinuity

Table 4.1 Test Results

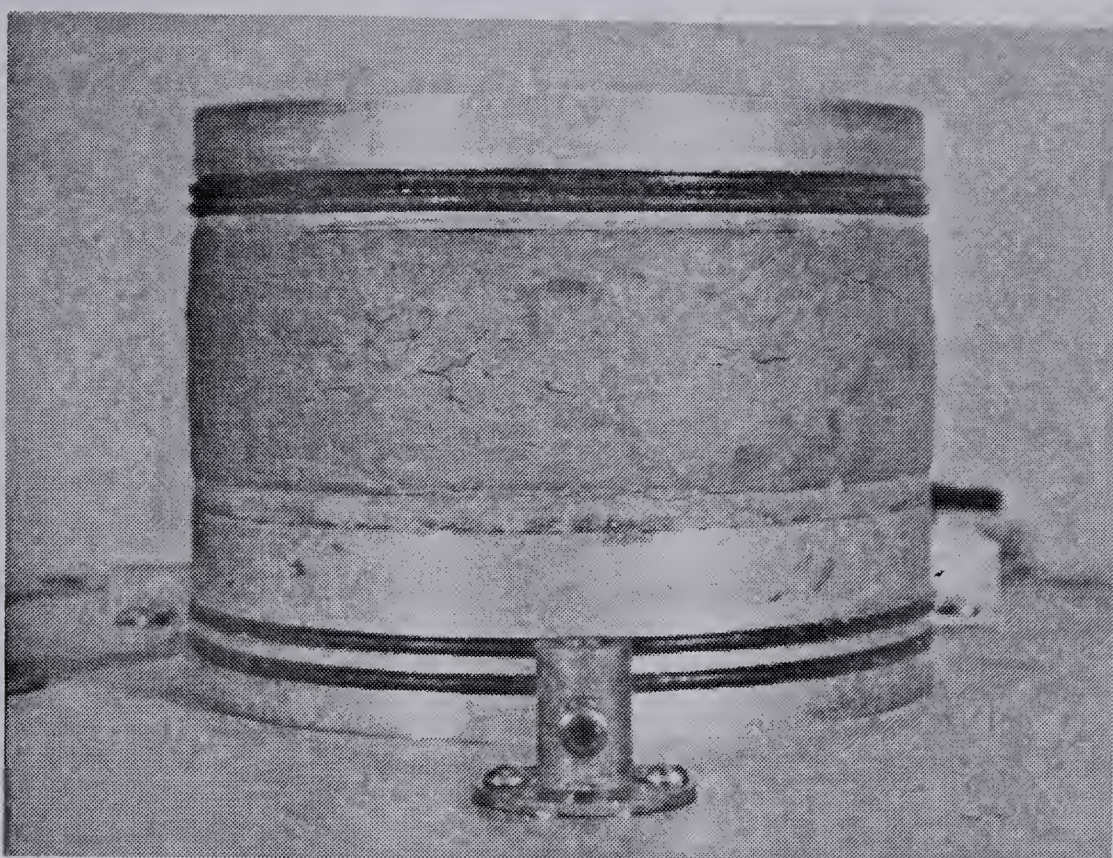


Figure 4.2 Views of Sample at End of Test #3

some nonhomogeneity of deformation is evident. However, it must be borne in mind, in drawing conclusions, that the sample shown had undergone large strains. The contact between the horizontal surfaces of the sample and the finned plates was smooth and without gaps. This was seen at the end of the test upon careful removal of the sample from the apparatus.

Figure 4.3 also shows the sample of the third test after failure. The wrinkling of the membrane is apparent. However, again, it must be remembered the sample had been subjected to excessive deformations. At the beginning of the test the fit of the membrane, on the sample, was excellent. It is believed that such distortion accompanied the large strains following failure of the sample. Further, the sample, as photographed, was not subject to any loads.

4.4 Evaluation of Test Results

In evaluating the test results, the first question to be answered concerns the nature of the expected outcome. Hence, in the following paragraphs, the factors determining such an outcome will be discussed. The experimental results will then be considered.

4.4.1 Factors Influencing Soil's Structure

Table 4.2 (after Mitchell, 1976, abridged) lists the variables governing the structure of the soil and, hence, its behaviour upon shear loading.

Compositional Factors

Chemical Processes

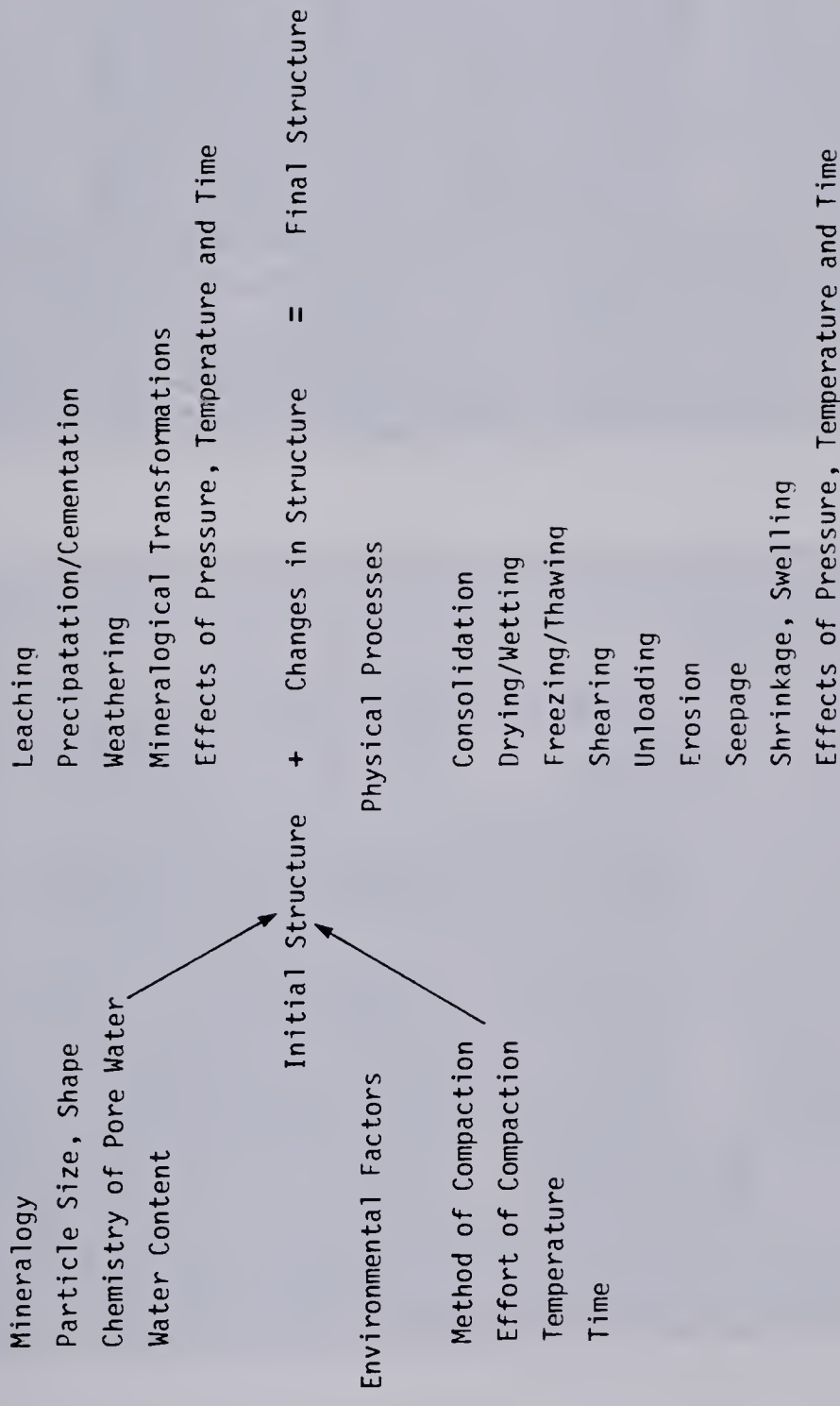


Table 4.2 Structure Determining Factors and Processes for Compacted Soil
(after Mitchell, 1976, abridged)

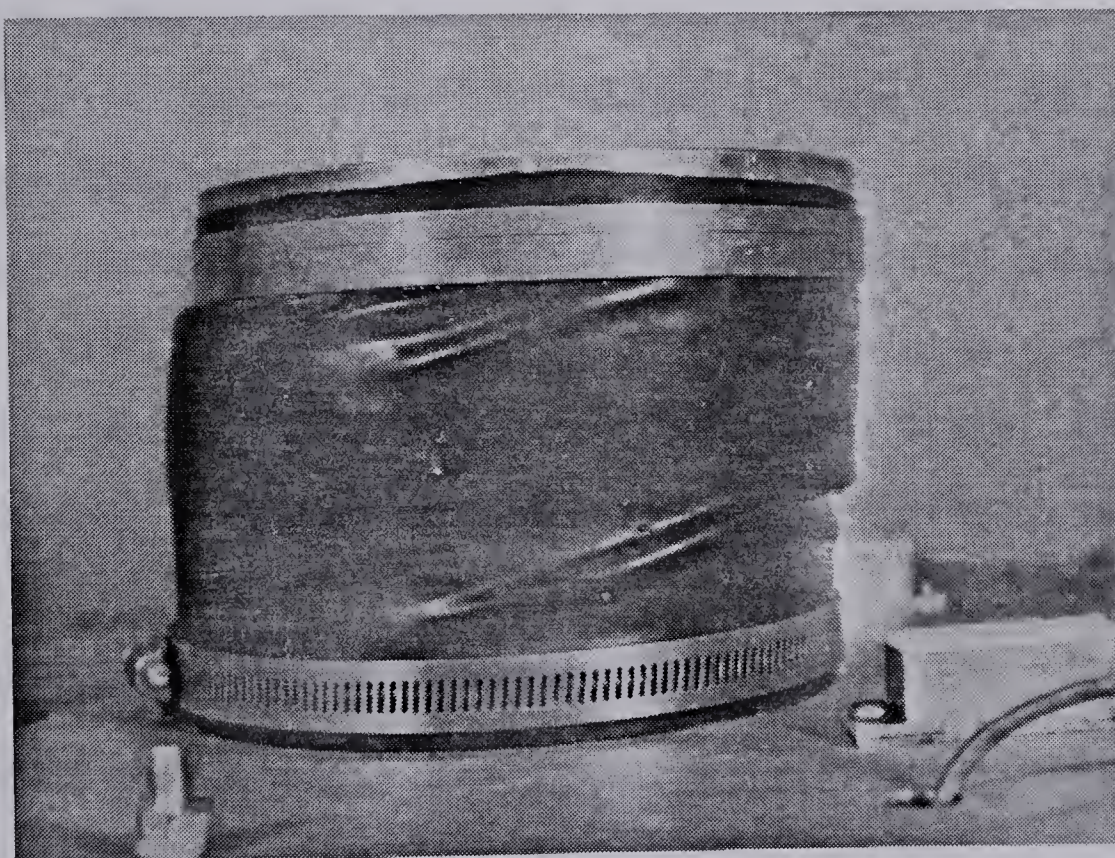
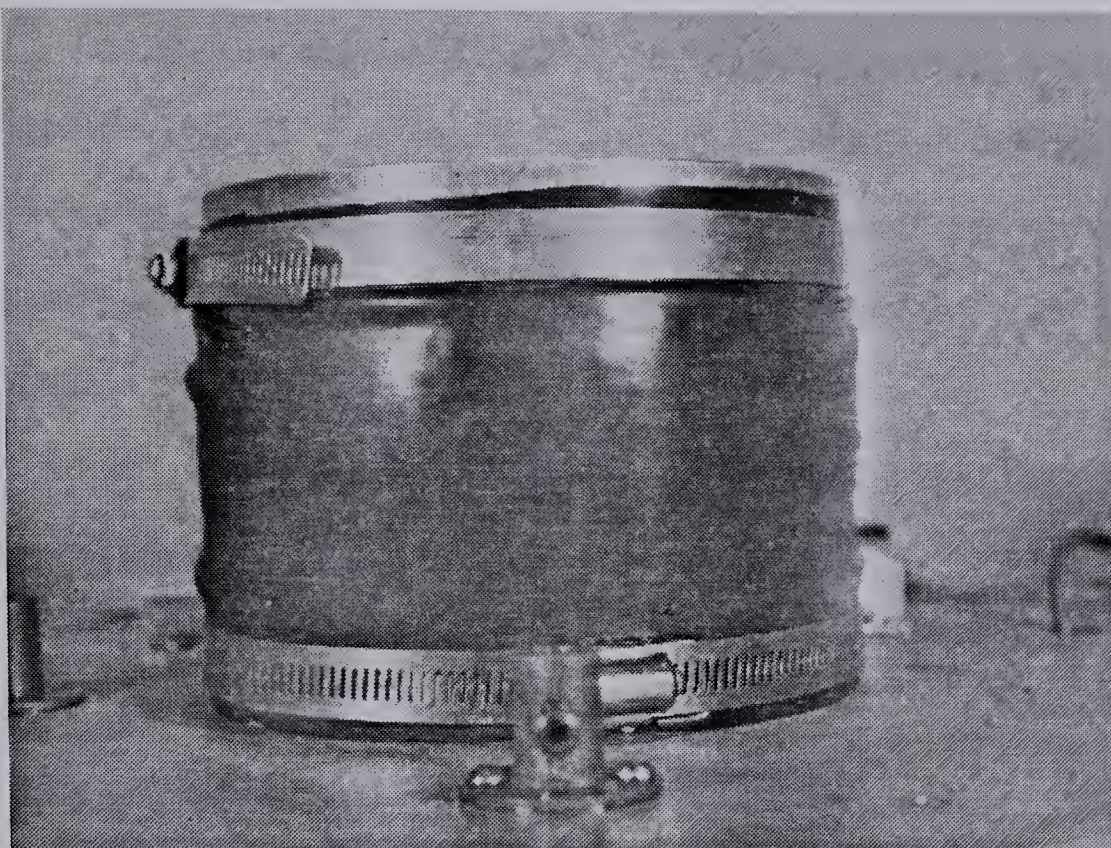


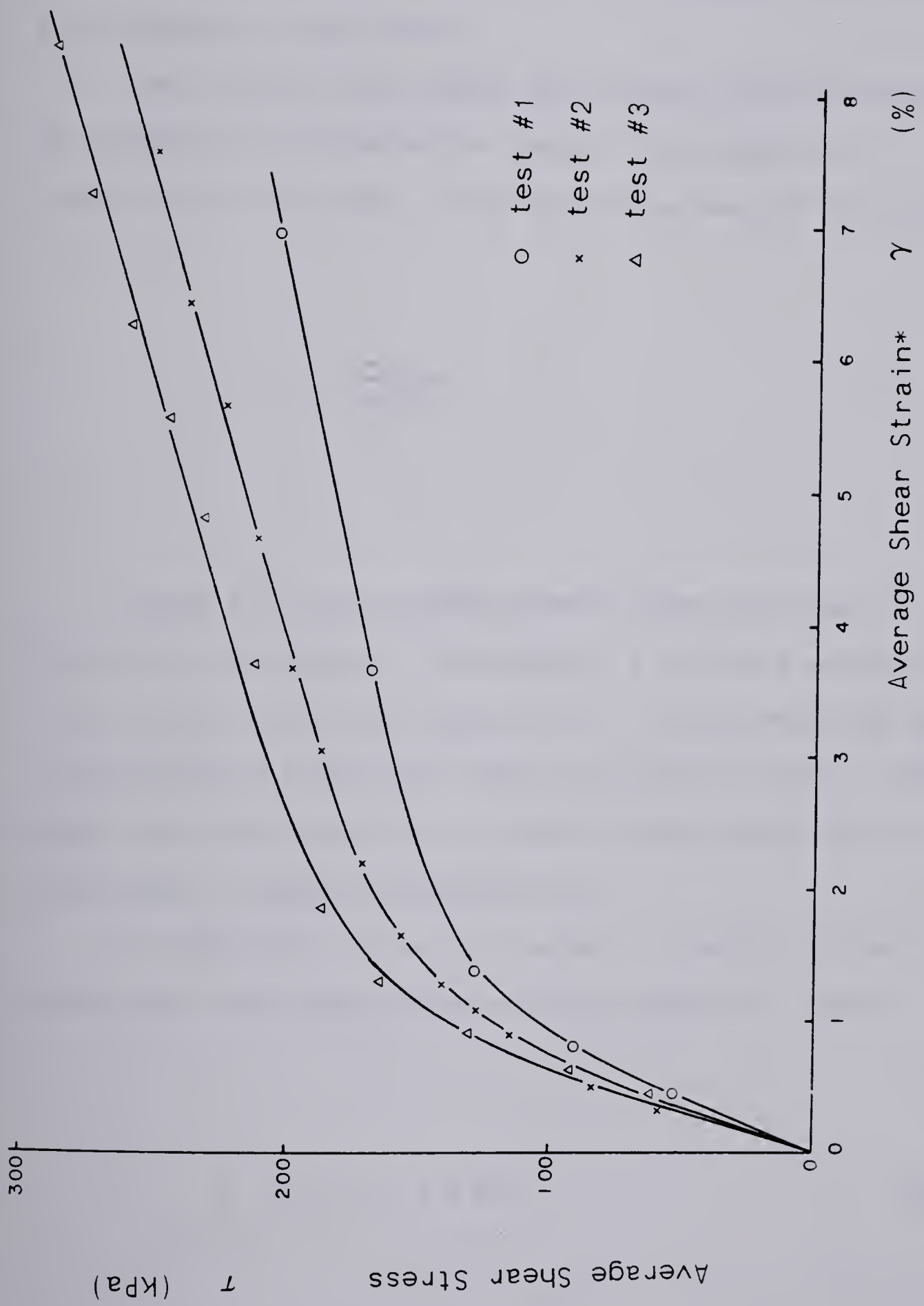
Figure 4.3 Views of Sample #3 Encased in Membrane

A description of the soil tested has been presented on page 69. In preparing a sample, enough distilled water was mixed with the soil to yield an initial water content of 15%. Following this, the sample was allowed to cure and it was then compacted. A Standard Proctor hammer was used for the purpose.

The total energy imparted to the soil was identical to that in a Standard Proctor compaction test. However, the volume of the mould is slightly larger than the conventional one; its shape, as well, is different. The resulting sample was quite soft with a high degree of saturation. This is reflected in the fact that, during compaction, the base of the hammer penetrated the soil's surface upon the application of each blow. Following curing of the compacted sample and apparatus assembly, embedding of the platens in the sample, undrained loading and consolidation would further modify the structure of the soil sample. With due consideration to the imposed boundary conditions, the behaviour during shear should reflect this final structure.

4.4.2 Average Stress Strain Curves

Figure 4.4 shows the average shear stress versus average shear strain curves resulting from the three tests. They all have an initially steep curvilinear portion followed by a second, approximately linear, segment that begins at an average shear strain of about 1.4%. The slope of the latter part of the curve is much less steep. Such a



* (hort. displ. of load cap/initial height of sample)

Figure 4.4 Average Shear Stress as Function of Average Shear Strain

bilinear stress-strain relation seems indicative of a brittle structure; the discontinuity in slope would then likely mark the beginning of its breakdown. In two of the three tests discrete failure planes formed. This is taken as evidence of the above.

The similarities among the stress-strain curves led to an attempt to characterize the data by means of a constitutive relation. The one chosen was of the form:

$$\tau = \frac{\gamma}{a + b\gamma} \quad 4.1$$

where τ is the average shear stress applied to the horizontal surface of the sample, γ is the average shear strain and a and b are constants. Citing previous work, a relationship of the same form was used by Byrne (1976) in modelling the plane strain shear stress-shear strain behaviour of compacted materials.

If the data fit such a curve, it would follow, as it does upon rearranging the previous equation, that:

$$[\gamma/\tau] = a + b\gamma \quad 4.2$$

with the relationship between γ/τ and γ being linear in form. Figure 4.5, showing the variation in magnitude of these quantities during a test, is based on the results of test #2. The relationship is linear until large strains occur where, with failure plane formation, the sample's behaviour would be expected to differ from that in the initial stages of the test.

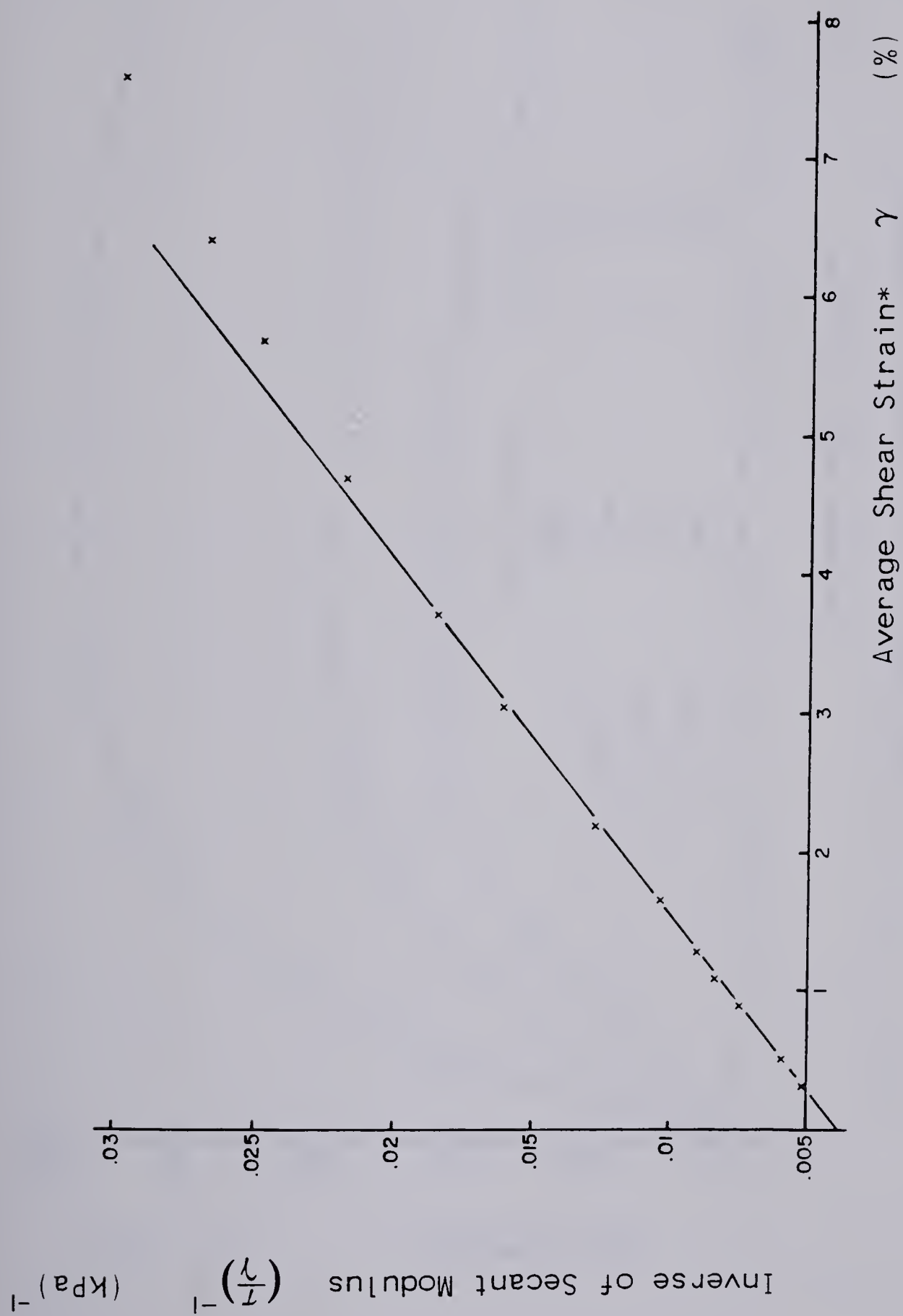
Hence, the stress-strain results are of the form expected.

4.4.3 Average Pore Pressure Shear Strain Curves

Figure 4.6 shows the average pore pressure as a function of average shear strain for each of the three tests. As with the stress-strain curves there is a similarity among the results. The slope of each of them decreases monotonically, reaching slightly negative values at large strains. It is felt that the general form of the curves is reasonable considering the extent to which the soil's structure was determined by the process of consolidation; an initially soft sample was seen, subsequent to consolidation, upon shear, to display a rather brittle structure. The decrease in pore pressure at larger strains would then be in response to a tendency toward volume increase upon formation of the failure plane.

4.4.4 Reformulation of Results

The interrelationship between average applied shear



*(hort. displ. of load cap/initial height of sample)

Figure 4.5 Inverse of Secant Modulus as Function of Average Shear Strain

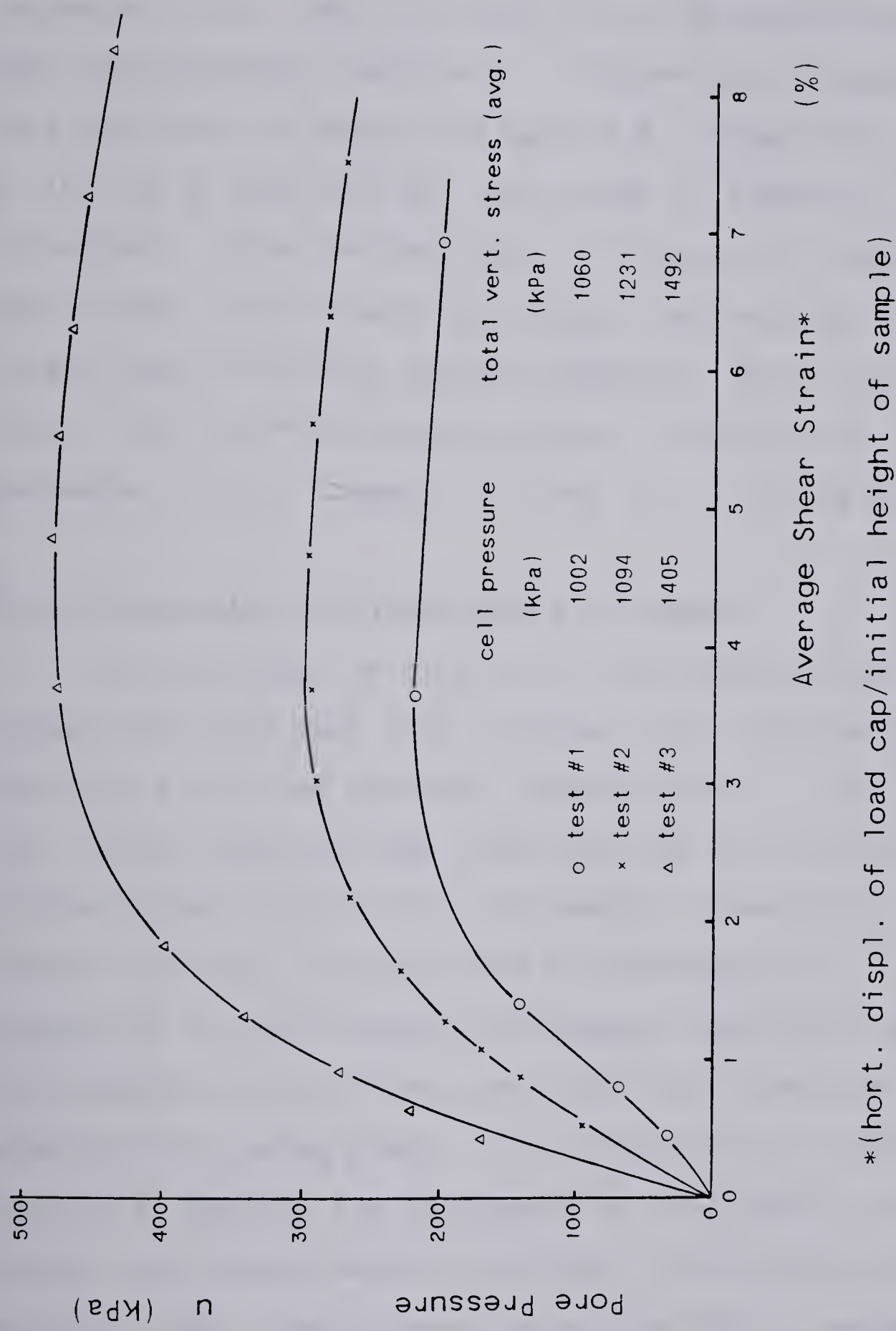


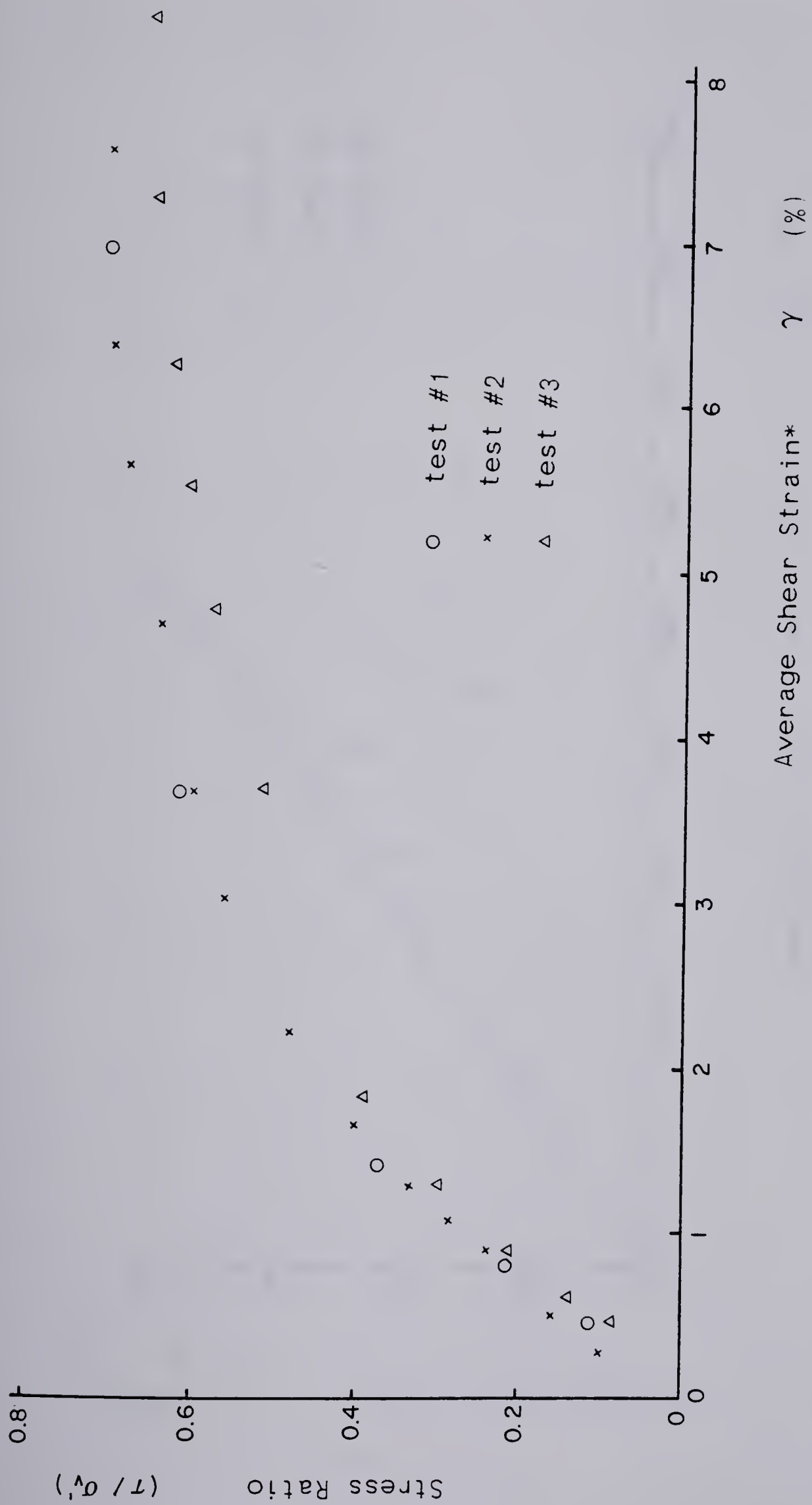
Figure 4.6 Pore Pressure as Function of Average Shear Strain

stress and pore pressure, during the three tests, is demonstrated in Figure 4.7. The independent parameter (τ/σ_v') may be thought of as an indication of the mobilized shearing resistance. Another way of representing this behaviour is shown in Figure 4.8. Except for a portion of the curve from test #3, the curves in Figure 4.7 are coincident. This implies that, in Figure 4.8, points of equal shear strain would lie along lines passing through the origin and inclined at various angles to the horizontal axis. Thus, with increasing strain, in each test, the parameter (τ/σ_v') appears to tend to a limiting value.

4.4.5 Discussion of Stress State in Sample

In discussing the results of the testing program, an attempt has been made only to prove their reasonableness, avoiding a detailed physical interpretation. The reason for this is the uncertainties that exist as to the actual nature of the stress state within the sample. Previously, the stress state was characterized as nonhomogeneous. The generation of pore pressure throughout the sample would then be expected to be similarly so, with pore pressure equalization taking place. For an apparatus of this particular design, the discrepancies that might exist between such experimentally derived relationships and ones based on ideal simple shear tests providing a homogeneous internal stress state are, as yet, unknown.

In light of these concerns, and because of the basic



* (hort. displ. of load cap/initial height of sample)

Figure 4.7 Stress Ratio as Function of Average Shear Strain

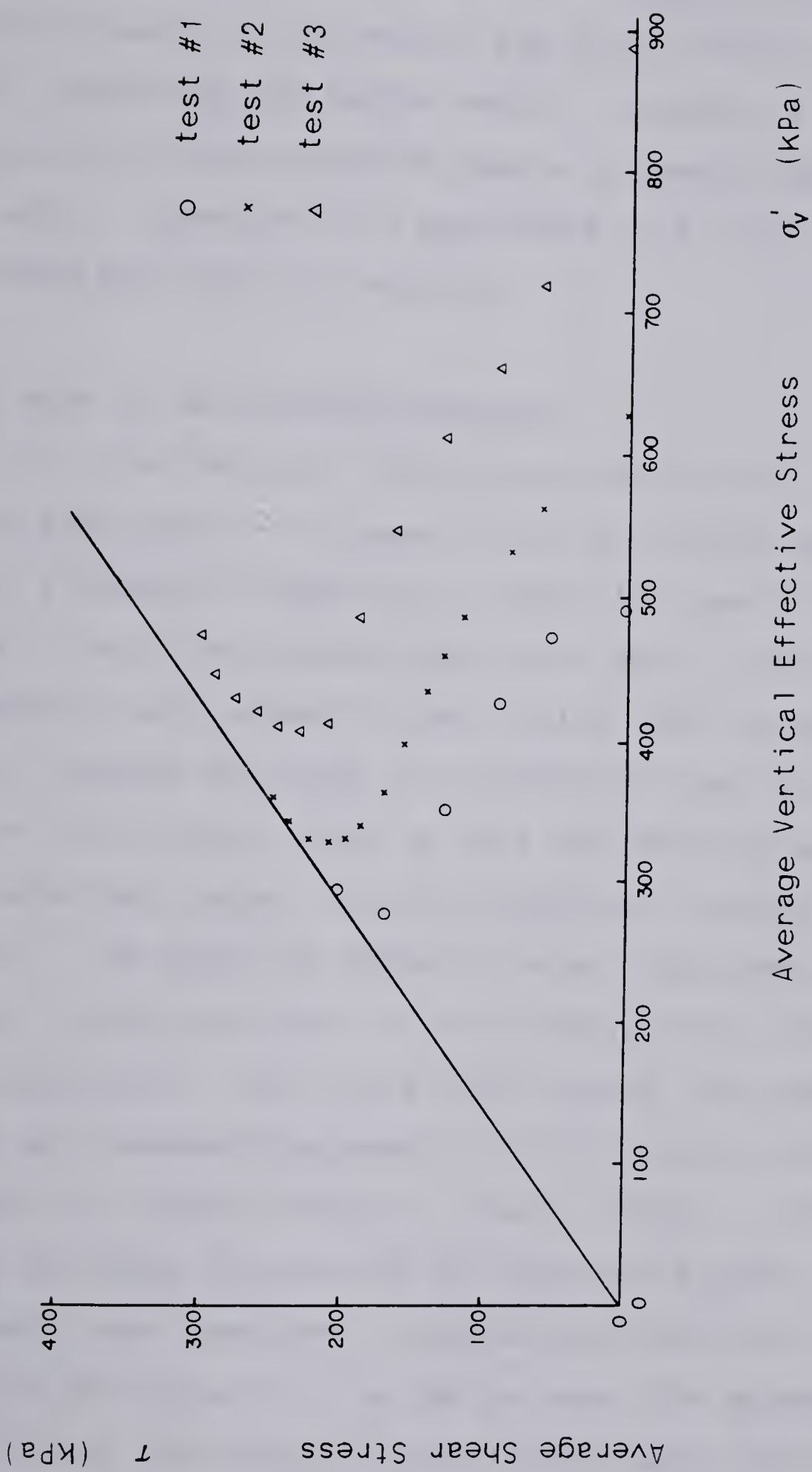
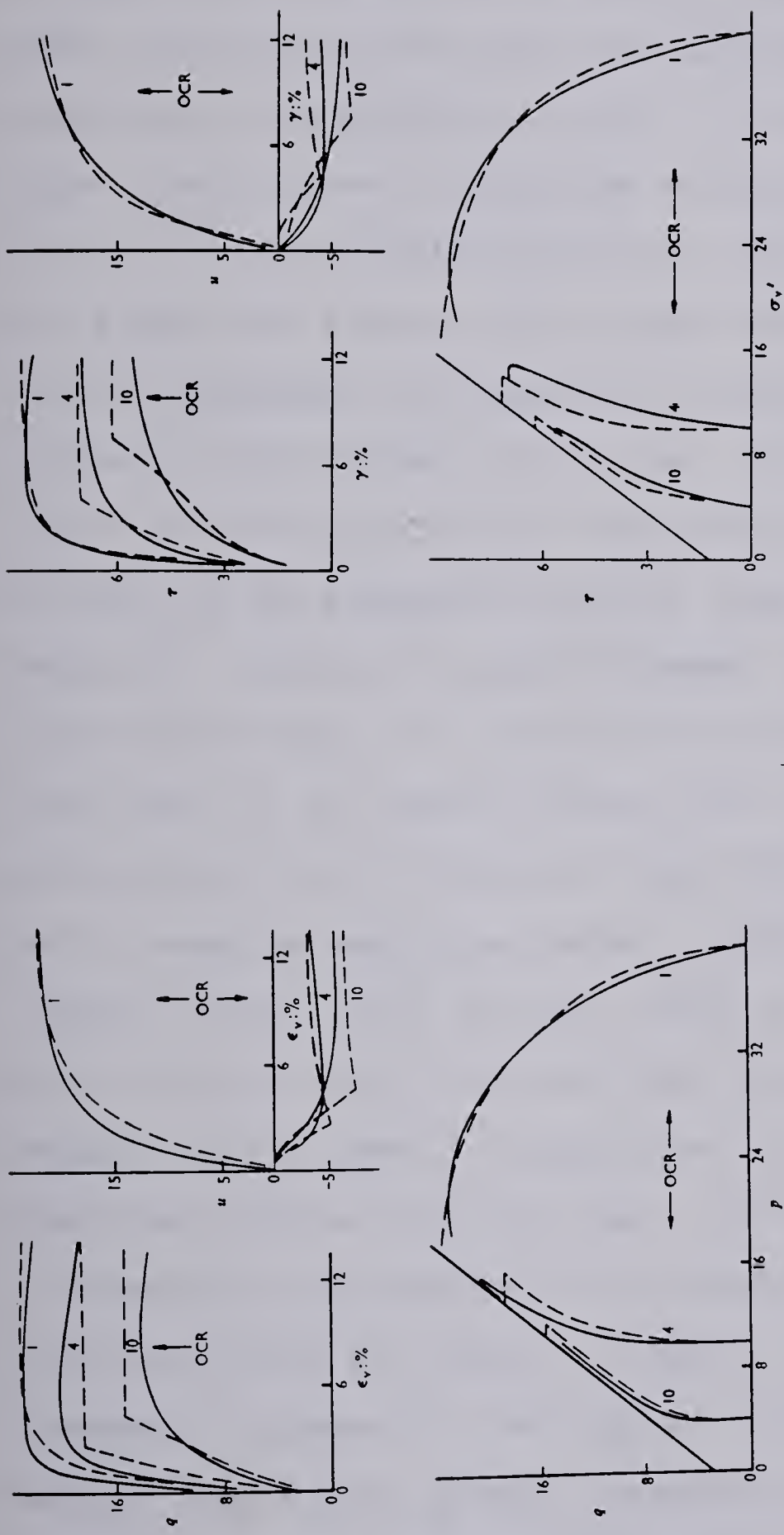


Figure 4.8 Average Shear Stress as Function of Average Vertical Effective Stress

similarities existing between the NGI apparatus and the one used in the present study, it is of interest to note the analytical work of van Eekelen and Potts (1978) and Prevost (1978) concerning the former device. However, a rigorous discussion of the respective papers is beyond the scope of this work. Therefore, the approaches will simply be described and results presented.

4.4.6 Work of van Eekelen and Potts

As a starting point for an analysis of data from cyclic simple shear tests on Drammen clay, van Eekelen and Potts (1978) attempted to construct a model that would predict static triaxial and simple shear test data, given certain fundamental soil properties and initial test conditions. Several changes were made to the Modified Cam Clay model (Roscoe and Burland, 1968) so that the observed and expected soil behaviour, under triaxial compression, would agree closely. The resulting formulation was then generalized, without further revision, to allow analysis of simple shear test conditions. The stress state inside the simple shear sample was assumed homogeneous with the reinforced membrane maintaining a condition of no lateral strain. Only average normal and shear stresses on the horizontal upper surface of the sample were measured. Expected and observed results are compared in Figure 4.9. As can be seen, the agreement is excellent for the normally consolidated case, less good for overconsolidated Drammen clay.



Triaxial Compression

Note:
 observed (—)
 predicted (---)

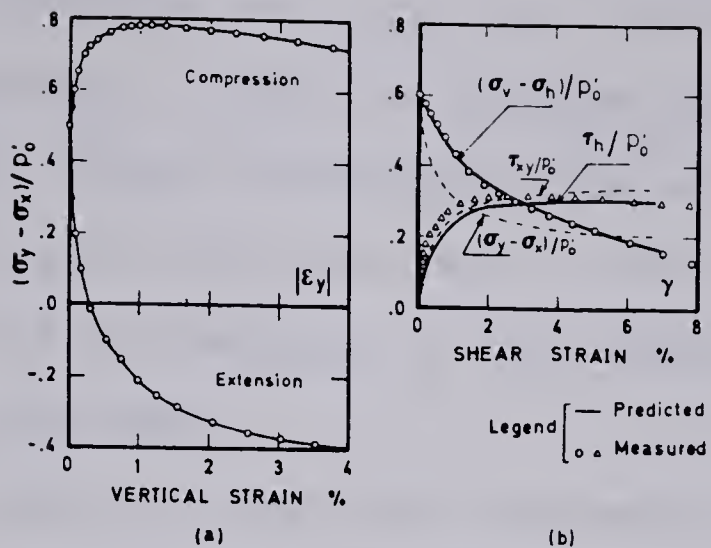
Simple Shear

ϵ_v - vertical strain
 γ - average shear strain

Figure 4.9 Predicted Behaviour of Drammen Clay
 (after van Eekelen and Potts, 1978)

4.4.7 Work of Prevost

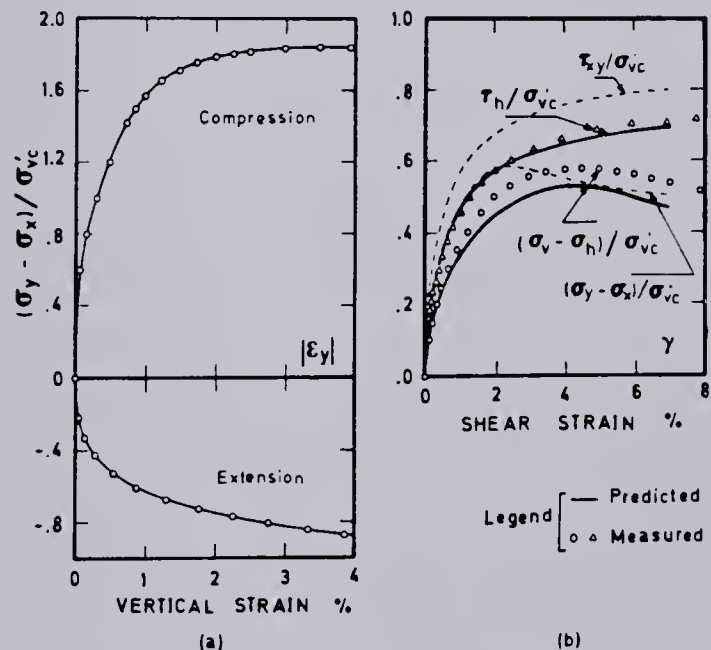
The work by Prevost (1978) draws upon the theories of isotropic and kinematic plasticity. Parameters for the model are derived from observed soil behaviour in triaxial compression and extension tests. In turn, the behaviour under simple shear loading can be predicted. However, contrary to van Eekelen and Potts (1978), Prevost (1978) did not assume the stress state within the simple shear sample to be homogeneous; an approach, it was said, dictated by the nature of the boundary conditions. During the simple shear tests, the average vertical and horizontal normal stresses as well as the average horizontal shear stresses were measured. Tests were run on Drammen clay. In the normally consolidated case, the samples were consolidated under conditions of no lateral strain until the vertical effective stress equalled that that was carried in the field. Another set of samples was consolidated, under conditions of no lateral strain, to a vertical effective stress greater than that carried in the field and then the vertical stress was reduced, again under K_0 conditions, to yield an overconsolidation ratio of four. Following consolidation, all samples were sheared in the undrained mode. The results and predictions are shown in Figures 4.10 and 4.11. The agreement is generally very good. Of interest also are the dotted lines on the graphs, accompanying the simple shear results. These represent the predictions of material behaviour for ideal simple shear tests, i.e. tests in which



dashed curves are material curves
see page 94

P'_0 - in situ vertical effective stress

Figure 4.10 Predicted Behaviour of Normally Consolidated Drammen Clay
(after Prevost, 1978)



σ'_{vc} - vertical effective stress upon K_0 unloading

Figure 4.11 Predicted Behaviour of Overconsolidated Drammen Clay
(after Prevost, 1978)

the boundary conditions are such that the internal stress state is homogeneous. Since van Eekelen and Potts (1978) did not consider stress nonhomogeneities within the sample, their predictions of soil behaviour in the simple shear test may be thought of as analogous to the material curves of Prevost, just mentioned.

Perhaps, their fit could be improved by consideration of such nonhomogeneities. However, regardless, it is felt that the preceding discussion of the two papers demonstrates the reasonableness of the data that can be obtained using the present apparatus and, hence, its role in a study of the material behaviour of compacted soil.

CHAPTER 5

CONCLUSIONS AND RECOMMENDATIONS FOR FURTHER RESEARCH

5.1 General

To begin the chapter, the ultimate goals and current aims of the present research program are stated. The conclusions which may be drawn from it are then discussed. Finally, recommendations for further research are outlined.

5.2 Review of Thesis

In the introduction to this thesis, some of the aims of earth dam design were recounted and the consequent desirability of the capacity to predict stresses and pore pressures, throughout the working life of the dam, then noted. Techniques such as the finite element method can be used to yield approximate results for this purpose. Attention was focussed on the periods of construction and first filling of the reservoir and, in that light, two constitutive models that might be incorporated in such analyses were reviewed. It was decided, keeping in mind the aims of earth dam design alluded to above, that research in the area of simple shear soil testing would be of value.

The aims were stated as follows:

- a. to design and build a simple shear apparatus for testing samples of compacted soil at elevated pressures, and
- b. to demonstrate, by comparing experimental and

expected results, that the data derived from such tests are meaningful.

The construction of a new type of simple shear apparatus was then advocated. In support of this decision, the level of technology reflected in the design, simplicity of accompanying laboratory procedures and recent work concerned with the modelling of soil behaviour in the simple shear apparatus were cited. A detailed description of the apparatus and experimental results, obtained, followed.

5.3 Conclusions

On the basis of the testing program, the following conclusions can be drawn:

- a. in general, in a mechanical sense, the cell and loading systems functioned well. There is some friction developed between the rams and associated bushings but this can be estimated and accounted for.
- b. the sensitivity of the lateral deformation measuring system must be heightened. This may require improvement of the present gauge or design of a new one; examples of different designs, such as that of Menzies (1976), may be found in the literature. Whichever route is chosen, the problems are not insurmountable.
- c. the sample preparation and apparatus assembly procedures allowed samples of a uniformly good

quality to be produced.

The second aim of the thesis was to show that the data produced by the apparatus are meaningful. In a qualitative sense, the average shear stress-strain and pore pressure-strain curves are as expected. This point was discussed in Chapter 4. Some uncertainties in interpretation are introduced by the inadequate performance of the lateral gauge, mentioned before, and the stress nonhomogeneities within the sample generated by the boundary conditions. However, the test results may still be taken as an indication of the usefulness of the apparatus in the course of this research.

As concerns the former problem, the performance of the gauge may be upgraded. The effects of the boundary conditions on the homogeneity of the stress state are perhaps more serious. However, it would appear from the review of the work by van Eekelen and Potts (1978) and Prevost (1978) that the results of an apparatus of this general type are predictable and, therefore, in another sense, meaningful. The material response under boundary conditions inducing a homogeneous stress state can then be recovered (see Figure 4.11, page 95). The ability to predict test results, in the case of the present simple shear device, would prove its validity as a model test on the same footing as the NGI device.

5.4 Recommendations for Further Research

As indicated in the first chapter of this thesis, the ultimate goal of this research is the formulation of a practical yet comprehensive model for compacted soil to be used in design. The necessary complexity and power of such a model is dictated by considerations such as the physical quantities to be predicted and uncertainties in the processes to be modelled. To reach this goal, the following recommendations are made:

- a. more testing should be done, using the present apparatus, over a wide range of pressures; the maximum working cell pressure is 2800 kPa. These tests might take the form of those run as part of the present program or another; for example, drained K_o loading followed by undrained K_o unloading and horizontal shear loading, as before.

This would require, in addition to the recommended modifications noted previously in the chapter, that the compliance of the drainage and pore pressure measuring systems be reexamined in order that the experimental results reflect only the behaviour of the soil sample.

Also, tests on unsaturated soils may be contemplated. Considerations involved in such testing may be found in the work of Fredlund (1973) and Law (1975), among others.

- b. a comprehensive model for the stress-strain

behaviour of compacted soil should be developed, capable of predicting soil behaviour in the simple shear test, under the above mentioned loading conditions.

The first recommendation will lead to a greater understanding of the material response of compacted clay under a wider range of loading conditions. The second will allow the recovery of the material response of such soils under ideal simple shear conditions, as done by Prevost (see page 94). Further, the prediction of field behaviour, based on analyses using hyperbolic and elastoplastic formulations, would provide more evidence of present abilities to model the processes ongoing during construction and reservoir filling and, hence, of the predictive capabilities required of models used in such analyses.

REFERENCES

- Berre, T. 1969. The latest design of the N.G.I. Simple Shear Apparatus. Proceedings, 7th International Conference on Soil Mechanics and Foundation Engineering, Contribution to Specialty Session No. 16, New Laboratory Methods of Investigating Soil Behaviour, Mexico, Vol. 3, pp. 525-526.
- Bishop, A.W., Green, G.E., Garga, V.K., Andresen, A., and Brown, J.D. 1971. A new ring shear apparatus and its application to the measurement of residual strength. *Geotechnique*, 21(4), pp. 273-328.
- Bishop, A.W., and Henkel, D.J. 1962. The measurement of soil properties in the triaxial test. 2nd ed. Edward Arnold (Publisher) Ltd., London, England.
- Bjerrum, L., and Landva, A. 1966. Direct simple-shear tests on a Norwegian quick clay. *Geotechnique*, 16(1), pp. 1-20.
- Black, D.K., and Lee, K.L. 1973. Saturating laboratory samples by back pressure. *ASCE Journal of the Soil Mechanics and Foundations Division*, 99(SM1), pp. 75-93.
- Chang, C.S. 1976. Analysis of consolidation of earth and rockfill dams. Ph.D. thesis, University of California, Berkeley, California, 225 p.
- Design of small dams. 1977. United States Department of the Interior, Bureau of Reclamation, revised 2nd edition, United States Government Printing Office, Washington, D.C., 816 p.

- Duncan, J.M., Byrne, P., Wong, K.S., and Mabry, P. 1978. Strength, stress-strain and bulk modulus parameters for finite element analyses of stresses and movements in soil masses. Office of Research Services, University of California, Berkeley, California, Report No. UCB/GT/78-02 to National Science Foundation, 83 p.
- Duncan, J.M., and Chang, C.Y. 1970. Nonlinear analysis of stress and strain in soils, ASCE Journal of Soil Mechanics and Foundations Division, 96(SM5), pp. 1629-1653.
- Duncan, J.M., and Dunlop, P. 1969. Behavior of soils in simple shear tests. Proceedings, 7th International Conference on Soil Mechanics and Foundation Engineering, Tokyo, Japan, Vol. 1, pp. 101-109.
- Dunlop, P., Duncan, J.M., and Seed, H.B. 1968. Finite element analyses of slopes in soil. Office of Research Services, University of California, Berkeley, California, Report No. TE-68-3 to U.S. Army Engineers, Waterways Experiment Station, 232 p.
- Finn, W.D.L., Pickering, D.J., and Bransby, P.L. 1971. Sand liquefaction in triaxial and simple shear tests. ASCE Journal of the Soil Mechanics and Foundations Division, 97(SM4), pp. 639-659.
- Fredlund, D.G. 1973. Volume change behaviour of unsaturated soils. Ph. D. thesis, University of Alberta, Edmonton, Alta., 878 p.
- Hvorslev, M.J., and Kaufman, R.I. 1952. Torsion shear

- apparatus and testing procedures. Waterways Experiment Station, Vicksburg, Mississippi, Bulletin 38, 76 p.
- Kjellman, W. 1951. Testing the shear strength of clay in Sweden. *Geotechnique*, 2(3), pp. 225-232.
- Kulhawy, F.H., and Gurtowski, T.M. 1976. Load transfer and hydraulic fracturing in zoned dams. *ASCE Journal of the Geotechnical Engineering Division*, 102(GT9), pp. 963-974.
- Ladd, C.C., and Edgers, L. 1972. Consolidated-undrained direct-simple shear tests on saturated clays. Department of Civil Engineering, Massachusetts Institute of Technology, Cambridge, Massachusetts, Research Report R72-82, 245 p.
- Law, S.T.C. 1975. Deformations of earth dams during construction. Ph. D. thesis, University of Alberta, Edmonton, Alta., 364 p.
- Lowe, III, J., and Johnson, T.C. 1960. Use of back pressure to increase degree of saturation of triaxial test specimens. *Proceedings, ASCE Research Conference on Shear Strength of Cohesive Soils*, Boulder, Colorado, pp. 819-836.
- Lucks, A.S., Christian, J.T., Brandow, G.E., and Hoeg, K. 1972. Stress conditions in NGI simple shear test. *ASCE Journal of the Soil Mechanics and Foundations Division*, 98(SM1), pp. 155-160.
- Menzies, B.K. 1976. Design manufacture and performance of a lateral strain device. *Geotechnique*, 26(3), pp.

542-544.

Mitchell, J.K. 1976. Fundamentals of soil behaviour. John Wiley & Sons, Inc., New York.

Nobari, E.S., and Duncan, J.M. 1972,a. Movements in dams due to reservoir filling. Proceedings, ASCE Specialty Conference on Performance of Earth and Earth-Supported Structures, Lafayette, Indiana, Vol. 1, Pt. 1, pp. 797-815.

Nobari, E.S., and Duncan, J.M. 1972,b. Effect of reservoir filling on stresses and movements in earth and rockfill dams. Office of Research Services, University of California, Berkeley, California, Report No. TE-72-1 to The Office, Chief of Engineers, U.S. Army, Waterways Experiment Station, 186 p.

Penman, A.D.M., and Charles, J.A. 1979. The influence of their interfaces on the behaviour of clay cores in embankment dams. Transactions, 13th International Congress on Large Dams, New Delhi, India, Vol. 1, pp. 695-714.

Prevost, J.H. 1978. Anisotropic undrained stress-strain behaviour of clays. ASCE Journal of the Geotechnical Engineering Division, 104(GT8), pp. 1075-1090.

Prevost, J.H., and Hoeg, K. 1976. Reanalysis of simple shear soil testing. Canadian Geotechnical Journal, 13, pp. 418-429.

Roscoe, K.H. 1953. An apparatus for the application of simple shear to soil samples. Proceedings, 3rd

International Conference on Soil Mechanics and Foundation Engineering, Switzerland, Vol. 1, pp. 186-191.

Roscoe, K.H. 1970. The influence of strains in soil mechanics. *Geotechnique*, 20(2), pp. 129-170.

Roscoe, K.H., Bassett, R.H., and Cole, E.R.L. 1967. Principal axes observed during simple shear of a sand. *Proceedings of the Geotechnical Conference, Oslo, Norway*, Vol. 1, pp. 231-237.

Seed, H.B., Duncan, J.M., and Idriss, I.M. 1975. Criteria and methods for static and dynamic analysis of earth dams. *Proceedings, International Symposium on Criteria and Assumptions for Numerical Analysis of Dams, Swansea, U.K.*, Edited by D.J. Naylor, K.G. Stagg and O.C. Zienkiewicz, pp. 564-588.

Seed, H.B., Leps, T.M., Duncan, J.M., and Bieber, R.E. 1976. Hydraulic fracturing and its possible role in the Teton Dam failure. In "Failure of Teton Dam, Report to United States Department of the Interior and State of Idaho by Independent Panel to Review Cause of Teton Dam Failure", United States Government Printing Office, Washington, D.C., Appendix D, 39 p.

Squier, L.R. 1970. Load transfer in earth and rockfill dams. *ASCE Journal of the Soil Mechanics and Foundations Division*, 96(SM1), pp. 213-233.

Stewart, R.A. 1979. Pore pressures in earth dams during impounding. M. Sc. thesis, University of Alberta,

- Edmonton, Alta., 161 p.
- Thurner, H.F. 1973. Testing machine for investigation of compacted soil. Proceedings, 8th International Conference on Soil Mechanics and Foundation Engineering, Moscow, U.S.S.R., Vol. 1, Pt. 2, pp. 447-451.
- Vaid, Y.P., and Campanella, R.G. 1973. Making rubber membranes. Canadian Geotechnical Journal, 10, pp. 643-644.
- van Eekelen, H.A.M., and Potts, D.M. 1978. The behaviour of Drammen clay under cyclic loading. Geotechnique, 28(2), pp. 173-196.
- Wilson, S.D. 1977. Proceedings, 9th International Conference on Soil Mechanics and Foundation Engineering, Contribution to Specialty Session No.8, Deformation of Earth/Rockfill Dams, Tokyo, Japan, Vol. 3, pp. 527-531.
- Wood, D.M., Drescher, A., and Budhu, M. 1979. On the determination of stress state in the simple shear apparatus. Geotechnical Testing Journal, 2(4), pp. 211-221.
- Wood, D.M., and Budhu, M. 1980. The behaviour of Leighton Buzzard sand in cyclic simple shear tests. In "Soils under cyclic and transient loading:proceedings of the International Symposium on Soils under Cyclic and Transient Loading", Edited by G.N. Pande and O.C. Zienkiewicz, Rotterdam:Balkema.

APPENDIX A
CALIBRATION OF APPARATUS

A.1 Procedure for Friction Determination

An aluminum spacer, of dimensions similar to those of an actual sample, was positioned on the pedestal. A small, cylindrical load cell was then placed on the aluminum spacer, its axis aligned with those of the pedestal and spacer. The line from the load cell was connected to the electrical lead, passing through the cell base, normally used for the lateral strain gauge. To prevent later difficulties such as displacement of the yoke upon increase in cell pressure, the load cap was rotated through 180° and, upon positioning the cell wall, the yoke was pulled towards the wall as far as possible. The cell was then assembled as usual; the load cell being located, ultimately, between the load cap and aluminum spacer. Finally, the cell was lifted from the movable plate and placed on the loading frame base proper. The vertical load cell was then screwed into place and the main crosspiece secured. Initial values of the output of the internal and external load cells and the cell pressure transducer were obtained.

At the beginning of a test, the air pressure in the line leading to the vertical belofram was increased to about 140 kPa. The cell pressure was then increased to the desired level. The vertical seating load prevented the ram's being forced upwards upon an increase in cell pressure. When the cell pressure had come to equilibrium, the pressure in the line to the Bellofram was increased to

about 275 kPa and then, successively, to 552, 827, 1103 and 1379 kPa. At each vertical load level, the internal load cell output was allowed to come to an essentially stationary value (usually taking a minute or two) and then readings were taken of the load cell's output and the output of the cell pressure transducer. Upon reaching a line pressure to the vertical Bellofram of 1379 kPa, the pressure was reduced to the levels previously mentioned (1103, 827, 552 kPa etc,) and readings taken. Tests, as described above, were run for various cell pressures from atmospheric pressure to 1535 kPa. The results will be presented later in this appendix.

At the time these tests were run, there was some question of the internal load cell's readings possibly being affected by elevated cell pressure. To determine the extent of this effect, with the cell assembled as described previously, the output of the internal load cell was noted, for a variety of cell pressures. Each was large enough that, in the absence of an applied vertical load, the loading cap was forced away from the load cell. At the end of the test, when the cell pressure was reduced to zero, the measured output of the load cell rose noticeably as the load cap came into contact with the load cell. Up until that time, for the complete range of pressures applied, the output had been sensibly constant. Thus, it was concluded that elevated cell pressures had no effect on the functioning of the internal load cell. Figure A.1 presents, schematically, the forces acting on the load cap-vertical

ram assembly during the friction determination test. The load due to the self weight of the ram-load cap system, load C, is reflected in the initial output of the internal load cell. The magnitude of load D may be calculated easily and is constant for a given cell pressure. Hence, with an increase in applied vertical load, the change in output of the internal load cell directly reflects the effect of the frictional force. Further, all parameters being known, the value of frictional force can be calculated. Figure A.2 presents the quantity (A-D) as a function of (E-C), for various cell pressures. The significance of the letters is as in Figure A.1 .

The horizontal displacement of any experimentally determined point from the no friction loss line is a measure of the frictional load, B, acting at that point in the test. There is a slight dependence of the frictional load on the magnitude of the net external load, (A-D), but it is essentially independent of cell pressure. The total vertical load to which the sample is subjected is composed of a deviatoric load and one due to the cell pressure. It is only the former that is plotted on the ordinate in Figure A.2 . As a percentage of the total vertical load, that lost to friction is quite small.

For present purposes. the above method of determining the frictional loads acting on the vertical ram is deemed sufficient. A more comprehensive study was required for determination of loads acting on the horizontal ram.

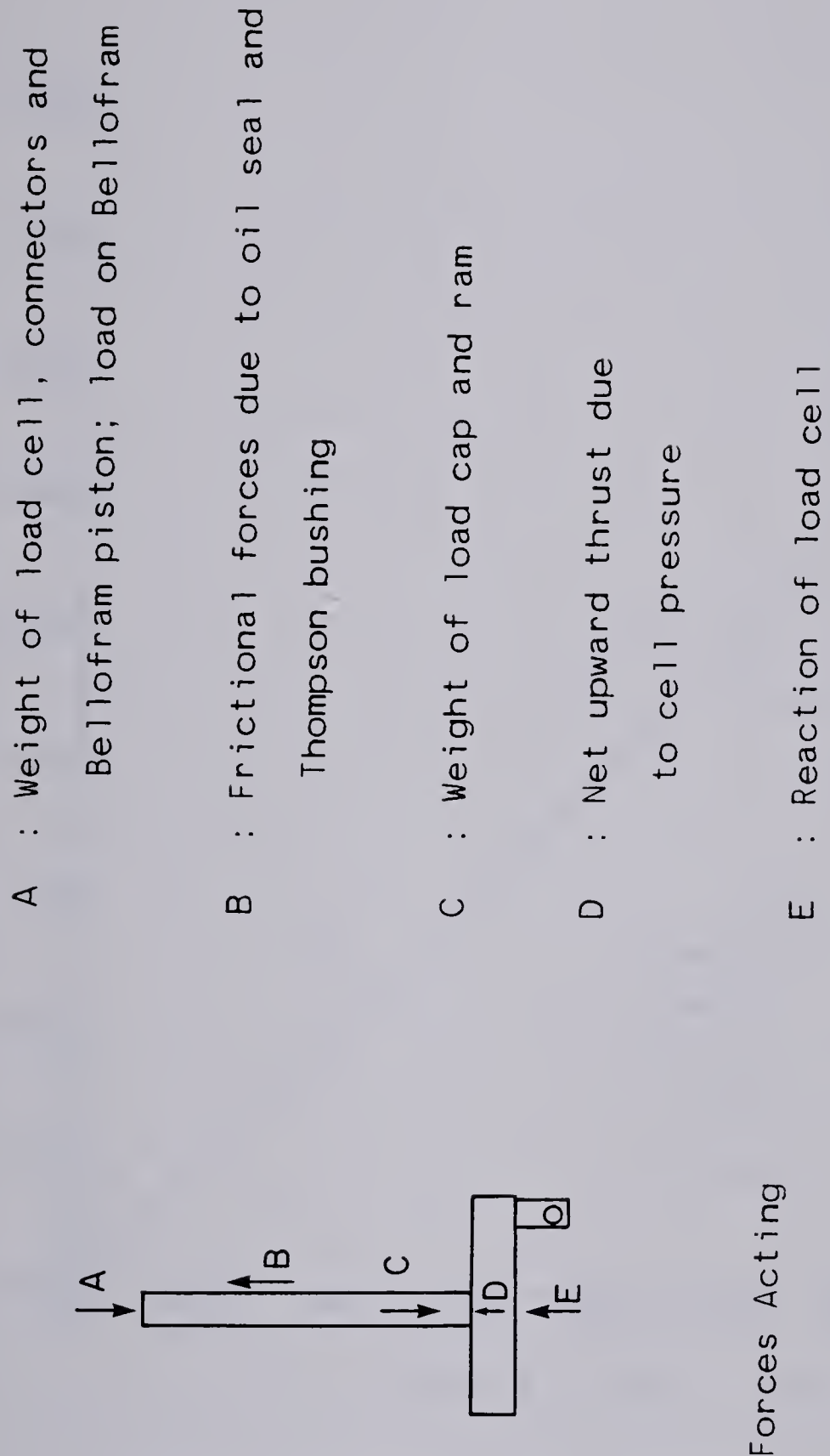
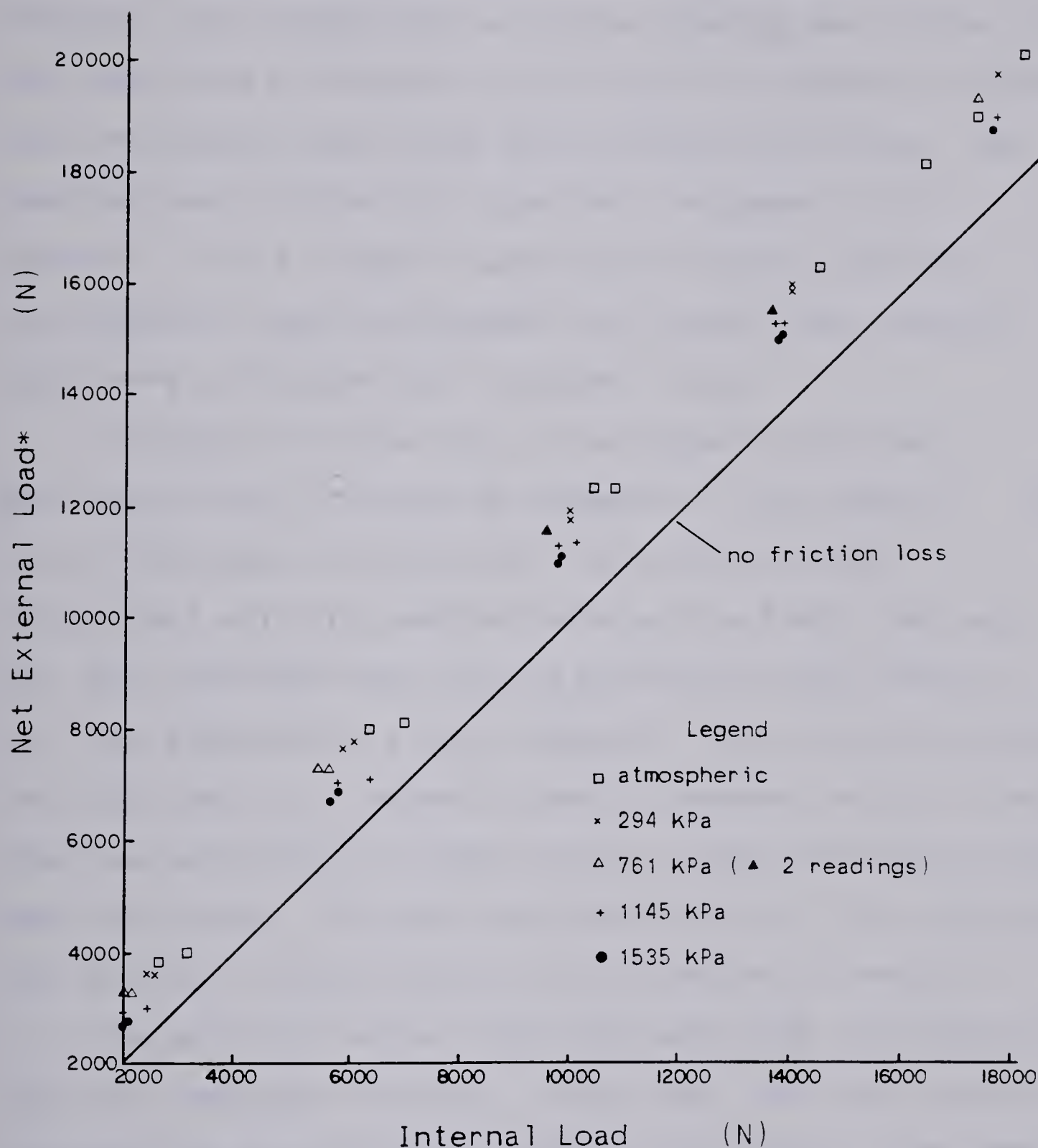


Figure A.1 Forces Acting on Load Cap-Vertical Ram Assembly



*(Bellotram load - cell pressure thrust)

Figure A.2 Net Internal Load as Function of External Load

A.2 Determination of Horizontal Friction Loss

The testing configuration used to determine the friction loss through the horizontal bushing was similar to that described previously for the vertical bushing. A known tensile load was applied by the horizontal belofram. The reaction was provided by a load cell anchored to the pedestal. For a range of such applied loads, whatever discrepancies appeared between the internal and external loads were attributed to frictional forces.

To prepare for the test, a rectangular plate was machined so that it could be screwed onto the pedestal. The head of the yoke, that portion that normally comes into contact with the vertical arms of the lower load cap, was then unscrewed from the one passing through the cell wall and replaced by a small adapter. This in turn screwed into the load cell, normally used to measure vertical loads, that was anchored by a stock bolted to the rectangular plate mentioned above. It should be noted that for this occasion the vertical load cell had to be calibrated in tension.

The vertical ram was then unscrewed from the load cap and both components removed. After that, the cell cap was attached and the cell positioned on the loading frame base. The tie rods were then removed and the cell cap raised. Upon connecting an electrical line to the internal load cell, two small wooden blocks were placed on the upper flange of the cell wall and the cell cap once again lowered until it came in contact with them. These blocks provided

support for the cell cap and, at the same time, ensured sufficient clearance for the line to the vertical (internal) load cell. The cell base was then bolted to the loading frame and the horizontal loading system finally connected.

During a test, a monotonically increasing series of loads was applied, using the horizontal Bellofram, and the outputs of the external and internal loads cells recorded. The procedure was then repeated as the applied loads were decreased. With the results of the first friction determination in mind (see Figure A.1) it was decided not to run tests at elevated cell pressures.

Normally, when a load cell is calibrated, the output is recorded for given range of known applied loads. Assuming the load-output relationship to be linear, a straight line is fit to the data. Thereafter, until a further calibration is deemed necessary, one determines the magnitude of a change in applied load based on the accompanying change in load cell output and the slope of the calibration curve. This approach is acceptable for applied loads greater than approximately 10% of the maximum working load. However, when the load cell is to be used in low load ranges, the nonlinearity of the calibration curve should be considered in detail.

To do this, a piecewise linear curve was selected to represent the actual calibration curve. Figure A.3 shows this function, as well as the assumed calibration curve. For a given load cell output, the true and apparent applied

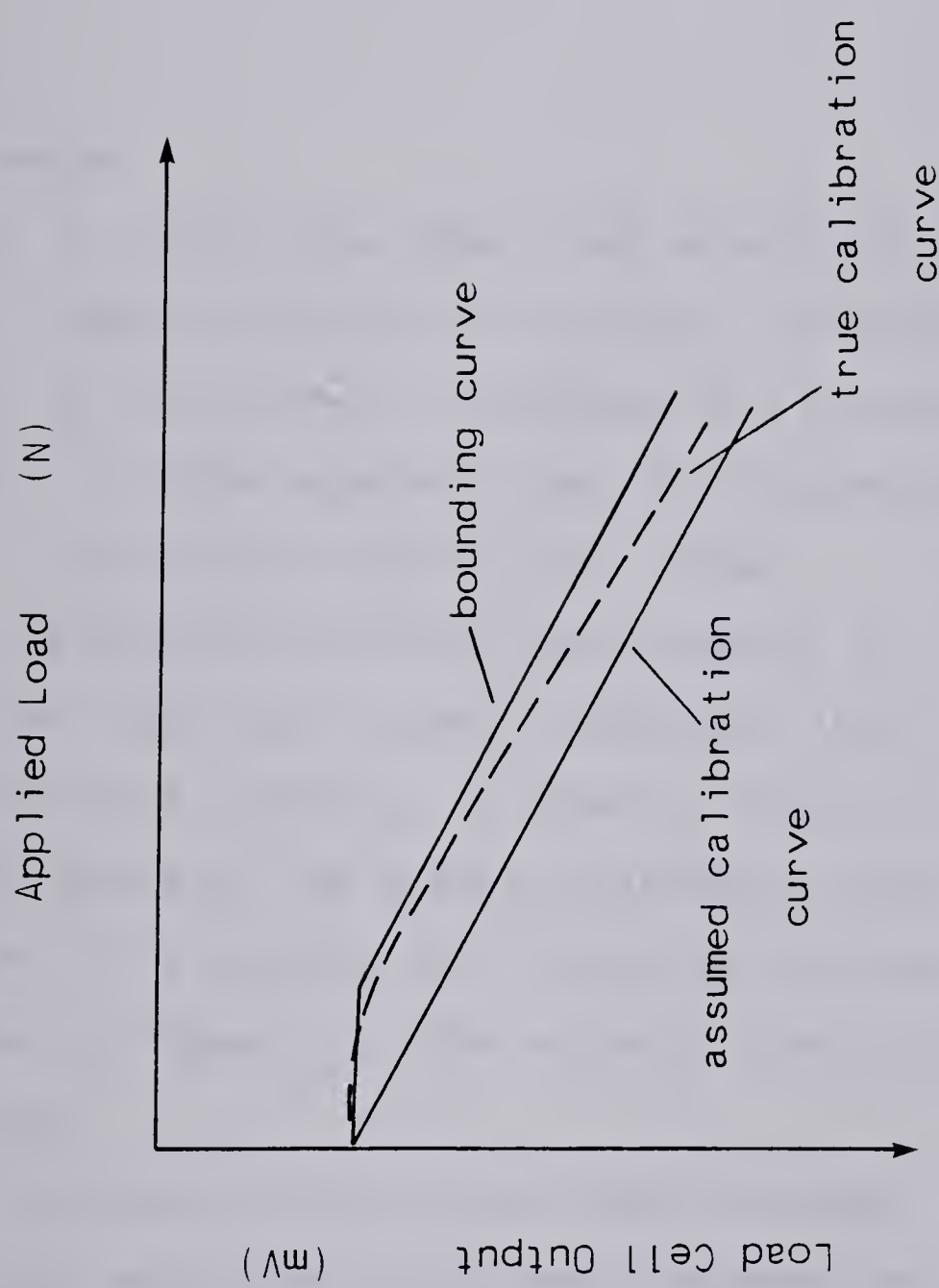


Figure A.3 Idealization of Calibration Curve

loads could then be linked by an equation of the form:

$$r = (1-q)t \quad A.1$$

where:

- a. r is the true load; that determined using the representation of the actual calibration curve
- b. q is the error, expressed as a percentage, and,
- c. t is the apparent load; that determined assuming the calibration curve to be linear.

The absolute value of the parameter q , for the two different load cells used to determine the friction loss in the horizontal bushing, is shown in Figure A.4. Depending on the nature of the actual calibration curve, that is, whether it is concave up or down, as portrayed in a diagram similar to Figure A.3, the value of q may be positive or negative.

The load cell data were then corrected. Figure A.5 shows the resulting relationship between the true external load and the true internal load. The load lost due to friction in the horizontal bushing system is apparently about 10% of the true external load.

However, since a stiff measuring element, the internal load cell, was utilized in determining the friction loss due

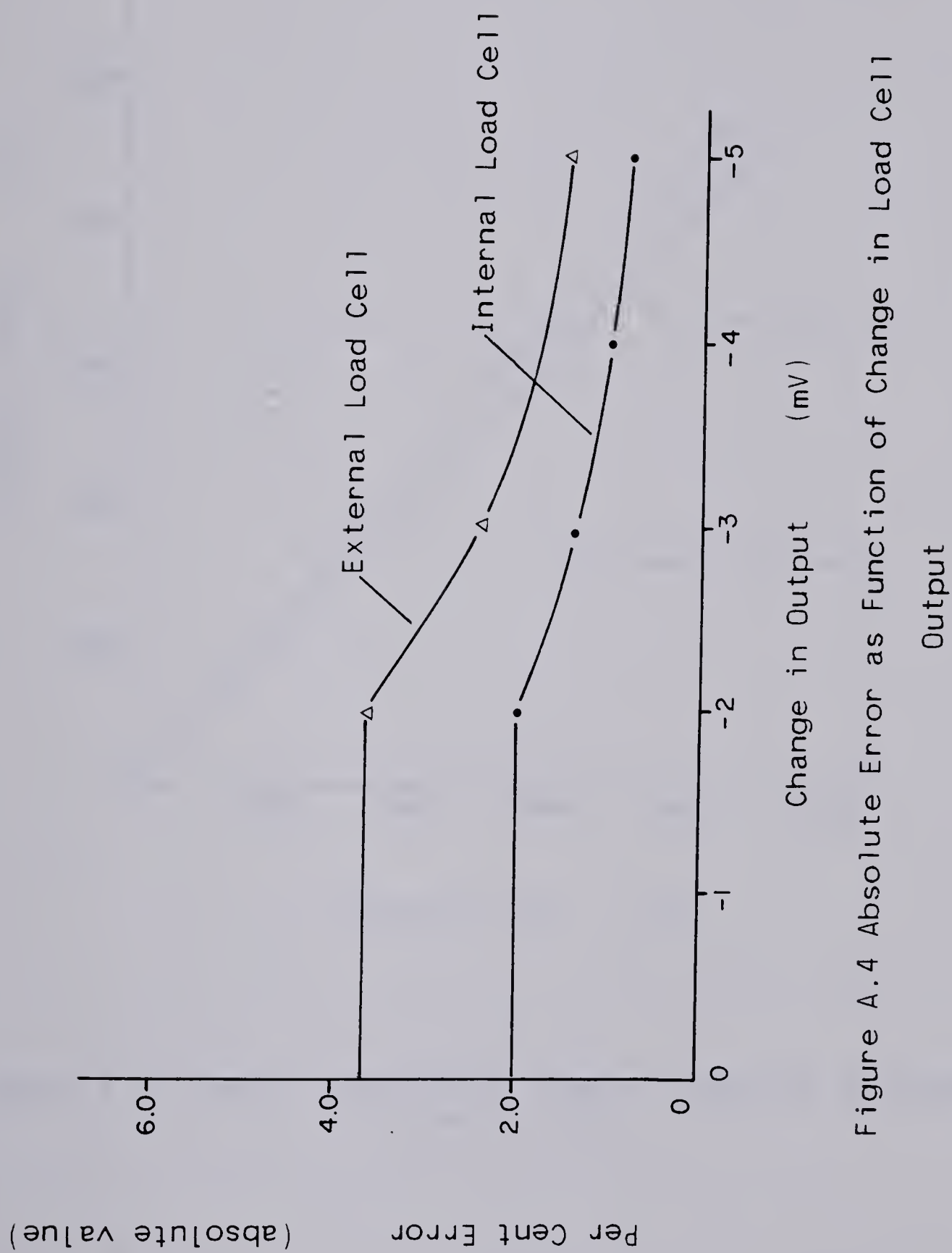


Figure A.4 Absolute Error as Function of Change in Load Cell Output

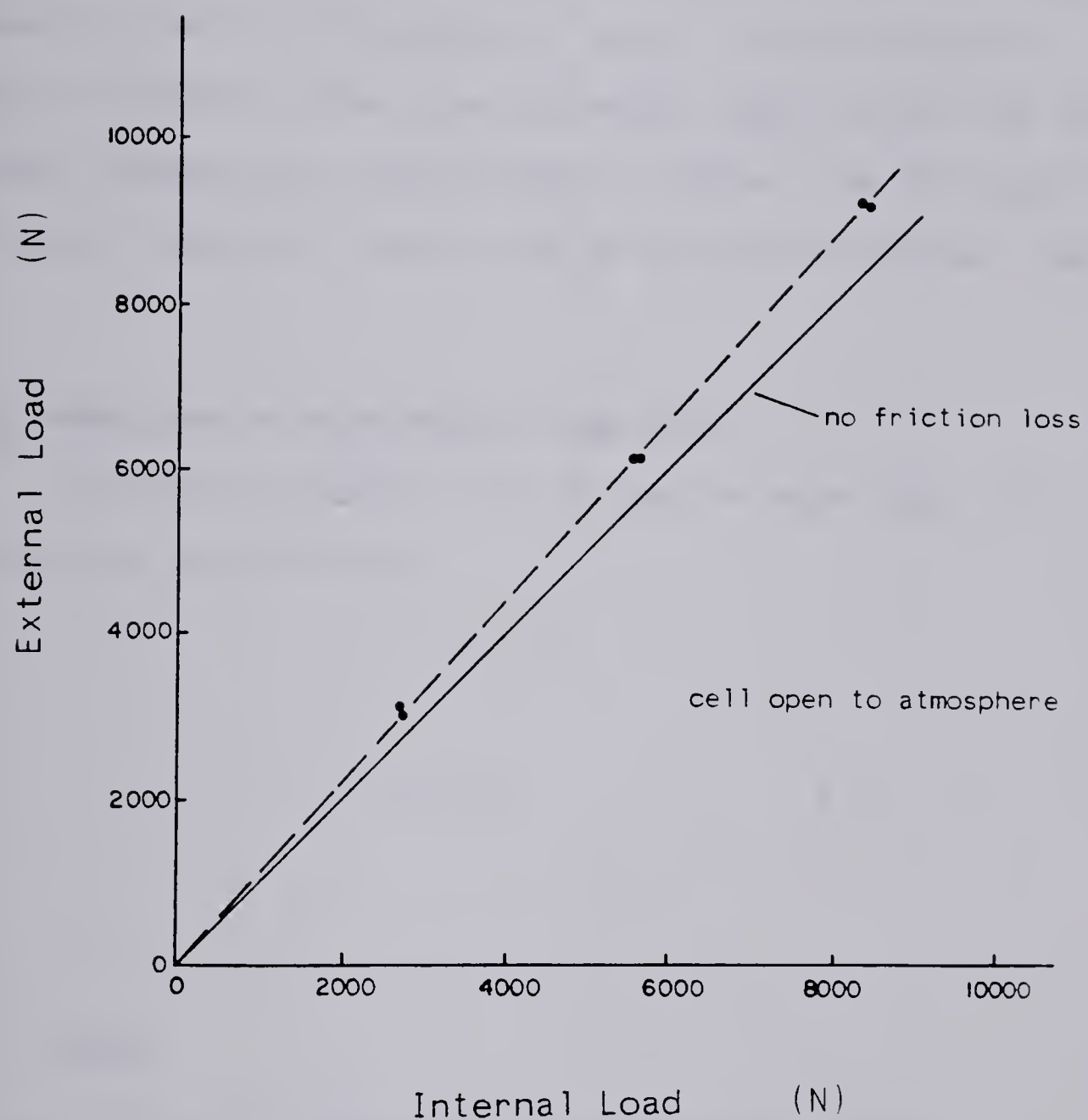


Figure A.5 Internal Horizontal Load as Function of Applied External Load

to the vertical and horizontal bushings, those values provide, if anything, an upper bound to the friction loss, under identical conditions in an actual test. The lower bound to the friction loss is zero. Thus, the best approximation to the true value was taken to be the value midway between the two extremes. Hence, the horizontal friction loss was taken as 5% of the true external load.

A.3 Reduction of Horizontal Load Data

Considering Figure A.6, it can be seen that, for horizontal equilibrium:

$$f = a + c - b \quad A.2$$

where:

- a. f is the load carried by the soil sample
- b. a is the load measured by the horizontal load cell
- c. b is the frictional force and,
- d. c is the load due to the cell pressure.

However, from the foregoing discussion, it is

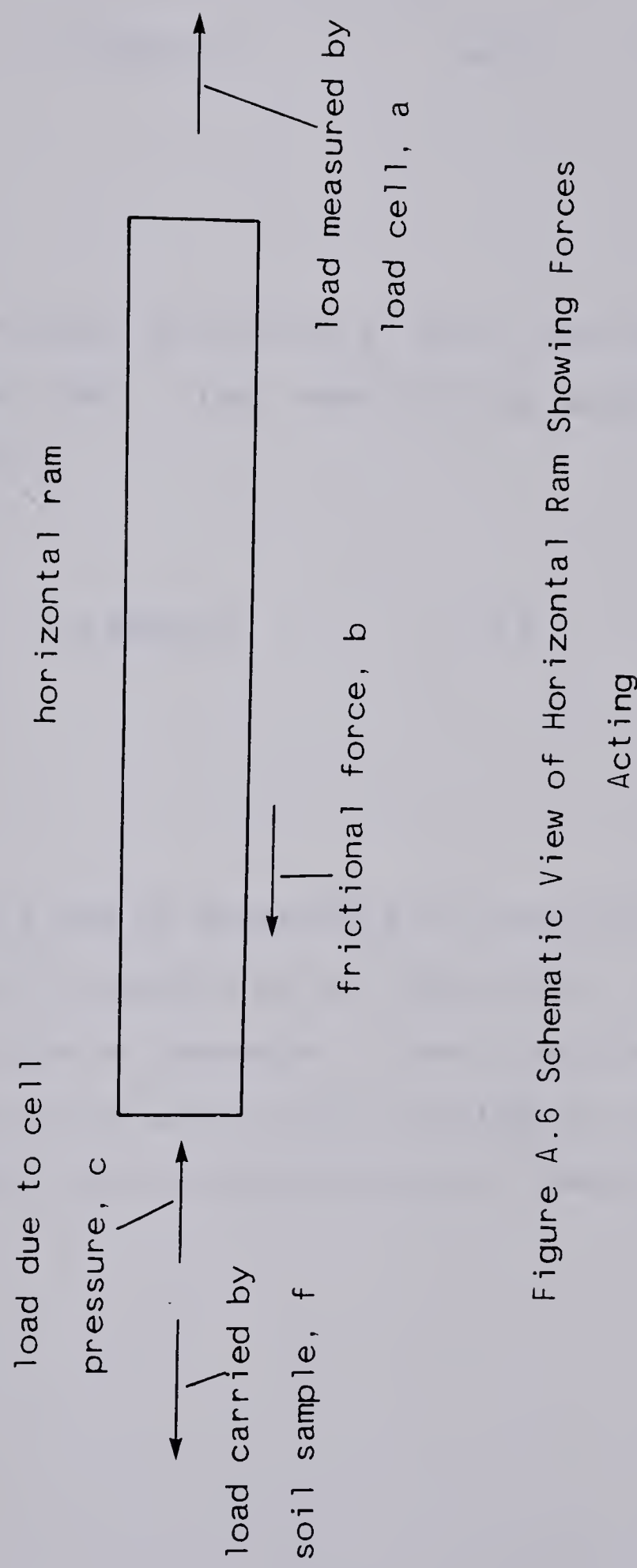


Figure A.6 Schematic View of Horizontal Ram Showing Forces Acting

Known that:

$$b = (.05)(a+c) \quad A.3$$

since the friction correction is 5% of the total applied horizontal load. Thus, substituting equation A.3 in equation A.2 yields:

$$f = (.95)(a+c) \quad A.4$$

The value of a may be determined by correcting the horizontal load cell readings as outlined above. In calculating the value of parameter c , one simply multiplies the value of the cell pressure that prevailed at the time load f acted by the cross sectional area of the horizontal ram.

APPENDIX B
SAMPLE PREPARATION

B.1 Preparation of Sample

The soil to be tested was derived from a block sample of Mica Dam core material. The initial maximum grain size of the block sample was far too large for present purposes and so, by sieving, the grain size distribution was altered as felt appropriate. Sieves, made by the Tyler company, numbers 4, 8, 16, 30, 50 and 100 were used. All material passing the number 100 sieve was collected in a pan. The soil retained in each of these groupings was placed in separate bags. Only that material passing the number 16 sieve was used for testing purposes.

To prepare a sample:

1. measured quantities of air dry soil from each of the bags are placed in a pan and mixed, by hand, till homogeneity is achieved.
2. distilled water is then added, in small amounts, and the soil is again mixed. This insures an even distribution of moisture throughout the mass.
3. a quantity of water is added to achieve a predetermined water content, allowing .5% extra for evaporation. Any lumps of soil are broken by hand.
4. the soil is then mixed for five minutes in a mechanical mixer.
5. finally, it is placed in a plastic bag which is tied, labelled and stored in a moisture room for approximately 24 hours.

To compact the sample:

1. plastic wrap is placed over the base of the mould and taped to the inside surfaces of the split rings. This is a good way to prevent the soil sticking to the base and sides of the mould. Care should be taken to see that the plastic is not wrinkled.
2. The split rings are then placed on the base of the mould, assembled and secured there. The compaction mould, assembled, is shown in Figure B.1 .
3. the weight of the base and mould is then determined.
4. the compaction mould collar is positioned and the sample formed, each of the three identical layers being compacted by 25 blows from a Standard Proctor hammer distributed evenly over the sample's area. The surface of the uppermost layer, when compacted, is almost level with the top of the collar.
5. after compaction, the collar is removed and the sample's upper surface trimmed level with the top of the mould, proper.
6. the mould, base and sample are then weighed. A water content sample is also taken.
7. with the sample still in the mould, it is placed in a plastic bag and stored in a moisture room.
8. the following day the water content sample is weighed. After a curing time of approximately 24 hours, the sample is ready to be tested.

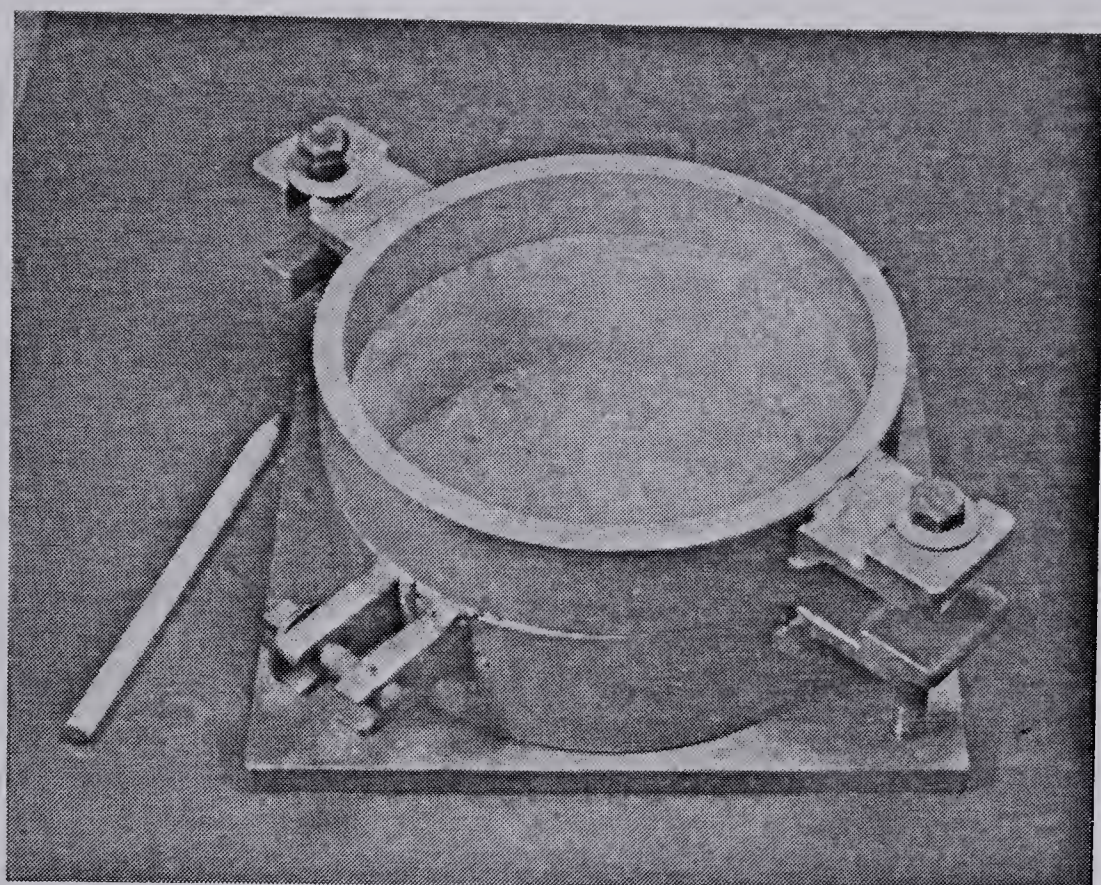


Figure B.1 View of Compaction Mould

B.2 Preparations Involving the Apparatus

In preparing the apparatus for a test:

1. organize all the components and required tools. This will save a great deal of time.
2. level the LVDT gauge pads on the load cap. To do this, a surface dial gauge is used. The probe of the surface gauge is drawn across the surface of the pad, parallel to the line of action of the shear load, and the change in dial reading noted. This change is relative to a reference datum. By altering the orientation of the pad, the deviation of points on its surface from the horizontal can be reduced to an acceptable level. The criterion of acceptability depends on the stringency of the requirements regarding rotation of the lower load cap; such rotation effects the sample's stress state.

For the following descriptions, reference to Figures B.2 and B.3 is required. At the outset, it may be assumed that all valves shown are closed.

3. deair the lines running from the back pressure reservoir to the cell. With valve V2 opened to the atmosphere, valve V1 is opened and the back pressure reservoir filled. The progress of the water's surface can be monitored using the sight tube.
4. when appropriate, valve V1 is closed and valve V2 is opened to the air pressure regulator. Valve V3 is then opened, and a slight pressure applied to the back pressure chamber. Care must be taken to NOT allow water

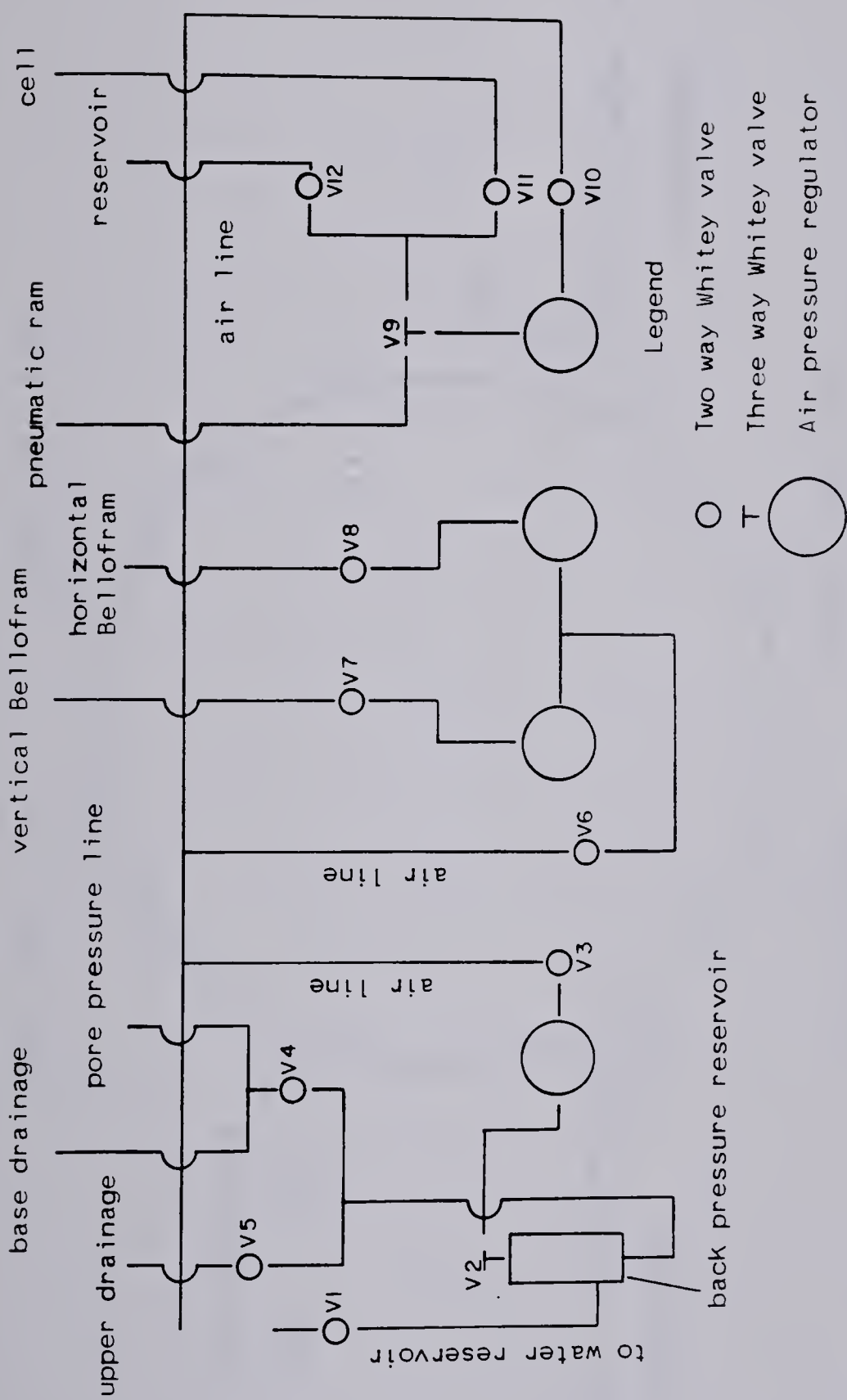


Figure B.2 Control System for Apparatus

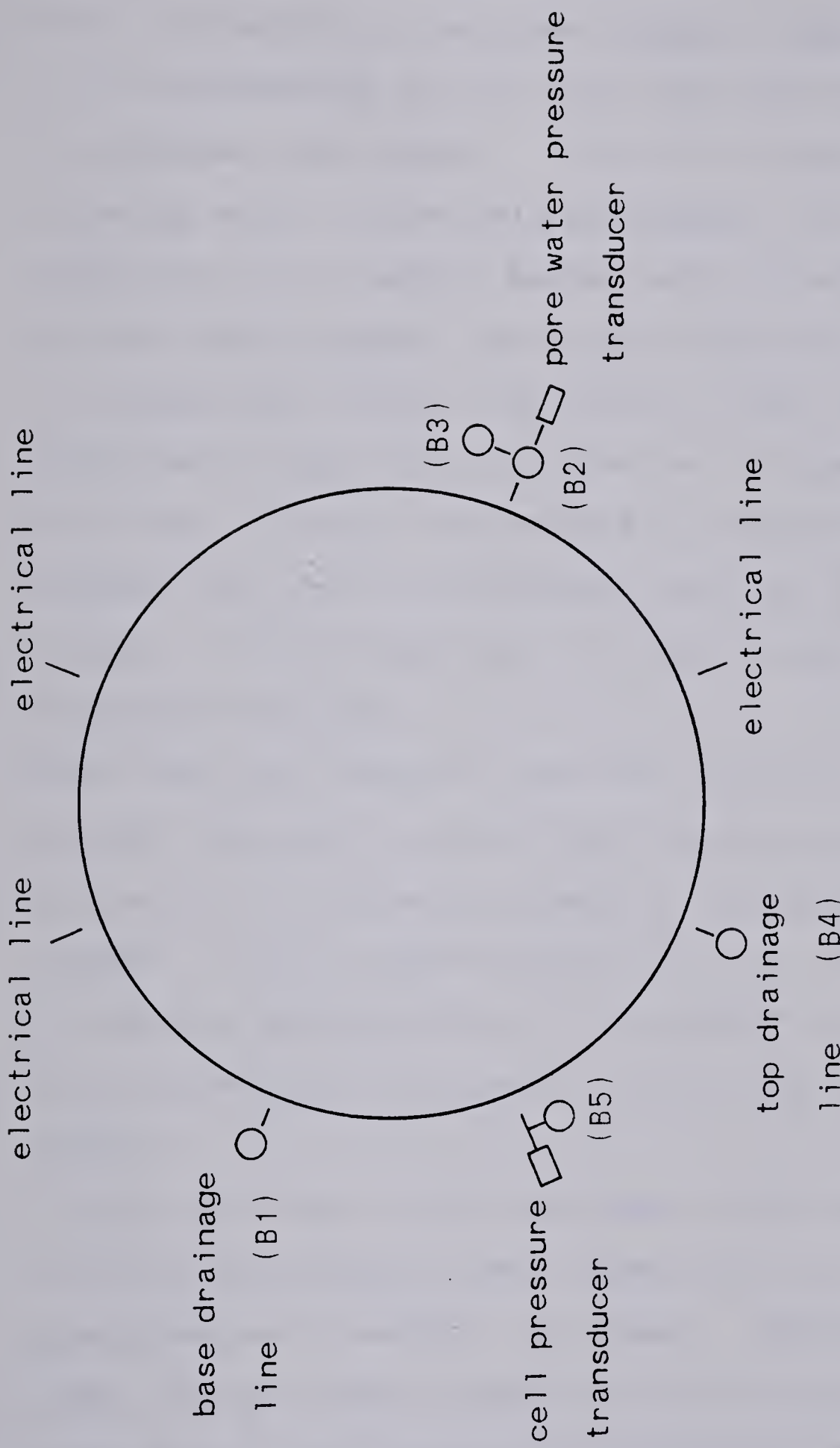


Figure B.3 Valves and Connections on Cell Base

to enter the air pressure regulator.

5. the line leading to the upper platen is deaired first.

It is disconnected at the cell's base and the end placed in a medium sized beaker. Valve V5 is then opened, allowing water to flow into the beaker. The reservoir should not be allowed to become empty of water. After no more bubbles appear during continued flow, valve V5 is closed and a visual inspection of the line is conducted to make sure that there are no bubbles left in the line. Finally, with valve B4 closed and valve V5 opened, the line is reconnected and valve V5 then closed. If found necessary, the back pressure reservoir should be refilled.

6. deair the pore pressure line then reconnect it. Note, at this time, that valve B1, on the base drainage line, and valve B3, at the pore pressure transducer, are closed. Prior to deairing the last line, that leading to the base drainage line, it is worthwhile to saturate the pore pressure transducer's cavity and that of the adapter.

7. tip the cell base so that the edge of the base where valve B1 is located is the highest point and that by the pore pressure transducer the lowest. Spacers are placed under the cell base to maintain this orientation.

8. open valve B1 and unscrew the transducer, draining any water in the adapter's cavity. If valve B2 is not open at this time, the transducer might be exposed to

negative pressures (absolute) and possibly destroyed.

9. fill the small cavity in the transducer with water
10. open valve B3 and allow the water to run into the adapter's cavity.
11. screw the transducer part way into place and hold it there till water is seen to seep along its threads; it can then be screwed in all the way. Note that the transducer should not be tightened too much as this risks stripping the threads in the brass adapter.
12. allow water to run through the cell base to the cell pedestal till it emerges, without bubbles.
13. close valves B2, B3 and V4. No excess water should be allowed to remain outside the recessed area of the porous stone.
14. remove the spacers from beneath the cell base.
15. saturate the base drainage line. The techniques described above are used where applicable. All open valves are then closed.
16. plug the LVDT's in to allow them time to warm up. This essentially eliminates drift of the instrumentation during the actual test. Also, the direction of movement of the probes indicated by a change in output should be noted.
17. prepare the line running from the cell fluid reservoir to the cell base. The cell fluid reservoir is shown in Figure B.4 . It is assumed that the line connecting the reservoir to valve B5 is partially full of glycerine,

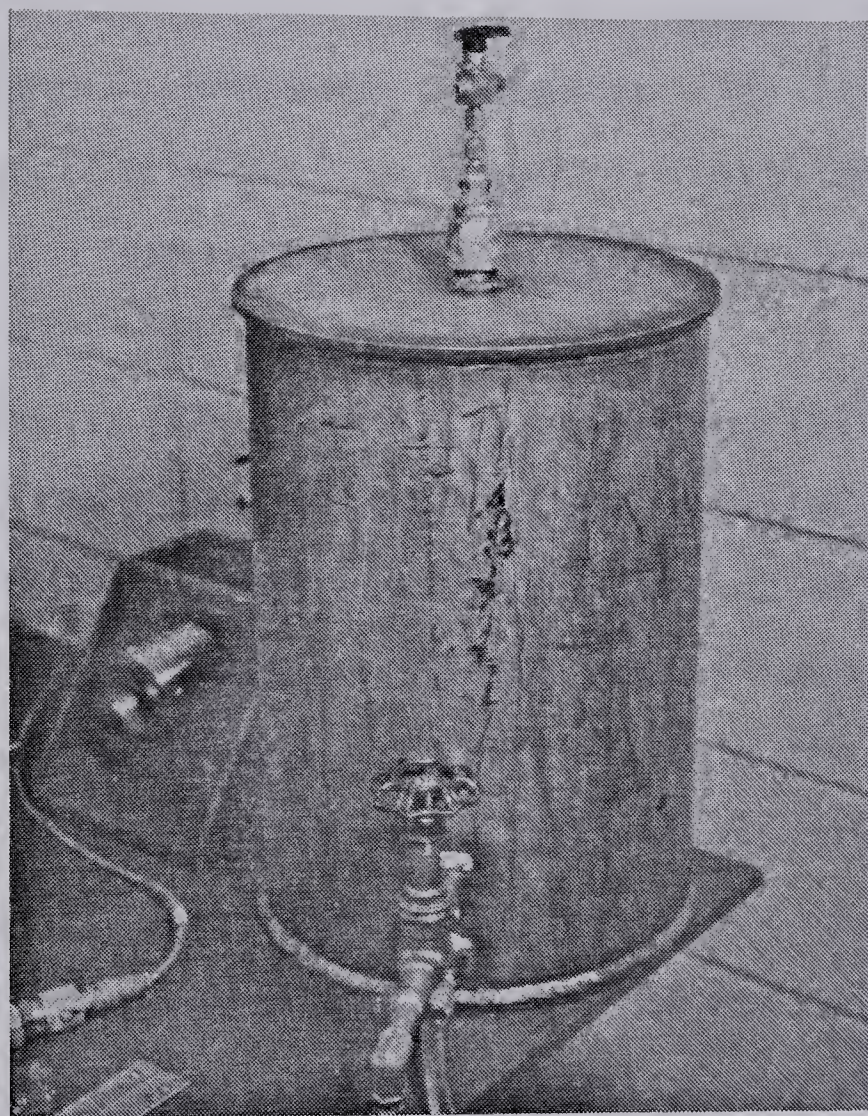


Figure B.4 View of Cell Fluid Reservoir

the cell fluid. The line is then disconnected at valve B5 and glycerine run through it till the fluid seeps into a beaker at the free end. If thought necessary, the glycerine reservoir is filled manually beforehand so that the flow, under gravity, is sufficiently fast. The line is then reconnected and the cell pressure transducer's cavity and that of the adapter saturated, as with the pore pressure transducer's cavity.

18. place the porous stones in a pan of distilled water and boil them for approximately 5 minutes to rid them of entrapped air.
19. open valves V2, V3, V4 and B1, as appropriate, and run water till the recessed area in the pedestal is filled.
20. close the valve on the base drainage line at the cell's base. After removing one of the porous stones from the pan, slide it onto the pedestal and into the recessed area. Any water displaced in the process should be cleaned up. Sliding the porous stone into position, it is hoped to prevent the entrapment of air beneath it.
21. cover the O-rings, to be positioned on the pedestal, with a light film of high vacuum grease and slide them into place. Use of such grease allows a better seal between the O-rings and the membrane surrounding the sample.
22. screw the thicker finned plate into position and run water through the base line, having opened valve B1, to fill the drainage holes in the finned plate. The

pedestal, as it appears at this stage of sample assembly, is shown in Figure B.5 . Care should be taken to align the fins in a direction normal to the line of action of the shear force.

23. trim strips of filter paper to fit between the fins themselves, place them in position and wet them completely.
24. assemble the upper platen. Open the appropriate valves and run water through that portion of the upper platen drainage line situated within the cell. Figure B.6 shows it, at a later stage of sample assembly, connected to the upper platen.
25. with the drainage line attached, turn the upper platen, proper, upside down. The plastic tubing, seen in Figure B.6, leading to the upper platen, should not be allowed to bend during inversion of the platen lest a constriction develop near the fittings at either of its ends.
26. run water through the top drainage line to fill the recess in the upper platen with water. It should be recalled that at all times the water level in the back pressure chamber must be monitored to ensure that the chamber does not run dry.
27. slide the remaining porous stone onto the platen and into the recess. Clean up any water forced out in the process.
28. clean the O-rings to be positioned on the upper platen,

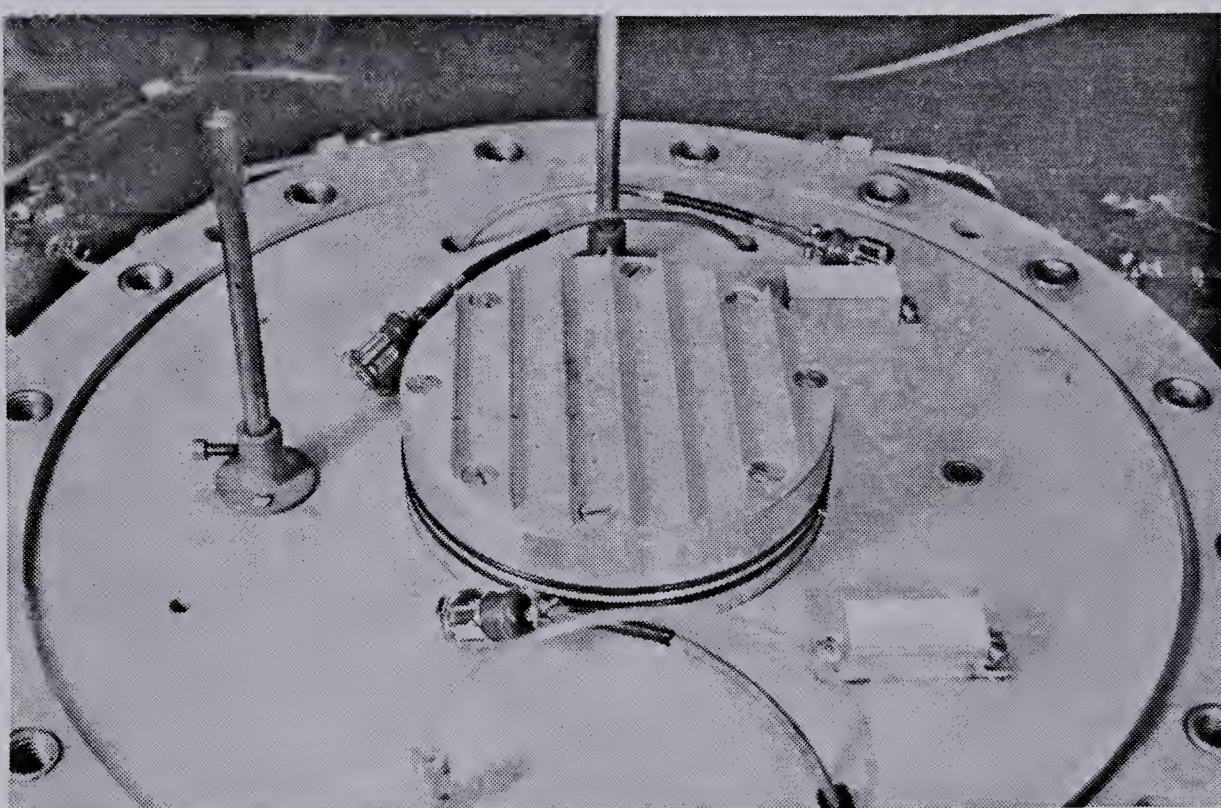


Figure B.5 View of Pedestal

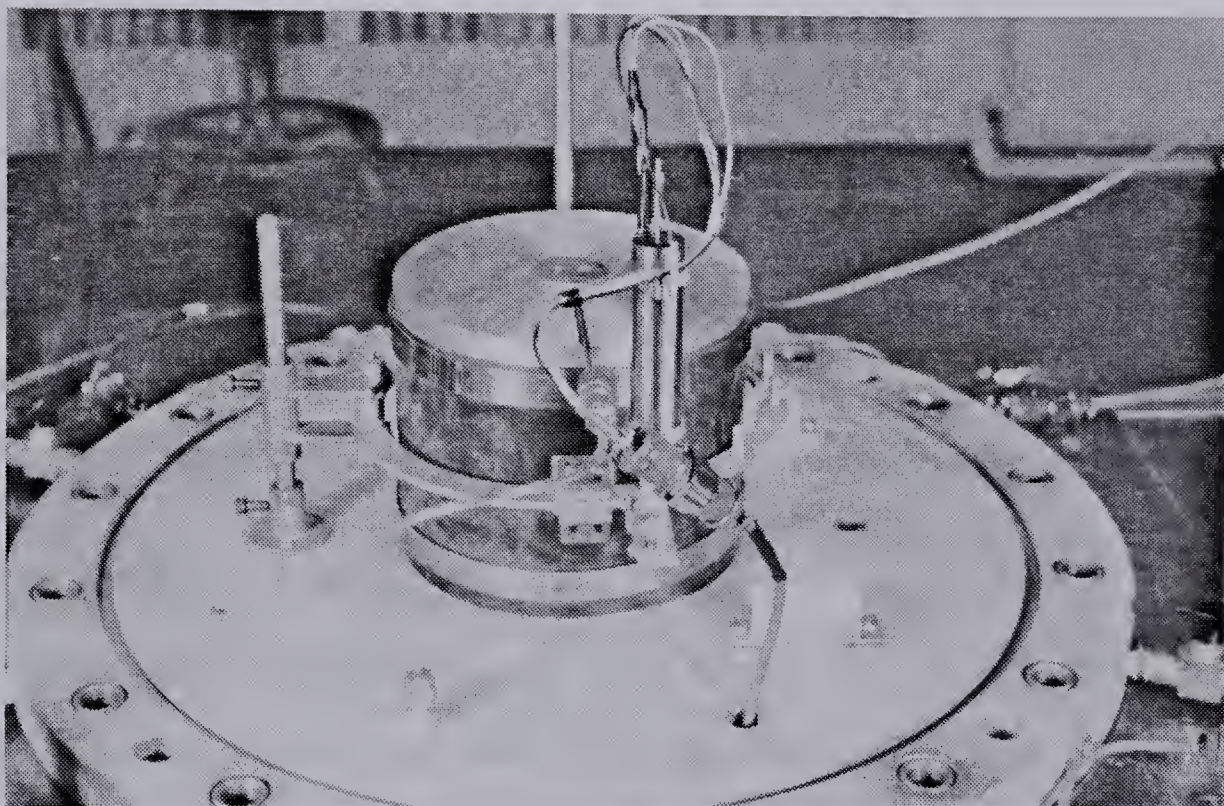


Figure B.6 Upper Platen with Drainage Line Attached

proper. Coat them with a light film of high vacuum grease and slip them into place.

29. attach the finned plate and run water through the upper drainage line to fill the drainage holes. Its orientation should be such that the fins are parallel to the long axis of the stainless steel portion of the drainage line.
30. trim strips of filter paper as before and place them over the drainage holes. The upper platen is left like this till the fins are about to be embedded in the soil.

B.3 Installation of Soil Sample

To position the sample on the pedestal:

1. remove the compaction mould from the moisture room and place it rightside up on the pedestal. The mould fits neatly over the pedestal so no problems are encountered in centering it.
2. screw the uprights for the embedding device into the cell base. Position the crosspiece as shown in Figure B.7 .
3. place the upper platen on the soil sample, approximately in its final position, and place the slotted disc on top.
4. insert the rod linking the crosspiece and slotted disc. This orients the disc in the manner required. By matching marks on the surfaces of the disc and upper platen, the finned plate can then also be positioned properly. At no point should the fins touch the side of

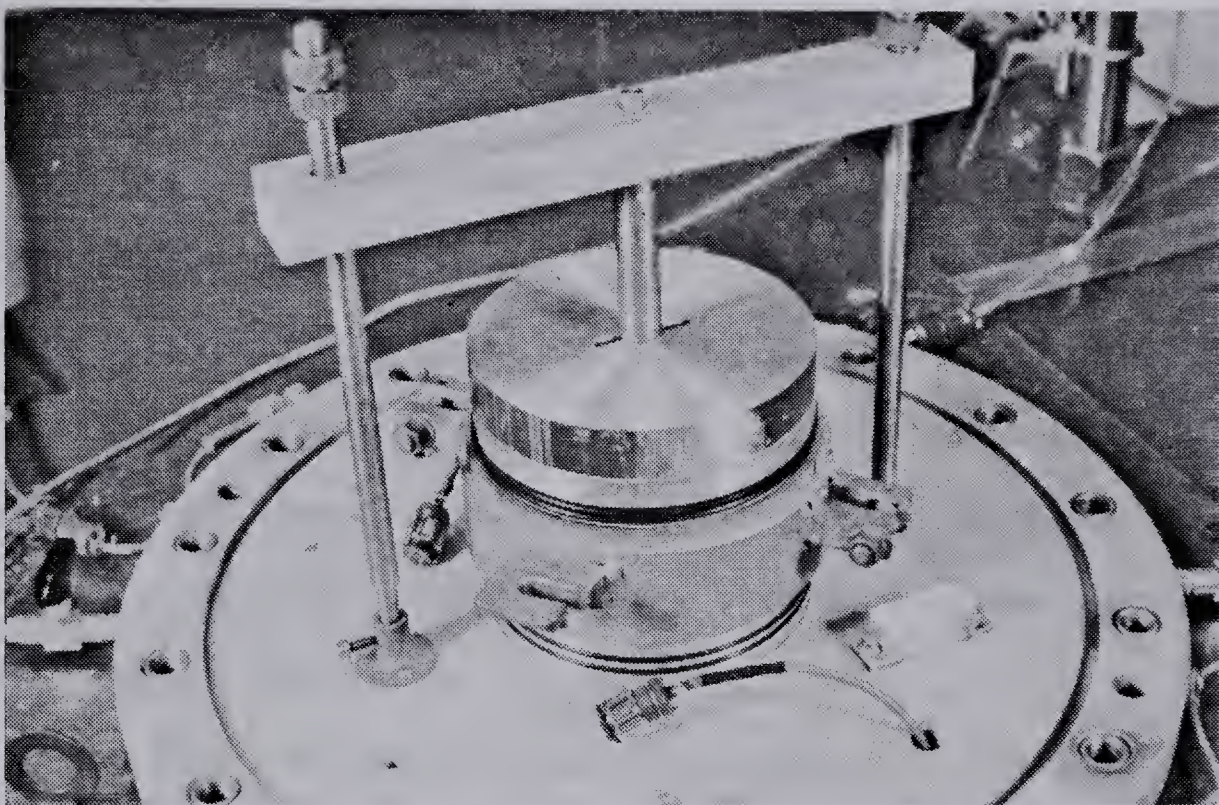


Figure B.7 View of Device for Embedding Fins in Sample

the compaction mould.

5. apply a uniform force to the crosspiece and embed the fins in the sample.
6. remove the membrane from the moisture room, trim it to size and position it on the membrane stretcher. Care should be taken to insure that the membrane is not wrinkled but lies flush on the inside surface of the membrane stretcher.
7. remove the crosspiece and upper platen drainage line and lay the membrane stretcher on top of the slotted disc.
8. reposition the crosspiece and tighten the nuts on the vertical uprights until a small pressure is applied to the top of the upper platen.
9. remove the compaction mould carefully - so as not to damage the sample - and position the membrane. With the membrane properly positioned, there is sufficient room near the upper surface of the platen to attach the collars. These should abut the upper platen and not touch the membrane or the strapping, which is about to be positioned and tightened.
10. remove the membrane stretcher, support bars, crosspiece and associated components and attach the metal strapping. To insure a good seal between the O-rings and membrane, the strapping must be positioned and tightened carefully. The membrane has a tendency to bunch if the strapping is tightened too much. This must be guarded against. It is a good idea to tighten the

lower strap first and then to stretch the membrane, in the region of the upper strap's screw housing, as it is being tightened. The upper strap should be positioned so that its screw housing does not interfere with the collars when they are attached.

11. position the lateral strain gauge. It is simply slipped over the sample, as shown in Figure B.6, and the electrical connections made. The upper drainage line is not attached at this time. If a lot of vertical deformation is expected during the test, the lateral gauge should be placed so that its midplane, that of the arms, is slightly below the horizontal midplane of the sample. In this way, the midplane of the gauge will remain close to that of the sample.
12. align the collar, to which the lateral gauge is attached, parallel to the line of action of the to be imposed shear load and fix its elevation by tightening the appropriate cap screw.
13. thread the wire, attached to the LVDT probe, seen in Figure B.6, around the various posts on the arm of the gauge and anchor it on the opposite arm. The wire should be made taut to prevent poor response of the measuring system upon sample deformation. Further, the probe of the LVDT should be positioned so that, upon sample deformation, it is not interfered with by the wires extending from the top of the LVDT. At this time, the output of the LVDT should be checked to insure that

the probe is not near the limits of its travel.

14. attach the top drainage line, the channel in the upper platen, having first been filled with distilled water; the level might have been drawn down due to swelling of the sample. The screws are not tightened too tightly to avoid stripping of the threads.
15. install the rotation LVDT's and stand, as pictured in Figure B.8. The proper elevation of the gauge is found by matching the guide notch on the support stand with the upper surface of the collar. The Allen head cap screw is then tightened. The lower horizontal surfaces of the barrels of the rotational LVDT's are set flush with the underside of the lower horizontal surfaces of the arms to which they are attached. During tests, springs extend from the heads of the LVDT probes to the bases of the LVDT's. If restraint is not provided while the sample is being set up, the probes will be forced out of the barrels of the LVDT's. Therefore, two strips of copper sheeting were cut to size with a short section at each end of the strips being bent to form a right angle. One end of the clip is then hooked around the top of the LVDT's barrel, the other supports the head of the probe. Using the thumbscrew, the arms of the gauge are rotated so there is sufficient room for the gauge points of the load cap to pass by as it is lowered into position; otherwise, the LVDT's might be damaged.
16. clean the large O-rings and corresponding grooves in the

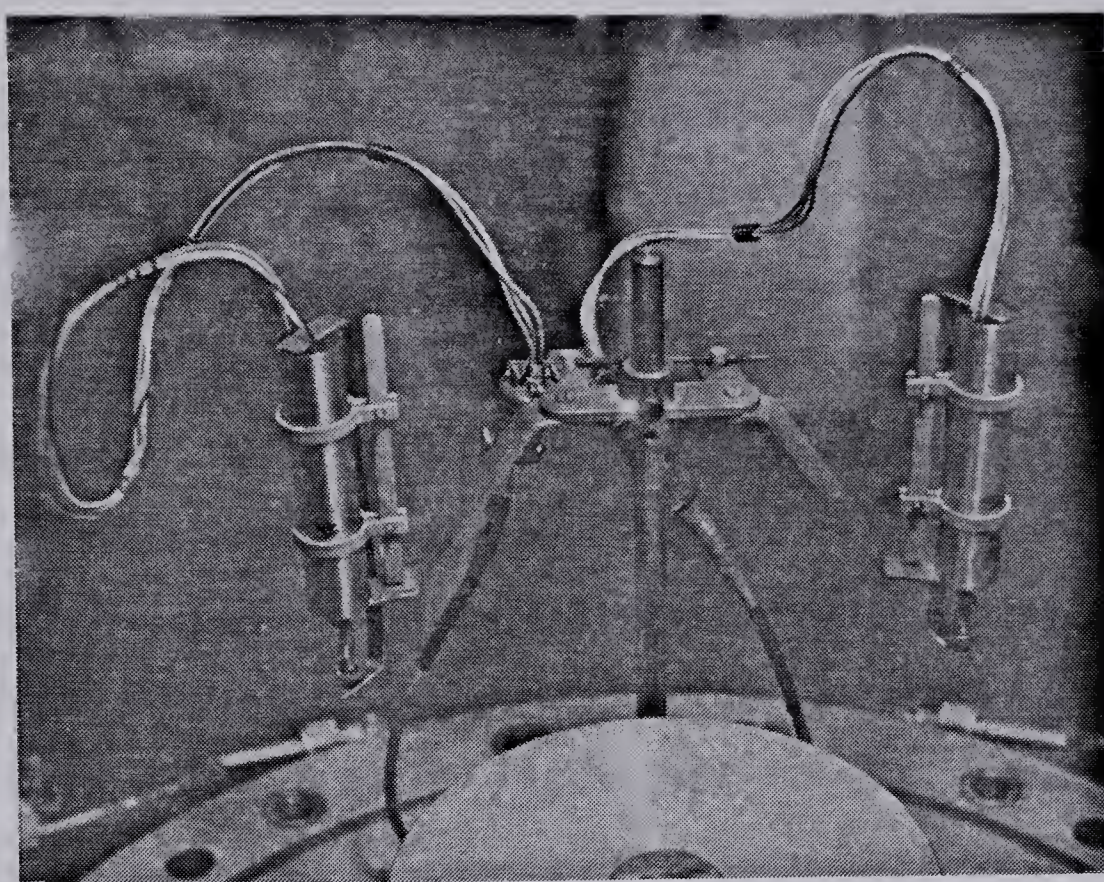


Figure B.8 View of Rotation LVDT's and Stand

- cell base and cap.
17. cover the O-rings with a light film of high vacuum grease and position them as required.
 18. position the cell wall. This step requires caution as the wall must be placed on the base, from above, without damaging any of the instrumentation surrounding the sample. For there to be sufficient room to do this, the cell cap and load cap must be raised. A workable procedure is outlined in the following steps.
 19. check the nuts normally used to secure the lowest crosspiece to make sure that they are positioned above the central threaded portion of the vertical uprights. They will then offer no resistance to the movement of the lowest crosspiece as it is raised. All relevant components should also be checked to see that they are bolted together properly and that no obstruction to the movement of the cell cap and load cap will be encountered.
 20. accompanying the apparatus are two steel rods, each about 13 cm long. These are extensions to the loading ram that screws directly into the upper load cap. The extension without the collar is screwed into the top of the loading ram.
 21. open valve V10 and turn valve V9 to the left. If the air regulator valve is opened, air will flow to the pneumatic ram.
 22. increase the air pressure slightly until the lowest

crosspiece begins to move. After movement commences it should continue rather uniformly except for a slight variability induced by the stick slip nature of the frictional interaction between the vertical supports and the sliding components.

23. when the cell cap collar, in which the vertical bushing is located, is about to rise above the elevation of the top of the first extension, decrease the air pressure in small amounts till the upward movement of the crosspiece is halted; when this happens, there will be a sharp increase in the blow by of the regulator.
24. screw the other extension into place and increase the air pressure once again. Due to the presence of the collar on the end of the upper extension, the load cap will be lifted as the cell cap continues to rise. When the load cap has been raised sufficiently, the pressure is reduced slightly, as outlined above, so that its elevation does not change further. If the components are raised too high, the middle crosspiece will come into contact with the upper crosspiece and its progress will be stopped. Care should be taken to prevent damage to the apparatus and minimize risk of personal injury upon malfunctioning of the air pressure system; a backup support system for the lowest crosspiece is recommended.
25. position the cell wall. The cell wall should be oriented so that the yoke rests on the two Teflon covered pads and the bolt holes in the lower flange line

up with those in the cell base.

26. remove the pin securing the moveable plate and push the plate into position, as shown in Figure B.9 . Recalling for the moment the discussion concerning the raising of the cell cap, this figure also shows the vertical loading ram that is screwed into the upper loading cap and, above it, the lower extension and part of the upper extension, distinguishable by their wrench flats.
27. lower the load cap into position. To aid in the process, two long aluminum rods are used. As the load cap is lowered, but before it nears the upper platen, its movement is halted and the two rods passed through sets of diametrically opposed holes in the cell cap and base. In this way, the load cap is automatically centered. Further, the holder for the horizontal displacement LVDT, which is on the ram of the yoke and seen in Figure B.10, is positioned so that when it abuts the bushing, the yoke is in the initial testing position. Thus, throughout the operation, one simply has to ensure that the arms of the rotation gauge are not hit by the load cap and that the collars, on the underside of the load cap, do not prevent it from sitting horizontally on the upper platen.
28. tighten the collars when the load cap is sitting on the platen. It is best to do this by hand as much as possible, using the appropriate Allen wrench when necessary. The cap screws are tightened greatly only

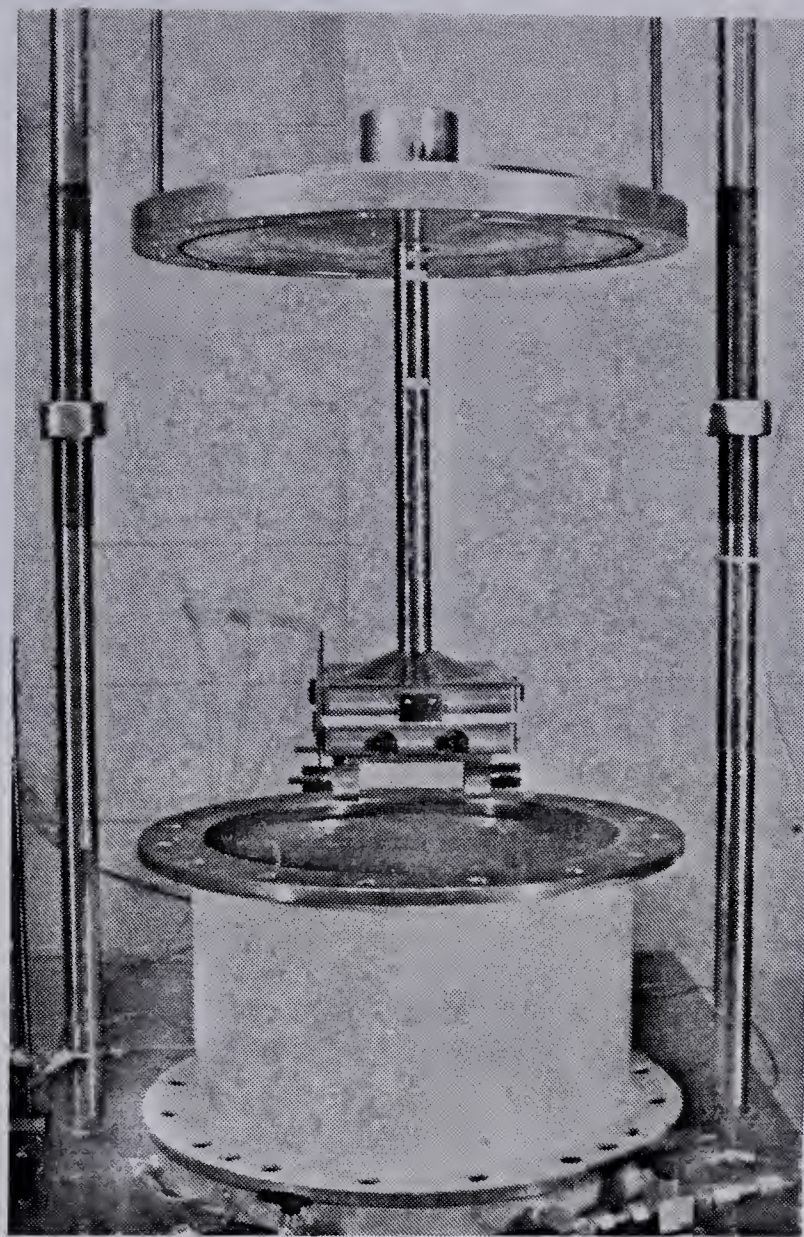


Figure B.9 View of Cell Cap, Load Cap and Cell Wall

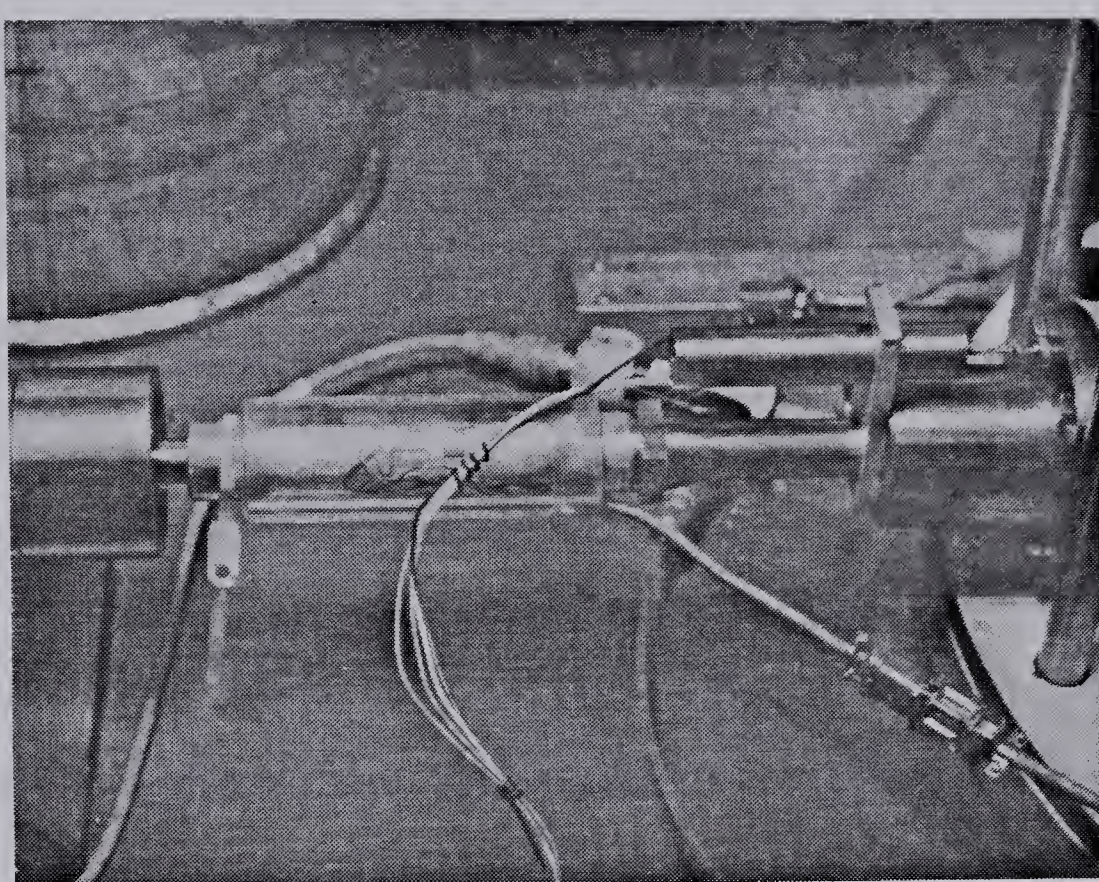
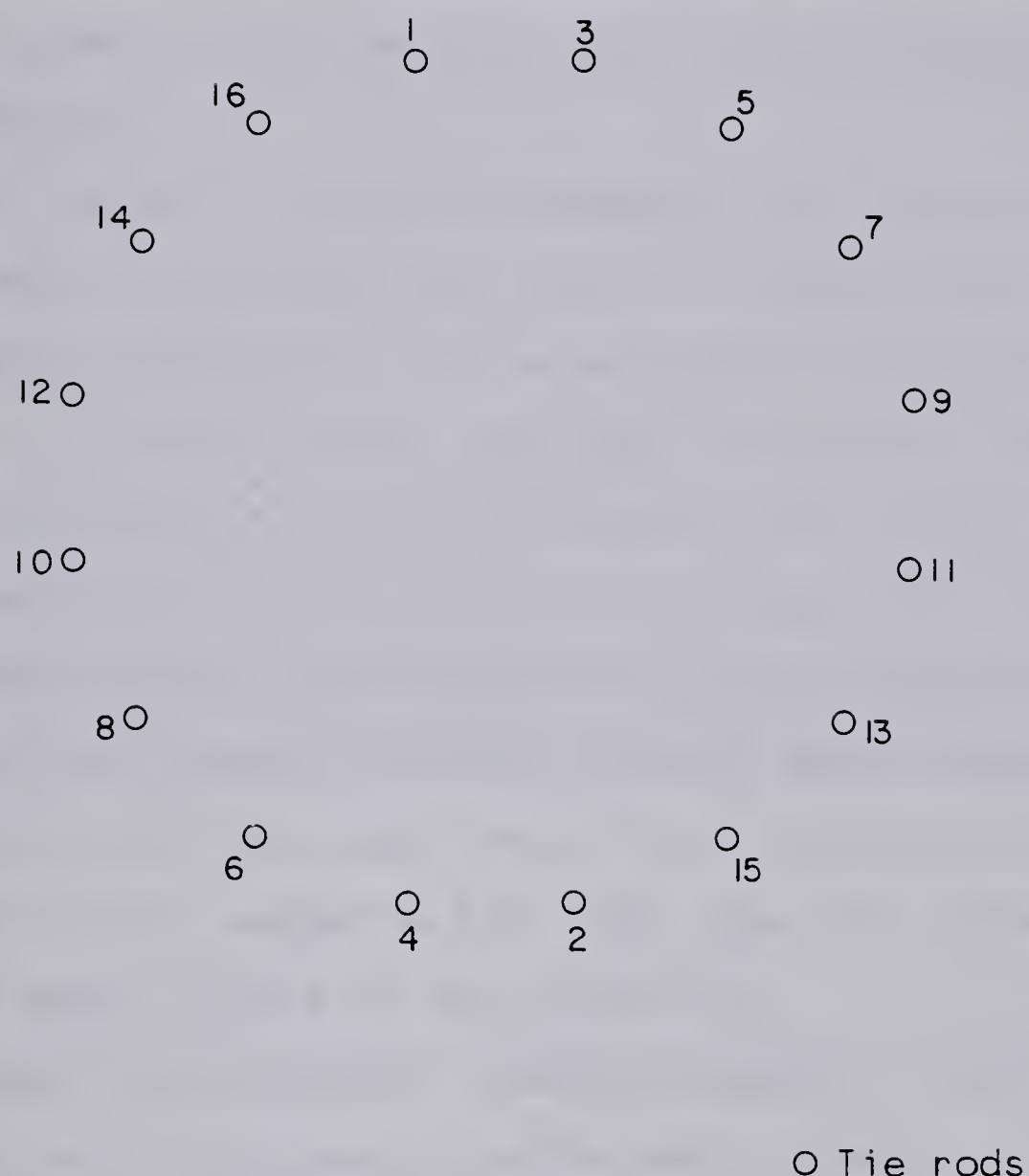


Figure B.10 View Showing Horizontal LVDT Holder Abutting Bushing Assembly

- after both collars fit snugly against the upper platen.
29. move the arms of the rotational gauge into position and remove the copper clips so that the LVDTs' probes rest on the gauge points bolted to the side of the lower load cap.
 30. lower the cell cap. As this is being done, remove the upper extension lest it interfere with the vertical Bellofram. When the cell cap rests on the upper flange of the cell wall, the two aluminum guide rods are removed and the tie rods positioned.
 31. check the cell cap to see that it is level. The tie rods are then screwed into the base of the cell.
 32. tighten the nuts on the tie rods till they are hand tight.
 33. tighten the nuts moderately, following the pattern shown in Figure B.11 .
 34. check to see if there are discrete spaces between the cell wall flange and cell cap. If so, the adjacent nuts are tightened. However, this should not be attempted if the observed spaces are quite large. Under those circumstances, one risks damaging the cell cap; it is best to start again.
 35. on completion of the previous step, tighten the nuts further, lodging them very securely against the cell cap.
 36. remove the lower extension then attach the vertical load cell assembly. The complete assembly consists of a



Note: numbers indicate sequence of tightening tie rods. Starting point is arbitrary.

Figure B.11 Procedure for Securing Tie Rods

small adapter that screws directly into the vertical load cell, the load cell itself and finally, the rotational adapter. This is shown in Figure B.12 . installed in the testing frame, the load cell should be oriented so that the electrical connection points downwards.

37. lift the cell, using the pneumatic ram, remove the moveable plate and lower the cell slowly toward the loading frame base. It is advisable to lower the cell till it is just above the table top and then to thread the four bolts, used to secure the cell to the loading frame base, part way into their holes. The cell is then lowered to the table top and the bolts tightened.
38. level the lowest crosspiece using a spirit level.
39. advance the nuts down the central threaded section of the vertical supports till they come into contact with the upper surface of the crosspiece.
40. connect the horizontal loading assembly. The horizontal load cell is screwed into the small connector, already attached to the yoke, with the plug on the load cell pointing toward the cell base. The horizontal spacer is then slid over the ram of the horizontal Bellofram and the appropriate small adapter screwed into the end of the ram. To link the small adapter and the load cell itself, the rotational adapter is then screwed into place. To complete assembly, the length of the spacer is adjusted so that it abuts the Bellofram stand on one

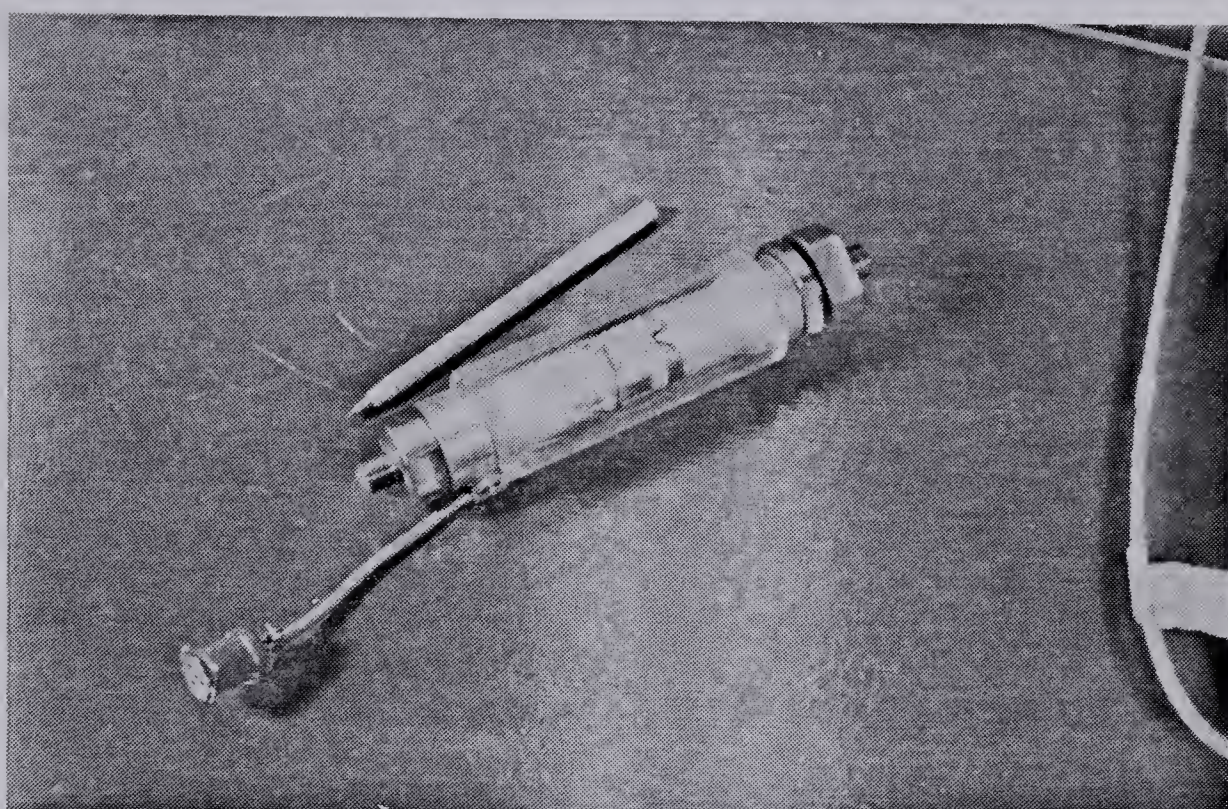


Figure B.12 View of Vertical Load Cell Assembly

side and the rotational adapter on the other. These components, as just described, can be seen in Figure B.13 .

41. connect the LVDT to measure horizontal deformation. The probe of the LVDT is placed in contact with the vertical face of the housing for the horizontal bushing, then the barrel is positioned so that the resulting output indicates the probe to be in the midrange of its travel.
42. fill the cell. With valve V10 open, valve V9 is turned to the right and valve V12 opened. Valve B8, on the reservoir, is then opened to the air line and valve B5 checked to make sure that it is closed (the reservoir and part of the low pressure line can be seen in Figure B.4). The air pressure is increased till the gauge reads approximately 205 kPa. The bleed plug on the cell cap is then removed and valve B5 opened. Cell fluid will flow from the reservoir, through the low pressure line, into the cell. The amount of fluid remaining in the reservoir can, at any time, be ascertained simply by closing valve B5, opening valve B8 to the atmosphere, and, when the rush of air has abated, opening the tap on the side of the reservoir. The fluid then flows, in the sight tube, to the elevation of the fluid in the reservoir itself. The tap is then closed once again, the fluid in the sight tube drained into a storage drum and valve B8 opened to the air line.
43. when sufficient pressure has built up within the

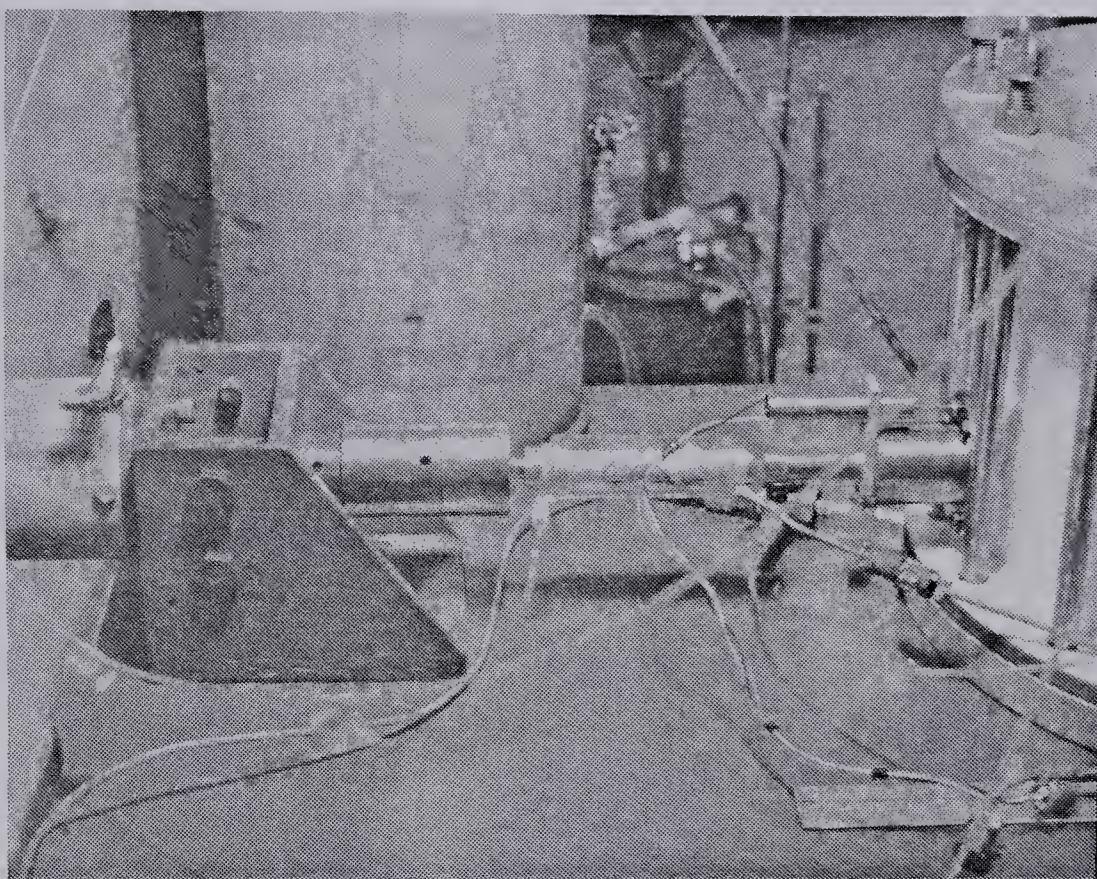


Figure B.13 View of Horizontal Loading Assembly

reservoir open valve B5.

44. fill the cell till the fluid begins to seep from the bleed hole on the cell cap.
45. close valve B5 and screw a blind ended plug into the bleed hole.
46. open valve B8 to the atmosphere and reduce the air pressure to zero.
47. check to ensure that all lines to the data acquisition system have been connected.

The sample is now ready to test.

APPENDIX C
TEST PROCEDURE

C.1 General

In this appendix, the procedure for conducting a test is outlined. As well, certain important aspects are discussed in detail.

C.2 Test Procedure

For simplicity, details of the testing procedure will be grouped under several major subheadings.

C.2.1 Initial Readings

In this subsection, the setting and recording of initial test conditions are described.

1. Before starting a test, make sure that the output of all appropriate channels in the data acquisition system is being read and, when required, recorded. Determine that the following conditions prevail:
 - a. the pressure within the cell fluid is due to atmospheric pressure and gravitational forces alone
 - b. all air regulator gauges indicate zero line pressure
 - c. all valves are closed except the one at the top of the vertical bellfram, which is open to the atmosphere, and that leading from the cell base to the pore pressure transducer
 - d. the horizontal load cell is in an unstressed condition

2. the output of the lateral gauge is displayed, the acquisition system being in the single channel mode with a reading interval of two minutes.

Under these conditions, the output of the various devices will be printed on paper tape, every two minutes, while the output of the lateral gauge will be displayed continuously. It is also advisable, during the course of a test, to record any other information that will facilitate later analysis and interpretation of the data.

C.2.2 Back Saturation of Sample

The first step in the test itself is to saturate the sample. Although a number of methods may be found in the literature (Bishop and Henkel, 1962; Lowe and Johnson, 1960), it was felt that for present purposes the desirable way to elevate the degree of saturation of the sample would be by undrained loading while maintaining a K_o condition. During the subsequent consolidation stage, the back pressure in the drainage line would be set at a sufficiently high level to maintain the degree of saturation as required. A more detailed discussion concerning the procedure may be found in the final section of this chapter.

1. open the appropriate valves leading from the vertical Bellofram to its accompanying air pressure regulator.

Increase the air line pressure to the vertical Bellofram to approximately (1/20) of the subsequent increment of cell pressure, each as read on the appropriate regulator

gauge.

The purpose of the seating load is to prevent the vertical ram's being forced away from the load cap upon an increase in the cell pressure.

2. opening the necessary valves, increase the cell pressure. Apply these two load increments in quick succession. As soon as possible after this, take another reading on the data acquisition system; readings being taken thereafter at two minute intervals. Continue the loading step until it is judged that a condition of stability has been reached. In the present series of tests, this usually took about 15 minutes. More will be said of this later in the chapter.

No steps were taken to restore the sample to a K_o condition if whatever deviations which occurred appeared small. The details of the procedure to use, if required, will be discussed later, in connection with the consolidation of the sample.

This pattern of undrained loading involving increments of seating load, cell pressure and, if necessary, further vertical load is continued until a suitable stress level is attained. At the end of each loading stage an apparent B value can be calculated.

C.2.3 K_o Consolidation

In consolidating the sample, the procedure is as follows:

1. with valve B4 closed (see Figure B.3), increase the back pressure to the desired value
2. take a set of initial readings
3. reset the data acquisition system as required, and have the lateral gauge's output displayed

The reading interval was chosen after studying the consolidation of the sample during the first test. It allows the consolidation process to be charted to insure that everything is proceeding as expected.

4. open valve B4. Take another reading as soon as possible.

When thought appropriate, the vertical load is altered to maintain a K_o condition. The procedure to maintain a K_o condition is given below. It assumes that the vertical Bellofram is open to the accompanying regulator. To increase the load slightly to maintain a K_o condition:

- a. close the valve on the vertical Bellofram to the air regulator
- b. increase the line pressure to more than the estimated level required
- c. open the valve to the air line slowly and for short periods of time, watching to see the effect on the lateral strain gauge's readings. When a K_o condition has been restored, keep the valve closed to the airline.

To decrease the load slightly:

- a. close the valve on the vertical Bellofram to the air regulator
- b. open that valve to the atmosphere slowly and for short periods of time
- c. when K_o conditions have been achieved, keep the valve closed to the airline

In view of the assumption of K_o loading, it is necessary to keep the lateral strain occurring to a minimum. Thus, the maximum allowable lateral strain was set at .25% .

The lateral gauge magnifies each change in diameter, Δd cm, by a factor of two. Further, the calibration factor of the lateral gauge LVDT is q volts/cm. Thus, if the diametral strain, $(\Delta d/d)$, is to be limited to .0025, where d is the diameter of the sample in centimetres, the corresponding change in LVDT output must be less than $(.005)(qd)$ volts.

5. with the dissipation of all excess pore pressures, close valve B4.

C.2.4 Shear Loading

The sample is now subjected to a horizontal shear load. When doing this:

1. reset data acquisition system to take readings at two minute intervals. Take an initial set of readings.
2. make sure the output of the lateral gauge is displayed
3. loosen the spacer on the horizontal ram. Take a set of

readings as soon as possible.

The spacer's length should be readjusted, if necessary and when convenient, to allow the horizontal displacement of the ram to attain a maximum value of only 1 cm. This will prevent horizontal loads being applied to the vertical bushing assembly.

The length of time of application of a shear load increment is on the order of 15-16 minutes. It may be set by the stipulation that, within it, some representative physical quantity, w , must achieve an approximately stationary state, satisfying the inequality:

$$(w_{t-4})(w_t)^{-1} \geq .95 \quad t \geq 4 \quad C.1$$

where:

w_{t-4} represents the magnitude of w after $t-4$ minutes

w_t represents the magnitude of w after t minutes

and it is assumed that w changes monotonically. If this criterion fails under certain circumstances, one simply makes the decision based on a further assessment of the data.

4. restore the K_o condition, if necessary
5. at the end of the loading period, take an initial set of

- readings for the next load increment
6. increase the horizontal load and take another set of readings as soon as possible.

In the present series of tests, the magnitudes of the load increments were selected to define the average stress-strain curves as clearly as possible. It is a good idea to try to estimate the desired loading pattern beforehand and then to plot the appropriate curves, as the test proceeds, determining if any changes in the loading sequence are required.

C.2.5 End of Test

Upon completion of the test, the procedure is as follows:

1. isolate the pore pressure transducer. If this is not done, and the transducer is subjected to negative pressures (absolute), it can be damaged.
2. remove the shear load and reduce the vertical load to the value required as a seating load
3. decrease the seating load and cell pressure together.

C.2.6 Disassembly of Cell

When disassembling the cell:

1. make sure all valves are closed, including the tap on the cell fluid reservoir
2. open valve B8 to the atmosphere and open the appropriate valves as one would to increase the cell pressure (V9, V10 and V11)

3. apply a pressure of 210 kPa (30 psi), as read from the air regulator gauge, to the cell fluid
4. open valve B5, on the cell base, to allow the fluid to flow into the reservoir
5. occasionally, check the level of fluid within the reservoir. Close valve B5 and, opening the tap on the base of the reservoir, allow the fluid to find its own level within the sight tube, held upright
6. if the reservoir is full, close the tap, insert the sight tube into one of the storage containers and open the tap once again. When the reservoir has been drained, close the tap and open valve B5 once again
7. if the reservoir is not full, close the tap, drain the fluid in the sight tube into a storage container and open valve B5
8. maintain the cell pressure till the fluid being forced from the cell turns to foam, then close valve B5. Reduce the cell pressure to zero; it will take a short while for the pressure to dissipate completely
9. close valves V9, V10 and V11. Remove the blind ended plug on the cell cap to ensure that all cell pressure has dissipated
10. put the vertical load cell channel in skip mode. Remove the tie rods and vertical load cell, the load cell being replaced by the lower extension
11. unscrew the collars in contact with the upper surface of the main crosspiece. They must not obstruct the

movement of the main crosspiece when it is raised

12. opening the valves to the pneumatic ram, V9 and V10, the cell cap is raised and the second extensison inserted. The collars on the load cap are then loosened, the rotational LVDT's and holder removed and the load cap raised. Care must be taken to avoid damaging the LVDTs' wires and probes

13. put the horizontal load cell and LVDT channels in skip mode. Loosen the clamp securing the horizontal LVDT and remove the LVDT

14. push the horizontal ram towards its initial position; to do this, it might be necessary to open valve B7, on the horizontal Bellofram, to the atmosphere

15. unplug the horizontal load cell and remove it

16. position the horizontal ram to accept the lower load cap. Lower the load cap

The guide rods may be used to center the load cap. Make sure the collars, used to secure the load cap to the upper platen, provide no obstruction

17. lower the cell cap, removing the second extension when necessary

18. secure the cell cap using four tie rods equally spaced about its perimeter. Remove the guide rods.

19. unscrew the bolts attaching the cell base to the loading frame base. Make sure that there are no cables or pressure lines that will obstruct the cell while it is being positioned on the moveable plate

20. raise the cell, position the moveable plate (with the hole for the anchoring pin pointing away from the cell) and lower the cell onto the moveable plate
21. reduce the line pressure to the pneumatic ram to zero
22. undo the tie rods, raise the cell cap, insert the second extension and raise the cell cap further
23. raise the load cap till the moveable plate can be pulled, without obstruction, to the working area; anchor the moveable plate by positioning the pin that passes through the plate and the loading frame base
24. remove the cell wall and lateral strain gauge
25. position a spacer beneath the load cap, with its upper and lower parts now aligned, and lower the load cap till it rests on the spacer.

The spacer should be of a diameter equal to that of the sample and of sufficient thickness that there is clearance between the vertical arms of the load cap and the loading frame base

26. remove the second extension and lower the cell cap till the main crosspiece comes into contact with the two collars positioned on the vertical supports
27. decrease the line pressure to the pneumatic ram to zero. Close valves V9 and V10.
28. clean up the cell fluid coating the inside of the cell wall and resting on the cell base.
29. the sample should then be inspected. The following should be considered:

- a. is the upper platen apparently horizontal to the base?
- b. what is the nature of the deformed profile of the sample in the direction parallel to the shear force?
- c. is there much lateral deformation along the diameter which is normal to the line of action of the shear load?
- d. was a failure plane formed; the homogeneity of deformation in general?
- e. the nature of any disturbance in the region of the finned plates (upper platen having been taken off)
- f. the presence of any cell fluid within the porous stones or around the sample; implications?

30. photographs should be taken as appropriate.

C.3 Detailed Discussion of Back Saturation

The following subsections deal with an approximate method for determining the degree of saturation of the sample during undrained shear loading.

C.3.1 Seating Load

As described on page 157, to begin the test the cell pressure and vertical load were increased. The vertical load was increased to prevent the displacement of the vertical ram upon application of the cell pressure.

Assuming that the cell fluid will exert pressure on every surface of the load cap assembly, the net load due to

the cell pressure, L_1 , is:

$$L_1 = (\pi/4)(d_1)^2 p_1 \quad C.2$$

where:

d_1 is the diameter of the ram, in metres

p_1 is the cell pressure, gauge, in Pascals

and it is directed vertically upwards. Similarly, the load exerted by the vertical Bellofram is:

$$L_2 = (\pi/4)(d_2)^2 p_2 \quad C.3$$

where:

d_2 is the bore of the Bellofram and,

p_2 is the internal pressure acting.

The units are compatible with those of the previous equation.

To insure static equilibrium of the vertical ram, it is required that L_1 equal L_2 . The self weight of the load cap-ram system is neglected as is the frictional force exerted by the vertical bushing assembly. This is

conservative.

Calibration procedures demonstrate that the air line pressures indicated by the air regulator gauges, of interest here, are below the true line pressures by about 10%. Hence, equating the two above relations and with primed variables representing the quantity as determined from the appropriate regulator gauge:

$$(\pi/4)(d_1)^2(1.1)p_1' = (\pi/4)(d_2)^2(1.1)p_2' \quad C.4$$

or,

$$(p_1'/p_2') = (d_2/d_1)^2 \quad C.5$$

Now, the diameter of the Bellofram cylinder is approximately 14 cm; that of the vertical ram is 3.18 cm. Thus, for equilibrium, the ratio of the regulator pressures must be approximately 20.

C.3.2 Increments of Cell Pressure

Following an increment in cell pressure, as discussed

on page 157, one need not make an attempt to maintain a K_o condition if the observed deviations from it are small. Further, one must be careful that the pore pressure does not exceed the lateral total stress.

An examination of the test data demonstrates that in interpreting the present stage of undrained loading, any vertical stress exerted by the vertical Bellofram on the sample may be neglected.

C.3.3 Changes in Degree of Saturation

It is assumed that the increase in cell pressure serves only to compress the free air within the sample and that no further air goes into solution. This is a conservative assumption. Further, following Bishop and Henkel (1962), pg. 179 et seq., it is taken that the pressure of the air in the voids of the sample does not differ greatly from the pressure in the pore water, with the air assumed to be at atmospheric pressure. Now, it is possible to derive a simple, conservative expression for the degree of saturation of a soil sample as a function of pore pressure and initial degreee of saturation. This will be done in the following paragraphs.

Let

V_w denote the initial volume of water in the sample

V_i denote the initial volume of free air within the sample

S_i denote the initial degree of saturation of the sample

S_2 denote the final degree of saturation of the sample

p_i denote the initial pressure (absolute) in the pore space and,

p_2 denote the final pressure (absolute) in the pore space.

As the pressure in the pore space rises from p_i to p_2 , the volume of free air decreases to:

$$V_2 = \frac{p_i V_i}{p_2} \quad C.6$$

where it is assumed that the pore air obeys Boyle's law and, again, that upon increase in the pore pressure no further air goes into solution. Now, by definition,

$$S_i = \frac{V_w}{V_w + V_i} \quad C.7$$

and,

$$S_2 = \frac{V_w}{V_w + V_2} \quad C.8$$

Therefore, using equation C.6, equation C.8 may be rewritten as:

$$S_2 = \frac{V_w}{V_w + \left[\frac{V_i}{P_2} \right] P_i} \quad C.9$$

Also, equation C.7 can be rearranged to yield an explicit expression for V_i :

$$V_i = \frac{V_w}{S_i} (1 - S_i) \quad C.10$$

which can be substituted in equation C.9 to give:

$$S_2 = \frac{1}{1 + \left[\frac{P_i}{P_2} \right] \left[\frac{1 - S_i}{S_i} \right]} \quad C.11$$

Therefore, knowing the initial degree of saturation and pore pressure, and final pore pressure upon an undrained increment in cell pressure, one can make a conservative estimate of the new degree of saturation. At the end of

consolidation, the volume of air and water considered during undrained loading to calculate the sample's degree of saturation occupies not only the pore spaces of the sample but a certain amount of the drainage lines as well. Equation C.11 may be used to calculate the final degree of saturation of that volume.

Since the pore fluid is assumed to remain homogeneous, this figure also represents the degree of saturation of the material occupying the pore spaces of the sample. It should be noted that although the pressure of the pore fluid decreases as consolidation proceeds, it is still greater than the pore pressure at the start of the test. Thus, since no air has been assumed to enter solution with any increase in pressure, the estimate of the degree of saturation of the sample is still conservative. Further, it should be noted that before testing is begun all drainage lines and lines in the cell base are rid of air bubbles.

C.3.4 Acceptable Degree of Saturation

Black and Lee (1973) assume that under certain conditions one can treat a soil sample, with a degree of saturation of .990 or .995, as fully saturated for the purpose of interpreting test results. It is chiefly a question of the stiffness of the sample. The advantage of this less stringent criterion is a saving of time. Since the samples presently being tested are of medium stiffness, following Black and Lee (1973), a degree of saturation of

.990 was accepted.

In the chapter on test results, data from the testing program will be reviewed.

B30300